OBSERVATIONS OF SOLAR CORONA AT
THE MEXICO TOTAL SOLAR ECLIPSE
OF JULY 11, 1991

「平成３年７月１１日メキシコ日食による太陽コロナの観測」

平成４年３月

平成２～３年度　科学研究費補助金
国際学術研究　研究成果報告書
（０２０４１０９４）

研究代表者　山下　泰正

N

E 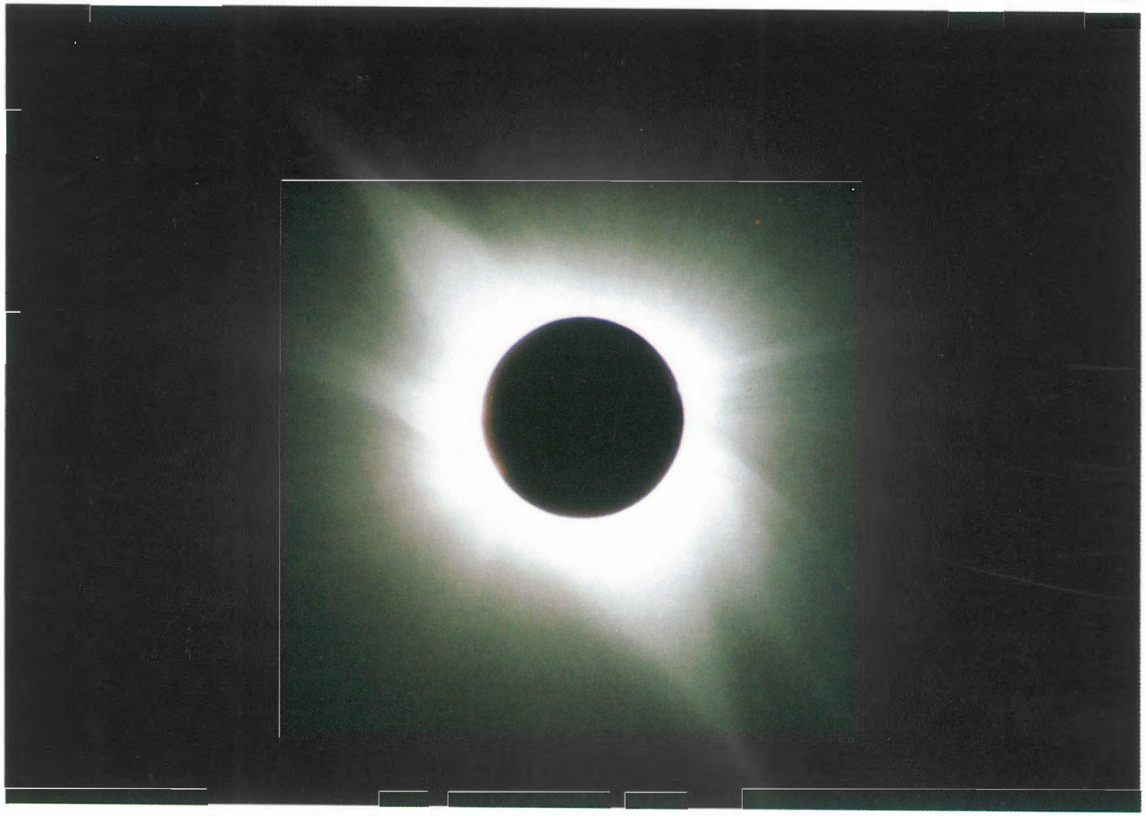 W

S

At La Paz,Mexico

OBSERVATIONS OF SOLAR CORONA AT THE MEXICO TOTAL SOLAR ECLIPSE OF JULY 11, 1991

「平成３年７月１１日メキシコ日食による太陽コロナの観測」

平成４年３月

平成２～３年度　科学研究費補助金

国際学術研究　研究成果報告書

（０２０４１０９４）

研究代表者　山下　泰正

「平成３年７月１１日メキシコ日食による太陽コロナの観測」

研究代表者

山下　泰正　　国立天文台・光学赤外線天文学研究系

研究分担者

平山　淳　　国立天文台・太陽物理学研究系

黒河　宏企　　京都大学・理学部

北井礼三郎　　京都大学・理学部

末松　芳法　　国立天文台・太陽物理学研究系

西野　洋平　　国立天文台・乗鞍コロナ観測所

磯部　琇三　　国立天文台・光学赤外線天文学研究系

田邊　俊彦　　東京大学・理学部

研究協力者

福島　英雄　　国立天文台・乗鞍コロナ観測所

野口　本和　　国立天文台・光学赤外線天文学研究系

小山　薫　　海上保安庁・水路部

奥村　雅之　　海上保安庁・水路部

石浦　清美　　京都大学・理学部

文部省科学研究費補助金
国際学術研究

平成２年度、３年度

課題番号　０２０４１０９４

OBSERVATIONS OF SOLAR CORONA AT THE MEXICO TOTAL SOLAR ECLIPSE OF JULY 11, 1991

Yasumasa, YAMASHITA — Optical and Infrared Astronomy Division, National Astronomical Observatory

Tadashi, HIRAYAMA — Solar Physics Division, National Astronomical Observatory

Hiroki, KUROKAWA — Faculty of Science, Kyoto University

Reizaburo, KITAI — Faculty of Science, Kyoto University

Yoshinori, SUEMATSU — Solar Physics Division, National Astronomical Observatory

Yohei, NISHINO — Solar Physics Division, National Astronomical Observatory

Shuzo, ISOBE — Optical and Infrared Astronomy Division, National Astronomical Observatory

Toshihiko, TANABE — Faculty of Science, University of Tokyo

Hideo, FUKUSHIMA — Solar Physics Division, National Astronomical Observatory

Motokazu, NOGUCHI — Optical and Infrared Astronomy Division, National Astronomical Observatory

Kaoru, KOYAMA Hydrographic Department
Maritime Safety Agency

Masayuki, OKUMURA Hydrographic Department
Maritime Safety Agency

Kiyomi, ISHIURA Faculty of Science, Kyoto University

A Grant-in-Aid for Overseas Scientific Research

Ministry of Education, Science and Culture, Japan

No. 02041094 (1990 and 1991)

(Summarized in March 1992)

日食研究会出席者名簿

（平成３年１１月２９、３０日、於：国立天文台）

氏　　名	所　　属
武田　　秋	京都大学・宇宙物理
河合　吾郎	〃
北井　礼三郎	京都大学・飛騨天文台
石浦　清美	〃
黒河　宏企	〃
久保　良雄	海上保安庁・水路部
小山　　薫	〃
金沢　輝雄	海上保安大学校
久保田　諄	大阪経済大学
椿　都生夫	滋賀大学・教育学部
花岡康一郎	国立天文台・電波天文学研究系
磯部　　三	国立天文台・光学赤外線天文学研究系
野口本和	〃
一本　　潔	国立天文台・太陽物理学研究系
坂尾　太郎	〃
平山　　淳	〃
桜井　　隆	〃
山口　喜助	〃
末松　芳法	〃
日江井栄二郎	国立天文台・乗鞍コロナ観測所
今井　英樹	〃
篠田　一也	〃
福島　英雄	〃
宮下　正邦	〃
西野　洋平	〃
入江　　誠	国立天文台・太陽活動世界資料解析センター
吉村　宏和	東京大学・天文学教室
田邊　俊彦	東京大学・天文教育センター
田鍋　浩義	
斉藤　尚生	東北大学・地球物理学教室
南　　繁行	大阪市立大学・工学部
川上　新吾	大阪市立科学館
當村　一朗	大阪府立高専
渡辺　　裕	東京学芸大学

CONTENTS

NAO: National Astronomical Observatory

JAPANESE EXPEDITION FOR THE OBSERVATION OF THE 1991 TOTAL SOLAR ECLIPSE

HIROKI KUROKAWA

Kwasan and Hida Observatories, Kyoto University, Kamitakara, Gifu 506-13, Japan

The total solar eclipse provides us with the best oppotunity when we can make detailed studies of solar corona with many types of observing devices from the ground. The 11-July-1991 Eclipse was one of the most important eclipses in this century because of its longest duration of totaity.

We started to discuss about this eclipse in the spring of 1986 at the National Committee for Solar Eclipse, Science Council of Japan. The astronomical circumstances of the eclipse, the climate conditions, the geographical situatoins and the environmental conditions along the path of totality were examined, and the purposes of the observations were discussed there in 1986-1989. Three institutes,i.e., National Astronomical Observatory, Kyoto University, and Hydrographic Department of Japan, decided to send the expedition to Mexico and started to prepare for the observing instruments from the spring of 1990.

During July 6-20, 1990, Two of us (Suematsu and myself) visited Mexico to investigate the climate conditions, transportation routes for the equipments, availability of electric power supply, lodging, security and other environmental circumstances for several sites. After the detailed investigation we selected the campus of UABCS (Universidad Autonoma de Baja California Sur) for the main observing site of the Japanese party according to the recommendation of COMES(Comite Mexicano Eclipse Solar). UABCS is situated in the suburbs of La Paz, the biggest city of the southern part of California peninsular.

Before the end of April of 1991 we finished the construction and final adjustment of the whole observing instruments at each institute. In the mddle of May, all the equipments were packed in three containers(each volume: 8 feet x 8 feet x 20 feet) and left Yokohama for Ensenada on 30 May, 1991.

The Japanese Eclipse Expedition consists of four observing teams with eleven members. One team of three members (leader: S. Isobe) climbed Mt. Popocatepetl (5452 m) together with the collaborators of UNAM (Universidad National Autonoma de Mexico). Three teams of eight members arrived at Ensenada on 13 July to receive the containers of the equipments. After the custom clearance, the three containers, loaded on two trucks(Figure 1), left Ensenada for La Paz in the morning of 15 July, and arrived, after 1600 km's ride, at the playground of UABCS near the noon of 17 July (Figure 2).

The Japanese party was the first to arrive at UABCS, and about three hundred persons from more than ten countries successively got together on the campus before the eclipse

day according to the announcement of CUPOE(Comite Universitario Para la Observacion del Eclipse). Figure 3 shows the press conference held at the campus on 9 July, or two days before the eclipse day. With great help of CUPOE(chairman: Ing. Manuel Oseguera) we set up the observing systems on the playground of UABCS and repeated the test observations, fine adjustments of the instruments and the rehearsals of the observation. The weather was also cooperative to us and it was very fine on the eclipse day(Figure 4). We successfully obtained a lot of data in the clear sky and in the good seeing condition.

In this report, the preliminary results obtained by the four teams of the Japanese Expedition for the 1991 Eclipse are presented as well as the purposes of the observations, instrumentations and observational procedures. Some other related papers, which were presented in the eclipse seminar held on 29-30 November, 1991 at National Astronomical Observatory, are also included.

In the course of preparing and carring out this project, we have received great deal of help and supports from many people and organizations. We would like to express our hearty thanks to them and especially to the following organizations;

- International Scientifc Research Division of the Ministry of Education, Science and Culture, Japan for a grant in aid of research in Mexico,
- The Ministry of Foreign Affairs, Japan (the Bureau of Middle-South America) for introducing us to Embassy of Japan in Mexico,
- Embassy of Japan in Mexico for providing us with useful informations of local conditions in Mexico and with kind help in Mexico city,
- National Committee for Solar Eclipse, Science Council of Japan for discussing many problems in preparing and organizing the Japanese Eclipse Expedition,
- COMES(Comite Mexicano Eclipse Solar) giving information on UABCS for the observing site and for negotiating with Mexican custom authorities for the smooth custom clearance of the equipments,
- UABCS and CUPOE(Comite Universitario Para la Observacion del Eclipse) for providing the observing site and various kinds of facilities and for their hospitality,
- Hotel Aquarios in La Paz for warm hospitality and kind help.

We also express our sincere thanks to Professors Y. Yamashita and T. Hirayama for their support and encouragement as the leaders of this research project, and to Professor E. Hiei for his continuous encouragement with valuable advices as the chairman of National Committee for Solar Eclipse.

Fig. 1. The containers of the equipments loaded on two trucks at Ensenada Port

Fig. 2. The three containers arrived at the playground of UABCS.

Fig. 3. Press conference held at the campus of UABCS on July, 1991.

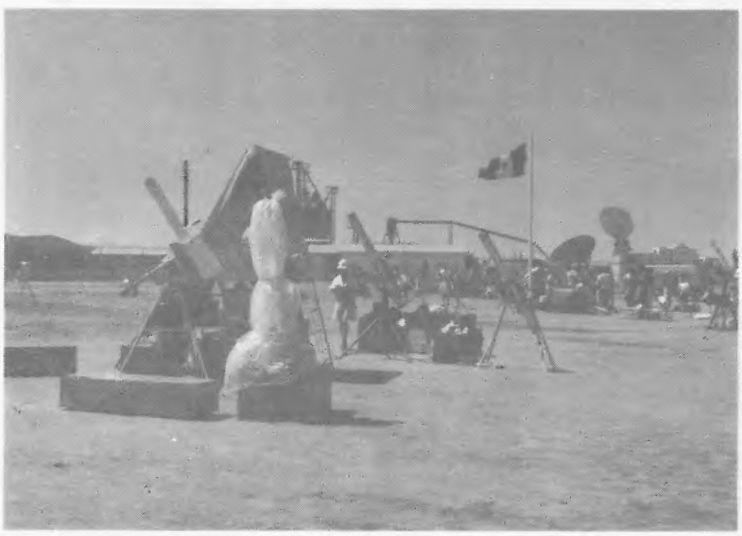

Fig. 4. A view of the observing site on the eclipse day.

CIRCUMSTANCES OF TOTAL SOLAR ECLIPSE OF 1991 JULY 11

YOSHIO KUBO
Hydrographic Department
Tsukiji-5, Chuo-ku, Tokyo, 104 Japan

A total solar eclipse occurred on 11 July 1991. The circumstances of this eclipse, especially focused on those in Hawaii and Mexico where many scientific observations were made, are presented.

1. General Situations

A total solar eclipse, which has the Oppolzer number 7614, occurred on 11 July 1991. This eclipse belongs to saros series number 136. The last eclipse in this series was the one which occurred on 30 June 1973 in northern Africa and other areas and the next one will be seen on 22 July 2009.

The global circumstance of the eclipse of 11 July 1991 is shown in Figure 1. About half of the central path passed over land, including densely populated areas.

The central path began at a point west-southwest of the Hawaiian Islands at about $17^h\ 23^m$ (The time is universal time UT throughout this article). It covered a large part of the Hawaiian Islands, passed Mexico, Guatemala and other Central American countries and, entering South America, ended at a place in Brazil at about $20^h\ 49^m$.

The central eclipse at local apparent noon occurred at $19^h\ 06.1^m$ at a point of 105° 10.7' western longitude and 21° 59.1' northern latitude near Tuxpan in the mainland of Mexico. The altitude of the Sun at this site was about 89°. The width of the central path reached its maximum, about 258 km, near this site. On the other hand, the muximum duration of totality occurred at about $19^h\ 00^m$ at a point in the Gulf of California and it was $6^m\ 58^s$, the longest of all remaining total solar eclipses in this cetury.

2. Circumstances in Hawaii and Mexico

Figure 2 are enlarged maps of the total paths near Hawaii and Mexico. The figures given along the paths in the maps show the times of muximum eclipse.

In Table 1 is shown the local circumstances at Mauna Kea in Hawaii Iland and La Paz and Popocatepetl in Mexico, where observations of the eclipse were made by many scientists including the Japanese expedition teams.

The computation for these local circumstances is based on the Japanese Ephemeris for 1991, which is accordant with IAU (1976) system of astronomical constants. 0.2725076 and 959.630"

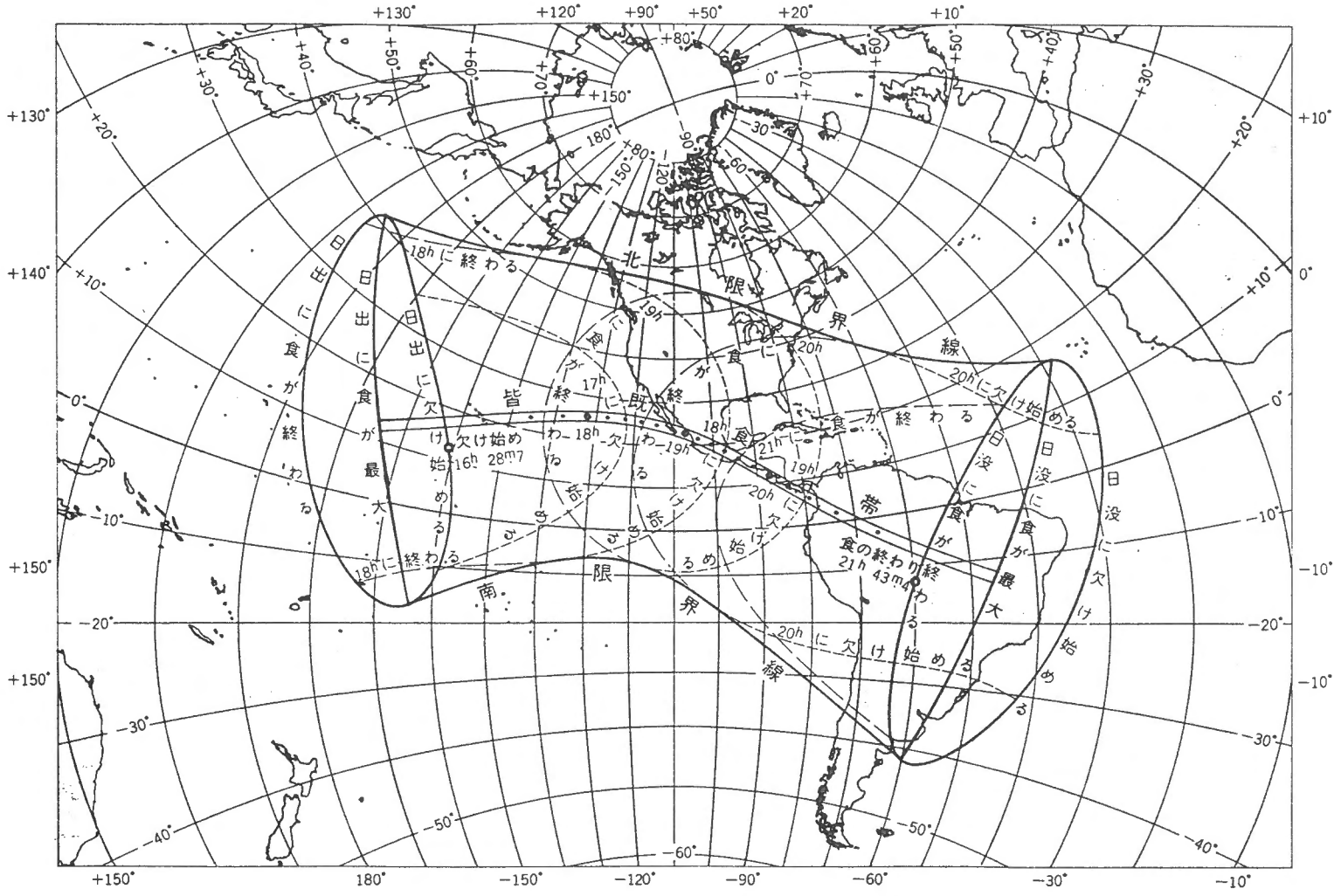

Figure 1. Map of the Total Eclipse of 1991 July 11

are adopted as the Moon's radius in the unit of the equatorial radius of the Earth and the semidiameter of the Sun at 1 a.u. distance, respectively. A correction of $\Delta\lambda$ = 0.38" and $\Delta\beta$ = -0.21", which is the differece between the center of figure and the center of mass of the Moon, is applied to the longitude and latitude of the Moon in the Ephemeris, respectively. ΔT of 58 secs is used as the difference TD (dynamical time) - UT.

Table 1. Circumstances of the Total Eclipse at Mauna Kea, La Paz and Popocatepetl

	Mauna Kea	La Paz	Popocatepetl
Longitude	155° 28' 20" W	110 18 50 W	98 37 20 W
Latitude	19° 49' 30" N	24 06 00 N	19 01 40 N
Height	4.2km	0.0	5.3
2nd contact	$17^h\ 28^m\ 08.73^s$	18 47 33.66	19 22 41.30
P.A.	93.9°	92.9	110.3
Maximum	$17^h\ 30^m\ 14.22^s$	18 50 51.54	19 26 04.20
R.A. of Sun	$7^h\ 21^m\ 57^s$	7 22 10	7 22 16
Dec. of Sun	22° 06'119"	22 05 53	22 05 42
S.D. of Sun	943.9"	944.0	944.0
S.D. of Moon	1009.0"	1020.2	1020.0
Alt. of Sun	21.3°	81.5	78.8
Az. of Sun	73.2°	101.9	287.8
3rd contact	$17^h\ 32^m\ 20.72^s$	18 54 09.59	19 29 26.15
P.A.	277.1°	308.2	301.4

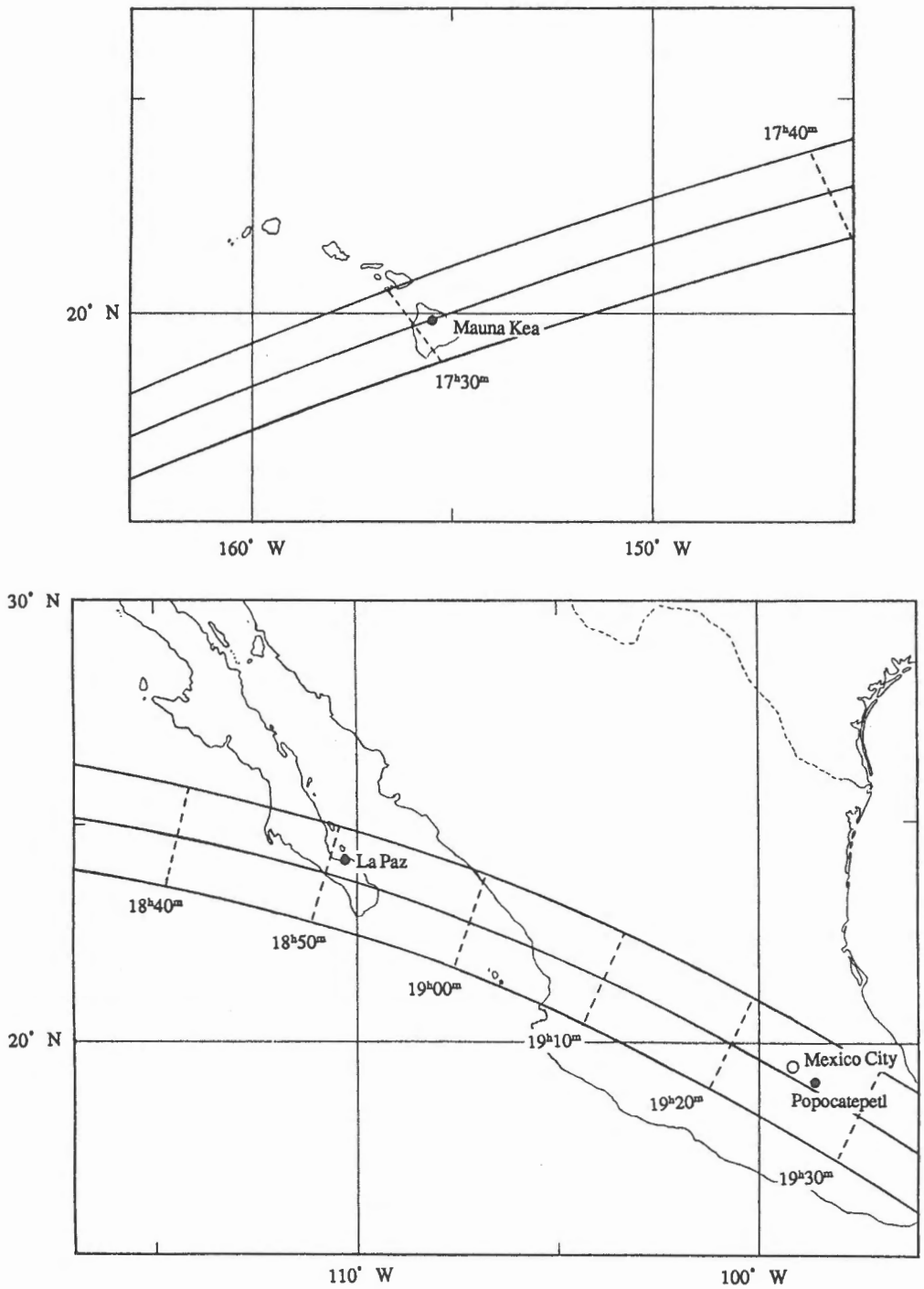

Figure 2. Circumstances of the Eclipse near Hawaii and Mexico

3. Profile of Lunar Limb

The profile of the lunar limb at this eclipse is shown in Figure 3. The figure is derived from the Watts' charts. The profile is based on the topocentric libration of the Moon at 18^{h} 51^{m} at La Paz. The parameters for libration are slightly different in Hawaii, but the general feature of the figure is almost the same. The directions of N and L mean those of the north in the sky and the north pole of the Moon, respectively.

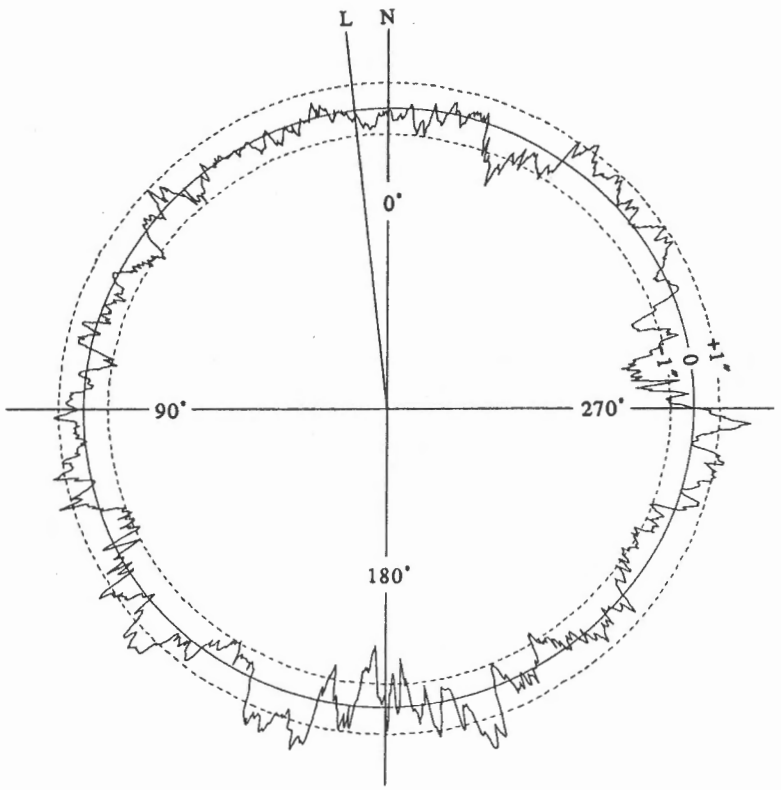

Figere 3. Profile of Lunar Limb

THE OBSERVATION OF THE INNER CORONA AT THE 1991 TOTAL SOLAR ECLIPSE

HIROKI KUROKAWA, REIZABURO KITAI AND KIYOMI ISHIURA

Kwasan and Hida Observatories, Kyoto University, Kamitakara, Gifu 506-13, Japan

ABSTRACT: The total solar eclipse of 11 July, 1991 was observed at La Paz, Mexico and high-resolution pictures of the inner corona were successfully obtained in the lights of FeX6374, FeXIV5303, CaXV5694, Hα lines and 6100Å continuum. The 6374 loop structures are found to be finer than any other 10^6K coronal loops which have ever been published. The emission-line images represent the fine structures of $1x10^6$K (FeX), $2x10^6$K (FeXIV), $3.5x10^6$K (CaXV) and $1x10^4$K (HI) respectively, and the continuum images show the electron column density distribution. The detailed comparison between them enable us to study the temperature-density structures of various types of coronal fine structures. The instruments and the observational procedure were described, and some examples of high-resolution pictures are presented. Preliminary examination and discussion of general characteristics of each monochromatic image are also given.

I. Introduction

The Kwasan and Hida Observatories team (the three authors) successfully observed the total solar eclipse of 11 July, 1991 at UABCS (Universidad Autonoma de Baja California Sur) campus in La Paz, Baja California Sur, Mexico. The primary purposes of our observation are to get the high-resolution images of inner corona in coronal emission lines of different ionization potentials, *i.e.*, Hα ($1x10^4$K), FeX6374Å ($1x10^6$K), FeXIV5303Å ($2x10^6$K), CaXV5694Å ($3.5x10^6$K) as well as in a continuum light, and to study the thermodynamic state of various types of cornal fine structures.

This research project of Kwasan and Hida Observatories dates back to the 1973 Mauritanian Eclipse when Kanno, Tsubaki and Kurokawa obtained the flash spectrograms of coronal lines with the slot spectrograph (Kanno *et al.* (1974)). Regarding the coronal lines of 5303Å, 6374Å and 7892Å(FeXI) in the spectrograms as the monochromatic images of the corona, Kurokawa (1975) first found a cool and dense core (10^6K, $6x10^9 cm^{-3}$) in the coronal condensation above the McMath region 12397 at the west limb.

In order to get higher resolution in space, we developed the four-channels monochromatic-image telescope for the 1976 Australia Eclipse (Hattori, Kubota and Kurokawa). The telescope consisted of three 15cm refractors, one 10cm refractor and four monochromatic filters of 5303Å, 6374Å, Hα lines and 6100Å continuum. Though clouds pre-

vented us from getting any coronal images in Australia, the four-channels telescope enabled us to obtain high resolution monochromatic images of coronal loops and post-flare loops at the 1980 Kenya Eclipse (Saito, Kurokawa and Ogimachi (1980), Hanaoka *et al.* (1986,1988)). From the detailed study of relationships among FeXIV5303 hot loops, FeX6374 cool loops and 6100 continuum loops, Hanaoka *et al.*(1988) presented a corona-loop model with several slender cool threads in a hot loop.

At the 1983 Indonesian Eclipse, Suematsu *et al.* (1984) observed a small coronal condensation related to a small transient Hα prominence with the same 4-channels monochromatic image telescope.

This expedition for the 1991 Mexico Eclipse is the fourth experiment with the monochromatic telescope. In order to study coronal fine structures in more detail with higher spatial resolution, we completely remodelled the rear part of the telescope to have simultaneously eight focuses, or eight coronal images. We adopted three high-sensitive video cameras as well as five photographic cameras.

Thanks to the clear sky and good seeing-condition on the eclipse day, we successfully got many high-reslution images of the inner corona in 5303, 6374, 5694, Hα lines and 6100 continuum both on the photographic films and on the video recorders. A detailed description of the instruments is given in the next section, and the observational procedures , in the section 3. Some examples of high resolution pictures are demonstrated and examined in the section 4.

2. Instrumentation

Our multichannel telescope consists of four refractors, installed on a spar of rigid tube of 50 cm in diameter and 1.5 m in length. The tube itself is mounted on a fork-type equatorial mounting. The basic design was developed by the 1976-expedition team to Australia (A. Hattori, J. Kubota and H. Kurokawa). Then with minor modifications, the telescope has been used by the following expedition teams : Kenya 1980 (S. Saito, H. Kurokawa and Y. Ogimachi) and Indonesia 1983 (S. Saito, Y. Funakoshi and Y. Suematsu).

We planned to get monochromatic images, as fine as possible in spatial resolution, at the total solar eclipse on July 11, 1991. We modified our multichannel telescope so that we could observe and record monochromatic images in video data format, in addition to photographic method thus far used. Highly sensitive and highly resolving video cameras were attached to the telescope to get faint coronal images in normal video rates. With this setup, we thought it promising to obtain high resolution coronal images without loosing any chances of good seeing conditions.

We describe the instrumentaion in five separate sections, namely the optical system design of the multichannel telescope, the photographic camera system, the video image system, the electric power supply, and setting-up procedure.

a) Optical system

First, we describe the original design of the optical system of the 4-channels telescope. The four refractors have the same optical system design each other. As is shown in Figure 1, the objective doublet (ϕ = 150 mm, f = 2250 mm) forms primary image of the sun of about 20 mm in diameter. The following relay-lens system enlarges the primary image to form the final solar image of about 30mm in diameter. A narrow band filter is set up at the rear of the relay-lens system to select out coronal emission lines. The relay-lens system consists of two lenses, the first one is concave and the second is convex. These two lenses, with their mutual distance fixed, are positioned so that the front focal point of the second lens coincides with the location of the exit pupil of the system, that is, the virtual image of the entrance aperture of the object lens formed by the first lens. In this telecentric lens configuration, every principal ray leaves the second lens parallel to the optical axis of the system, and the spectral transmittance of the filter is made to be homogeneous all over the field of view. This design was developed so that four monochromatic images of different coronal lines could be taken simultaneously on photographic films of standard 35 mm format.

We modified this basic design so that we could observe eight images simultaneously. A beam splitting element was introduced for every refractor light path, in front of the relay lens system (Figure 2). As images of coronal emission lines were expected to be faint, we used dichroic cube prisms for beam splitting elements so that we could have as much light as possible in the wavelength of each coronal line. For every refractor, we selected a pair of coronal emission lines to be observed and installed a suitable dichroic cube prism. Transmittances and reflectivities of these cube prisms were about 90 % in respective wavelength ranges. For continuum images of sufficient brightness, we used a normal cube prism for beam splitting. The combination among refractors, prisms and detectors for the eight wavelengths is summarized in Table 1.

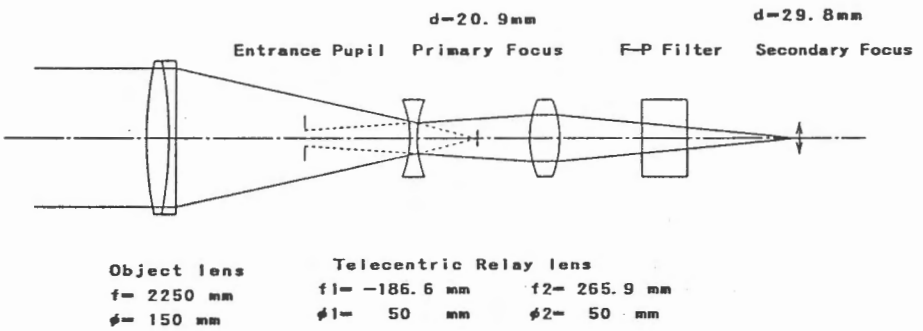

Fig. 1. Basic optical system of the four-channels telescope.

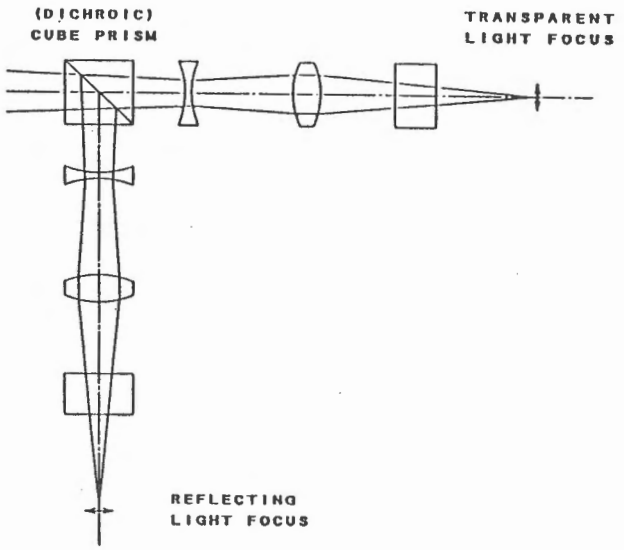

Fig. 2. Beam splitting part of the eight-channels telescope.

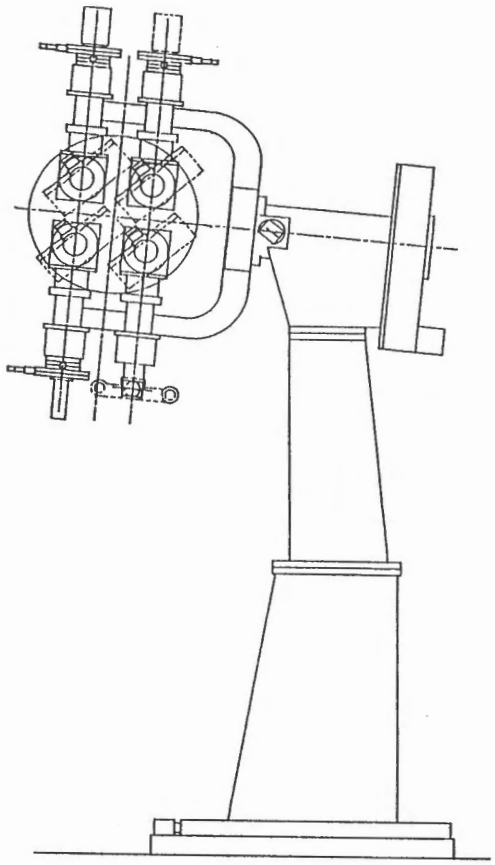

Fig. 3. Overall structure of the eight-cahnnels telescope.

Table 1.

Refractor Number	Beam splitter element	T/R	Wavelength	Dectector
1	Noraml beam splitter	T	6100 cont.	Photo (2415 film)
		R	6100 cont.	Video (HARP camera)
2	Dichroic cube prism	T	5303 line	Photo (T-max 400 film)
		R	6374 line	Video (SIT camera)
3	Dichroic cube prism	T	6374 line	Photo (T-max 400 film)
		R	5303 line	Video (HARP camera)
4	Dichroic cube prism	T	6563 line	Photo (2415 film)
		R	5694 line	Photo (T-max 400 film)

* T : Transmitted-light channel, R : Reflected-light channel

Table 2. Characteristics of filters

Channel	Central Wavelength(Å)	Filter Type	Pass Band FWHM(Å)	Peak Transmission(%)	Aperture (mm)
1T	6100.0	DIF	61	75.7	50
1R	6100.0	DIF	57	83.5	50
2T	5302.9	F-P	3.01	37.3	47
2R	6374.5	F-P	3.36	42.0	32
3T	6374.5	F-P	2.95	37.9	47
3R	5302.9	F-P	3.20	32.2	32
4T	6562.8	F-P	2.47	45.5	47
4R	5694.5	F-P	3.43	50.1	47

Characteristics of narrow band filters used in the observation are summarized in Table 2. For coronal line observations, we used interference filters of Fabry-Perrot type (F-P type). Temperatures of these filters were kept constant by thermo-controlled electric ovens. As atmospheric temperatures at the observing site were expected to be high, we setted the operating temperature of the filters at relatively high values (around 45 °C), above the atmospheric temperatures. Calibrations of central wavelengths of these filters were

performed through the vertical spectrograph of the DST telescope at the Hida observatory, Japan. On the other hand, we used dielectric multi-layered interference filters (DIF type) for 6100 continuum images .

b) Photographic devices

As is summarized in Table 1, five photographic cameras were used in the observation. All the cameras were of the same type, *i.e.*, motor driven NIKON FIII. We attached 250-film-backs to the camera for Hα images and to the one for 6100 continuum images, with which we could use 250-frames film magazines. For the other cameras, films were loaded with 36-frames patrones. In the observation, we photographed images in a pre-programmed sequence of various exposure times. Automatic exposure controls and power supply to the cameras were done by a sequence controller, in which we installed exposure control programs by hard-wiring. Detailed description of the observational programs will be given in the next section.

Spectroscopic sensitivity and granularity of photographic emulsions were key factors for our selection of appropriate films for our observations. The final selection is summarized in Table 1. The film 2415 is KODAK Technical Panchromatic 2415 film. T-Max 400 is also supplied by KODAK.

c) Video devices

Three kind of images, *i.e.*, 5303, 6374 and 6100-continuum images, were taken and recorded in video data format. Cameras and recording devices used in the observation is summarized in Table 3. As was stated above, we planned to take video images in normal video rate (30 frames/sec). This required us to use highly sensitive video cameras. After the sensitivity tests of various video cameras observing the full moon brightness as the test target, we finally selected out two cameras, SIT and Super-HARP, for our eclipse observation. The SIT camera, as is well known, is a Silicon-Intensified-Target device. This camera was found to have the highest sensitivity to red light among the tested cameras, and was adopted for the 6374 image observation. On the other hand, for the shorter wavelengths, we used Super-HARP cameras. These cameras had been developed at NHK (Japan Broadcasting Corporaion) and were kindly lent to us during the eclipse expedition. HARP is a video camera using High-gain Avalanche-Rushing amorphous Photoconductor. When high voltage around 600-700 volts is applied on thin layer of amorphous photoconductor, an electron produced by an incident photon produces an avalanche of secondary electron-hole pairs. Through this avalanche effect, quantum efficiencies of this detector reaches around 70, and the sensitivity to green lights is 80 times superior to usual saticon detectors. Owing to the thinness of photoconducting layer, avalances do not deteriorate spatial resolution of the detector. See Yamasaki *et al.* (1991) for details. Two Super-HARPs were used for the observation of 5303 images and of 6100-continuum images.

As the image areas of the video cameras were small compared to the image size of the Sun (Solar Diameter $\approx$ 30mm), only a part of solar corona could be seen through these

video cameras. So we put the video cameras on X-Y slide mounts equipped at the focal plane, and scanned the whole corona along the solar limb by manually moving the cameras in the focal plane.

Video recorders, which have high horizontal resolution matching the resolution of the cameras, were used in the observation, *i.e.*, a laser video disk recorder and two MII format video tape recorders.

Table 3.

Wavelength	Video Camera	Video recorder
FeX 6374	SIT camera Resolution 500 TVL Image Area 12.7 × 9.5 mm	Sony Laser Video Disk Recorder Resolution 550 TVL
FeXIV 5303	Super-HARP camera Resolution 600-800 TVL Image Area 8.8 × 6.6 mm	Panasonic MIIVTR(AU-665) Resolution 500-600 TVL
Conti. 6100	Super-HARP camera Resolution 600-800 TVL Image Area 8.8 × 6.6 mm	Panasonic MIIVTR(AU-520) Resolution 500-600 TVL

d) Electric power supply

At the observing site, we used a number of devices which required electric power of AC 100V, AC 220V or DC 12V. In fear of possible failure of commercial power supply during the total eclipse, we decided that all the neccesary electric power for the observing system should be supplied by DC batteries. For AC 100V devices, we supplied electric power by inverting DC 24V battery power. For this purspose, we used two rotary inverters and one thyristor inverter. DC 12V devices received power from 12V batteries. For AC 220V devices, which would not make serious troubles to the observation in case of power failure, we directly utilized commercial power supply. In Figure 4, all the cable connections between devices are shown including electric power supply, control signal lines and video signal lines.

e) Setting-up

The instruments were set up on the playground of Universidad Autonoma Baja California Sur (UABCS) in the suburb of La Paz, the biggest city of Baja California Sur. The longitude and latitude of the site are W 110°18' 51.1", and N 24°06' 02.1", respectively according to the observation of the Hydrographic Department team. We arrived at La Paz

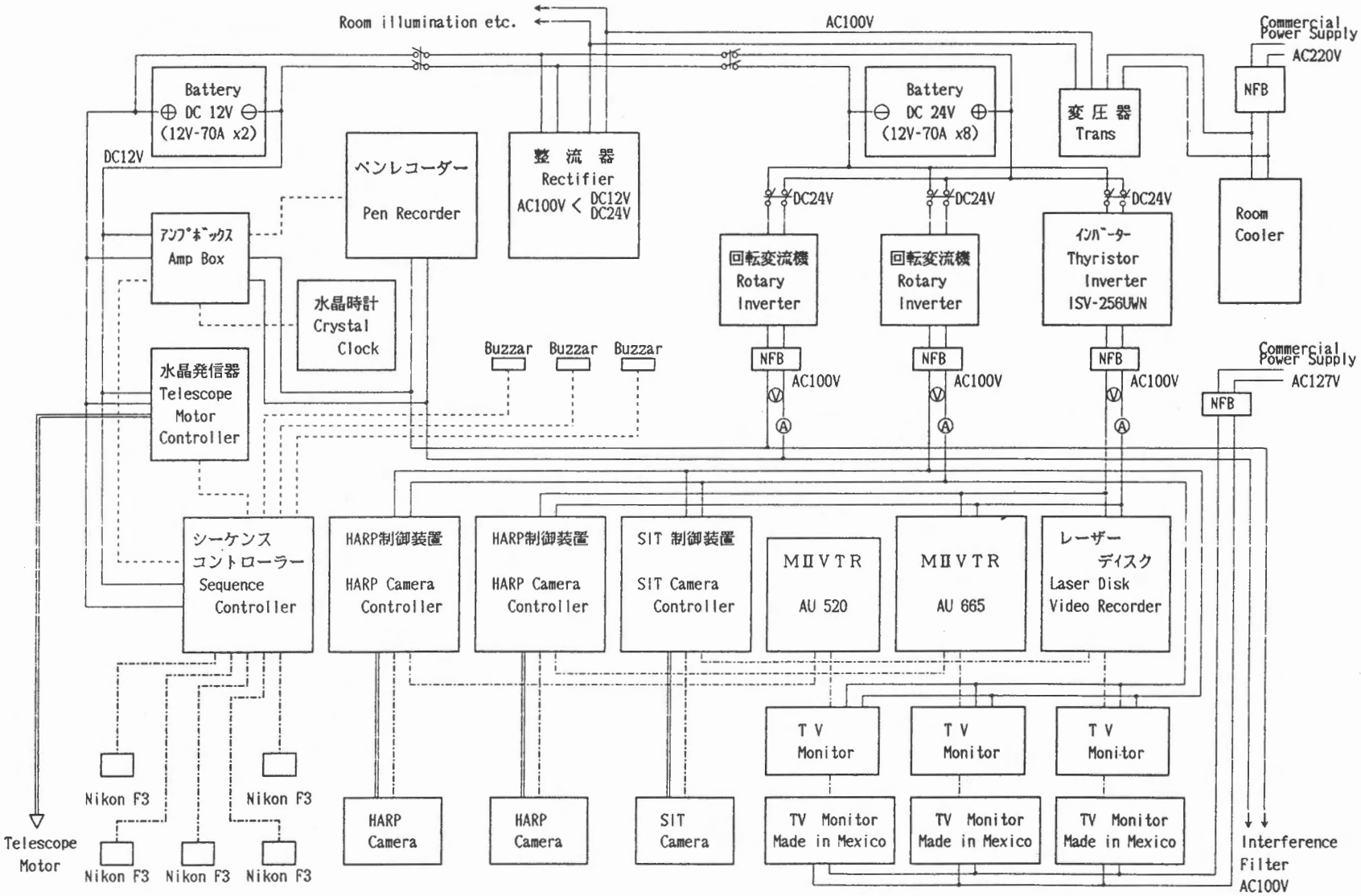

Fig. 4. Power supply and cable connections of the observational system.

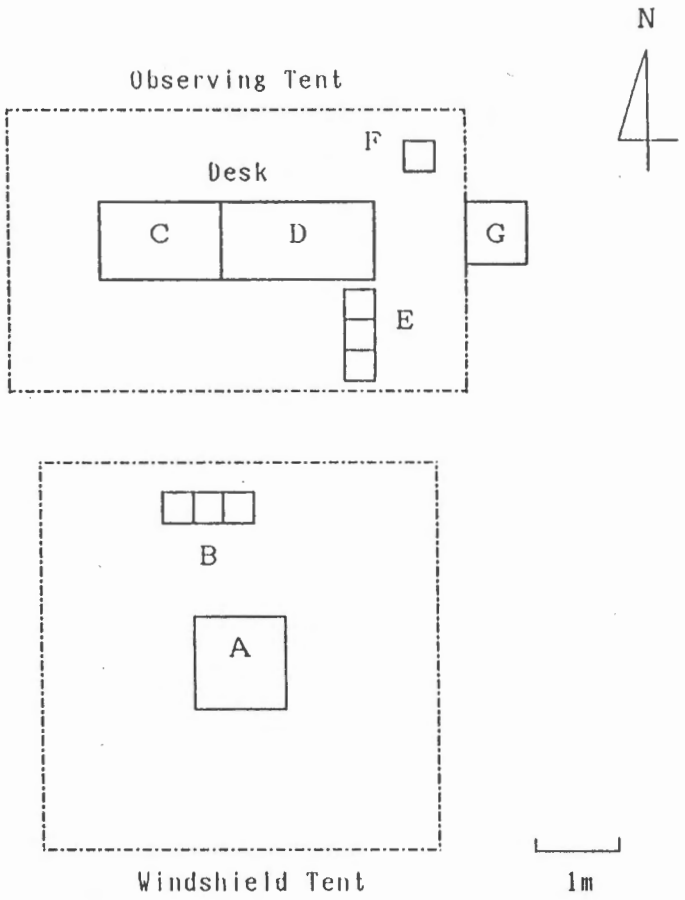

A : 8-Channel Telescope
B : TV Monitor x 3 (Made in Mexico)
C : HARP Camera Controller
HARP Camera Controller
Sequence Controller
Telescope Motor Controller
Crystal Clock
Amp Box
Buzzar x 3
Pen Recorder
Rectifier
Battery (12V-70Ah) x 2

D : Laser Disk Video Recorder
M2 VTR (AU 665)
M2 VTR (AU 520)
SIT Camera Controller
Thyristor Inverter
Rotary Inverter x 2
Battery (12V-70Ah) x 8
E : TV Monitor x 3
F : Trans (AC220V～AC100V)
G : Room Cooler

Fig. 5. The arrangement of the observing system of Kyoto University team.

on June 16 and the equipments, next day. We started to set up the instruments on June 18.

The housing tent for the instruments was equipped with an air-cooler. The maximum atmospheric temperature was about 38°C in the daytime at the playground of UABCS. The temperature rose up to even 50°C inside the tent without the air-cooler, but dropped to less than 35°C after the air-cooler began to work.

The telescope was installed on the concrete base of cement 30 cm deep in the ground (Figures 7, 8(a) and (b)). The main observing system was completed before June 27 when the moon became full. The arrangement of the observing system is shown in Figure 6. We examined the focus positions of the eight cameras, exposure times for the photographic films and the sensitivities of video camera by observing the full moon on June 28 and 29.

The last ten days were spent for the fine adjustment of the optical axes of the eight channels, improvement of the tracking accuracy of the telescope, the determination of the focus positions, exposure tests of the photographic films, and the rehearsal.

Figure 9 shows the telescope fully equipped with eight cameras and three video-monitors. Figure 10 shows the sequence cotroller, the pulse-generator for telescope-driving, three video-camera controllers, and three video recorders on the desk in the observing tent. The two pictures were taken on the eclipse day.

3. Observation

It was fine from the morning on the Eclipse day. The sky was completely clear and was never disturbed by any clouds during the eclipse at our observing site. The seeing condition was also found to be good by the visual observation of Hα solar prominences at about ten minutes before the second contact.

Here we describe our observational schemes and operations in details at the eclipse day and summarize some supplementary works after the observation.

The drive of the telescope and the exposures of photographic cameras were completely controlled by a sequence controller, which ran automatically following a prescribed program. The details of the program used in this observation is shown in Figure 6. We made the plan of the program based on the ephemeris calculation of the eclipse at the observing site, which was done in advance by Hydrographic Department of Japan. As the field of our photographic cameras covered nearly half of the solar disk, we divided the totality-duration into two periods, the former of which was used for the observation of east limb corona, and in the latter for the observation of west limb corona. The change of the telescope pointing was done in high speed around the mid-totality. The sequence controller had the ability to execute four different exposure-control sequences in parallel. We utilized three of them in this observation. The first one was used for controlling the camera of λ5694 images through the connector C2. The second one was for two cameras of Hα and λ6100 images through the connector C3 and C4 respectively. The third one was for two cameras of λ5303 and λ6374 images through the connector C5 and C6. The time necessary to

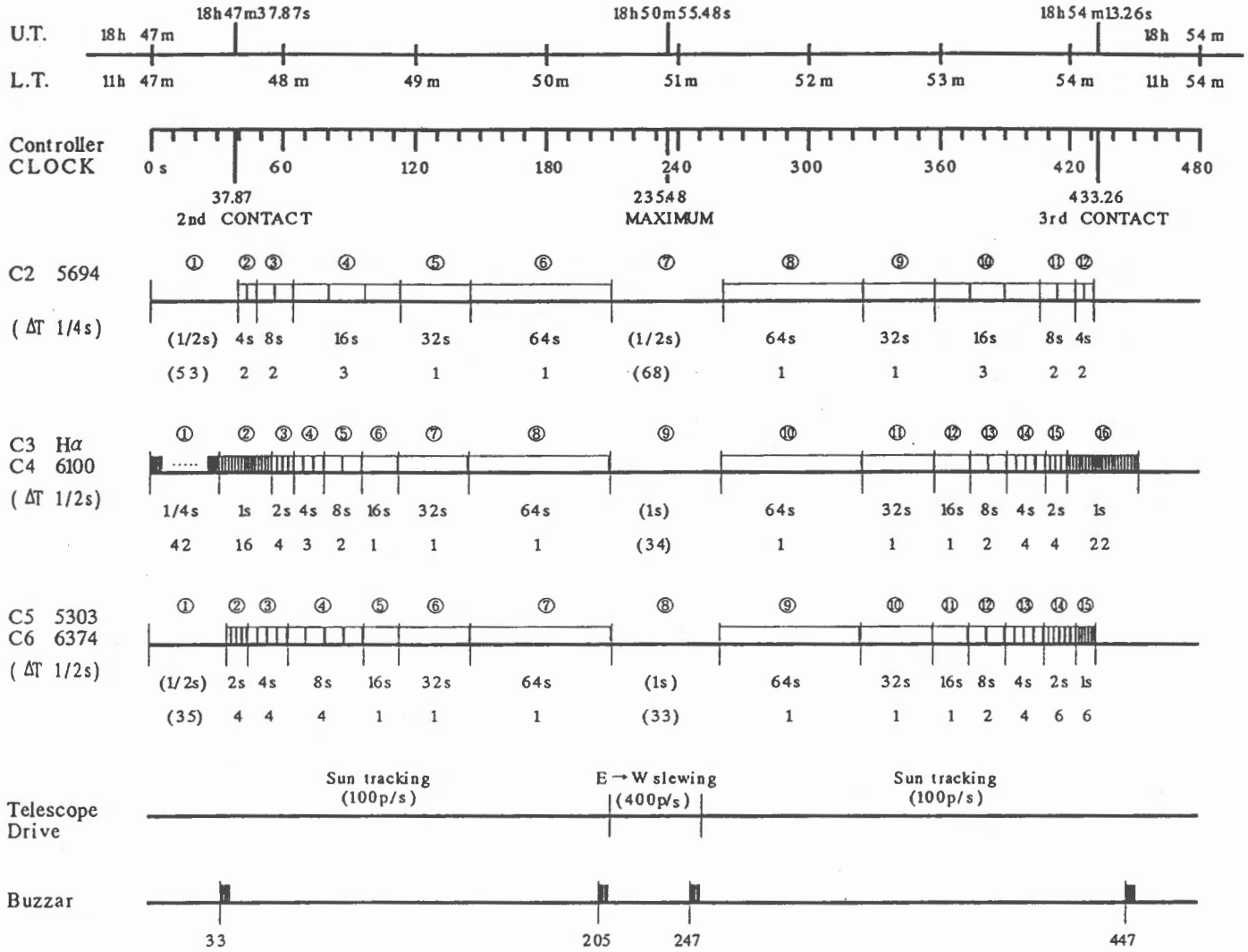

Fig. 6. Time-chart of the observational sequence programmed in the sequence controller.

advance a frame of film (ΔT) was 1/4sec for the first control sequence, while 1/2sec for the others. Layout of exposure times and number of frames taken are given in Figure 7, where parentheses indicate dummy exposures. Circled numbers show step numbers in each sequence. Buzzars were also controlled by the sequence controller and used for signaling changes of the observational stages to the observers.

On the other hand, the video-recording systems need some manual operations in the observation. We, three persons, were in charge of operation of three video cameras during the observation. The video cameras needed adjustment of gains and high voltages for getting images in good contrast. This adjustment were done in two steps at the early stages of the observation. Before the adjustment, a cover-plate and a ND filter (Transmittance $\approx 10^{-6}$) were inserted in front of the focal plane of each camera head for protection purpose. First adjustment was done when the Sun was eclipsed deeply. We took out cover plates, and increased and roughly adjusted high voltages of the cameras, assuming that the brightness of the partially-eclipsed Sun was equal to or less than 10^6 times the coronal brightness. Second adjustment was a fine tuning of the voltage for the best contrast, and was done just after the second contact, removing ND filters and monitoring the video images of the real corona . After finishing adjustment, we started to scan the corona along the limb by manually moving video cameras on X-Y slide mounts. Finally just at the end of the totality, we put cover plates again in front of the camera heads for protection from too bright light. In the observation, three video monitors were used inside the observing tent for the adjustment of the camera gains, and the other three were located near the telescope outside the tent for monitoring the spatial scanning.

The outline of the observational procedure for the eclipse day is summarized in order of time as follows.

(0) Checking all the cable connections and loading films to photographic cameras were finished by 30 min before the totality. Power supplies to the devices were started.
(1) After putting a light-reducing cap on the top of each refractor, we pointed the telescope to the Sun at the east limb (second contact point) and kept it tracking the east limb.
(2) We started our pen-recorder which ran automatically, recording clock pulses and shutter timings of five photographic cameras.
(3) Around 15 min before the totality, we removed light-reducing caps of the four refractors.
(4) Three video recorders were started manually one after another, not to overload DC-AC inverters.
(5) We roughly adjusted gains and high voltages of three video cameras with reduced light of partially eclipsed Sun.
(6) At the pre-determined start time, we put on the start-button of the sequence controller.
(7) Just after the second contact, we finely adjusted gains and high voltage of three video cameras.
(8) After the adjustment of video gains, we scanned the east limb corona by manually moving video cameras on the X-Y slide mounts.

(9) Around the mid-point of totality, the telescope was drived in high speed to point at the west limb (third contact point), by the sequence controller.
(10) We continued scanning of video cameras along the west limb.
(11) Just after the third contact, we put in cover plate protecting video camera heads.
(12) After the automatic stop of the controller, we put on light-reducing caps on four refractors.
(13) Stopping all video devices, and the pen-recorder, we finished main part of the observation.

Although we were, regrettabley, about 14.5sec late in putting on the start-button of the sequence controller, all the photographic devices and video devices worked compleletely well. Concerning the photographic observation, we succeeded in getting 18 frames of λ5694 images, 105 frames of Hα images, 105 frames of λ6100 continuum images, 36 frames of λ5303 images, and 36 frames of λ6374 images. Video images were also successfully recorded in good contrast, showing fine structures of coronal loops.

After the end of totality, we photographed monochromatic images of the partially eclipsed Sun, reducing the brightness by ND filters and aperture stops, in various exposure times. This supplementary works were done to get data for absolute calibrations of the photographic observation. Details are summarized in Table 4.

Table 4.

Wavelength	Diameters of Aperture Stop	ND filter	Exposure time
5303	5cm	1% + 10%	1/8, 1/15 sec
5694	5cm	1% + 10%	1/15, 1/30 sec
6100	5cm	1% + 10% + 10%	1/4, 1/8, 1/15 sec
6374	5cm	1% + 10%	1/4, 1/8 sec
Hα	5cm	No filters	1/125, 1/250, 1/500 sec

Supplementary works were performed when we returned back to Japan. To derive characteristic curves of Density-Intensity relations of photographic films, we photographed intensities of light beams from a standard white-light lamp, attenuated through a seven-step wedge filter, on films, cut out from the same rolls used in the observation. We used narrow band filters, FWHMs of them were around 50nm, to select out wavelengths of observation. Adjusting additive ND filters and supplied current strength to the lamp, we took photographs in the same exposure times as the eclipse observation. Development of the photographic films, obtained in the observation, were also performed at Hida observatory, in Japan. We simultaneously processed the films of the observation and the wedge films,

manually with small processing tanks. Data of development are given in Table 5.

Table 5.

Wavelength	Developper	Temperature	Develop time	Fixer
5303	T-MAX	24°C	8 min	Fuji Superfix 10 min
5694	T-MAX	24°C	8 min	Fuji Superfix 10 min
6100	D-19	20°C	8 min	Fuji Superfix 5 min
6374	T-MAX	24°C	8 min	Fuji Superfix 10 min
Hα	D-19 1:2 dilution	18°C	4 min	Fuji Superfix 5 min

4. Preliminary Results

The image quality of the obtained material is satisfactory both on the films and on the video recorders. They show many fine structures in the inner corona. Some examples of them are demonstrated in Figures 11 through 23. In the following we examine the characterstic features of the monochromatic images of five different wavelengths obtained with the eight cameras.

(I) Photographic Films

(a) FeX 6374 images

Figure 11 is a composites of two pictures taken with the 6374Å filter at different times; the upper half of Figure 11 shows the 6374 corona above the east limb taken at 12 s after the second contact, and the lower half, above the west limb at 4 s before the third contact. The central parts of the both limbs are enlarged in Figure 12. Notice various types of fine loops and streamers above the both limbs. Such coronal fine structures have never been obtained before. They are much slender than those of any other 10^6 K-corona published before. The diameter of the slenderest 6374 loop in Figure 12 is found to be about 2 seconds of arc according to a preliminary measurement.

Another composite picture of 6374 is given in Figure 13. Due to the longer exposure time (16 s), It shows fainter 6374 structures extending to the higher corona than in Figure 11. Notice many slender 6374 streamers extending radially in Figure 13 by comparing them with 5303 and 5694 images in Figures 14 and 16.

(b) FeXIV 5303 images

The monochromatic images of 5303 corona are given in Figures 14 and 15 which were taken at the same times as those of Figures 11 and 13, respectively. Figure 14 shows many fine structures at the innermost corona. Some 5303 loop structures are found at the same

locations as the 6374 loops, but most of 5303 fine structures seem to be different in shape from the 6374 fine strucrures. Notice also the different appearance between 6374 (Figure 13) and 5303 (Figure 15) images in the higher corona. The detailed study of the spatial relationships between 5303 and 6374 fine structures is in progress by the microdensitometer-tracing of the original negatives.

(c) CaXV 5694 images

This is the first observation which tried to get a monochromatic image of CaXV 5694 corona by using the interference filter. The result is shown in FIgure 16. The general appearance of Figure 16 is very differnt from the 6374 and 5303 images, but similar to the continuum images shown in Figures 17 and 18. This means that the 5694 pictures include a large amount of the continuum intensity which is transmitted through the 3Å passband of the 5694 filter. We must carefuly subtract the continuum intensity before studying the real structures of CaXV line emission.

(d) 6100 continuum images

Figure 17 shows five frames of 6100Å continuum corona of the east limb taken with different exposure times. We can study the intensity distribution of 6100 continuum from the lowest to higher parts of the inner corona by using these pictures. Four frames of Figure 18 also shows the intensity distribution of 6100 continuum corona of the west limb. Notice the bright and sharp images of the prominences seen at the middle part of each limb.

(e) Hα images

Since our primary purpose for Hα images was to observe the faint structures of Hα emission in the corona, the main bodies of the prominences are overexposed , especially for the bright prominence of the west limb. Some frames of 0.25 s and 1 s exposure, however, show very beautiful fine structures of the prominence at the east limb. Notice the fine loops and knots at the faintest parts of the enlarged image of the prominence in Figure 19. The smallest diameter of the loops and knots is found to be less than one second of arc. Such a picture of high spatial-resolution has never been reported at any other total eclipses.

(f) Comparison among five different wavelengths

The five monochromatic images of different wavelengths are aligned and compared in Figures 20 and 21 for the east and the west limbs, respectively. Preliminary results of the comparson are summarized below.

(1) The general appearances of fine structures are very different among the three coronal emission lines, *i.e.*, FeX 6374, FeXIV 5303, and CaXV 5694. The 6374 corona consists of many slender loops and streamers. The 5303 corona also consists of many loops and arch structures, but they are more diffuse than those of the 6374 corona. The 5694 images are much more diffuse and only show fine structures of the prominences and several dffuse coronal streamers and arches.

(2) There seems to be no clear correspondence between most of 6374 and 5303 fine structures, though some loops are located very close to each other. For examples, no clear 5303 loops can be found for the 6374 loops at the location (A) in Figure 20. The 5303 arches do not have any counterparts of 6374 structures at the location (B) in Figure 21.

(3) It is not easy to compare the 6100 continuum images with the emission-line images because of the large difference in the photographic contrast. Kodak technical pan 2415 film used for the 6100 continuum has much higher contrast than Kodak TMAX film for the three emission-lines. By combining several images of different exposure times, however, we can identify some continuum structures with those of 5303 and 5694 structures. For example, the arch structure of 6100 continuum is found at the same location (B) as the 5303 and 5694 arches.

(4) The brightest parts of Hα prominence (C) in Figure 20 and (D) in Figure 21 are clearly identified in the 6100 and 5694 images. The similar appearance of the prominences in the 6100 and 5694 images suggests that most of 5694 intensity is contributed by the continuum transmitted through the 3Å passband of the 5694 filter.

(5) The intensity distributions along the prominences (C) and (D) are very different among the 6100, 6374 and 5303 images. These differences must be important in the study of the physical conditions of the corona surrounding the prominences.

(II) Video Images

The three video images of FeX 6374 line, FeXIV 5303 line and 6100 continuum were also obtained in fine quality. The fine structures of the 6374 image is especially impressive. They are found to be as slender as those obtained on the phtographic film (Figure 12). Here, we only present the iso-intensity colour-maps of some frames of 6374 and 5303 video images in Figures 22 and 23.

5. Summary

We observed the total solar eclipse of July 11, 1991 by using the Eight-Channels Monochromatic Telescope at UABCS, La Paz, Baja California Sur, Mexico. Many monochromatic images of the inner corona were successfully obtained in five wavelengths, *i.e.*, FeX 6374 Å, FeXV 5303 Å, CaXV 5694 Å, Hα, and 6100 Å continuum with the photographic films, and in 6374Å, 5303Å and 6100Å with the video-recording systems. They show various types of fine structures in the corona and the prominences. The 6374 strucutres are especially fine and slenderer than any other 10^6 K coronal loops which have ever been published.

The detailed comparisons between these monochromatic images of emission-lines and continuum are expected to give us some essental informations about the thermodynamic structures of the inner corona. The precise comparison between the 6374 and 5303 loops is especially important to examine the coronal-loop models. The detailed photometry and the image-processing of these data are in progress. The results of the analyses will be published in some separated papers.

Acknowledgement

We are grateful to COMES(Comite Mexicano Eclipse Solar) for arranging the observing site and helping the custom clearance of our equipment, especially to Dr. Joaquin Bohigas for his help at the custom office in Ensenada, and to Dr. Julieta Fierro for her providing useful informations. We also thank to UABCS for providing the observing site and other facilities, and to Ing. Manuel Oseguera and the staff members of CUPOE(Comite Universitario Para la Observacion del Eclipse) of UABCS, for their invaluable help and warm hospitalites.

We would like to express our hearty thanks to NHK Science and Technical Research Laboratories for providing HARP cameras, and especially to Mr. J. Yamazaki for his kind guidance to the HARP Tubes.

We are grateful to Mr. H. Tokumaru and Mr. A. Fukushima of Minolta Camera Company for examining the optimum arrangement of the telecentric lens-system with a dichroic prizm set in the 8-channels telescope.

We express our hearty gratitude to Professor M. Makita, Dr.Y. Nakai and the staff members of our Observatories for their support and encouragements throughout this project. We also thank the central offices of Kyoto University and the Faculty of Science, especialy the Budgetary and Accounting Section for their support in realizing this project.

We also thank to Dr. S. Saito for offering the ephemeris data and the records of his past eclipse expeditions.

References

Hanaoka, Y., Kurokawa, H., and Saito, S.: 1986, *Solar Phys.*,**105**, 133.

Hanaoka, Y., Kurokawa, H., and Saito, S.: 1988, *Publ. Astron. Soc. Japan*,**40**, 369.

Kanno, M., Tsubaki,T., and Kurokawa,H.: 1974, *Memoirs of Faculty of Sci. Kyoto Univ. Series of Phys., Astrophy., Geophys., Chemist.*, Vol.**34**, 281.

Kurokawa, H.: 1975, *Solar Phys.*,**43**, 385.

Saito S., Funakoshi Y., Suematsu Y. and Suratono : 1985 in E. Hiei (ed.) "Research on the Sun, Earth and Moon at the Total Solar Eclipse in Indonesia on 11 June 1983", pp 35-45

Saito, S., Kurokawa, H., and Ogimachi, Y.: 1981, in "Observation of Total Eclipse of 16 February 1980", ed. S.K. Trehan, Indian Academy of Sciences, p.31.

Suematsu, Y., Saito, S., Funakoshi, Y., and Kurokawa, H.: 1988, *Solar Phys.*,**116**, 285.

Yamazaki J., Tanioka K., and Shidara K. : 1991, "Development of the Super-HARP camera, a rival to the human eye, for the next generation of broadcasting", the 25th SMPTE television conference, pp100-108

Fig. 7. The construction of the concrete base for the telescope.

Fig. 8. (a) Assembling the telescope. (b) Adjusting the optical axis of the telescope.

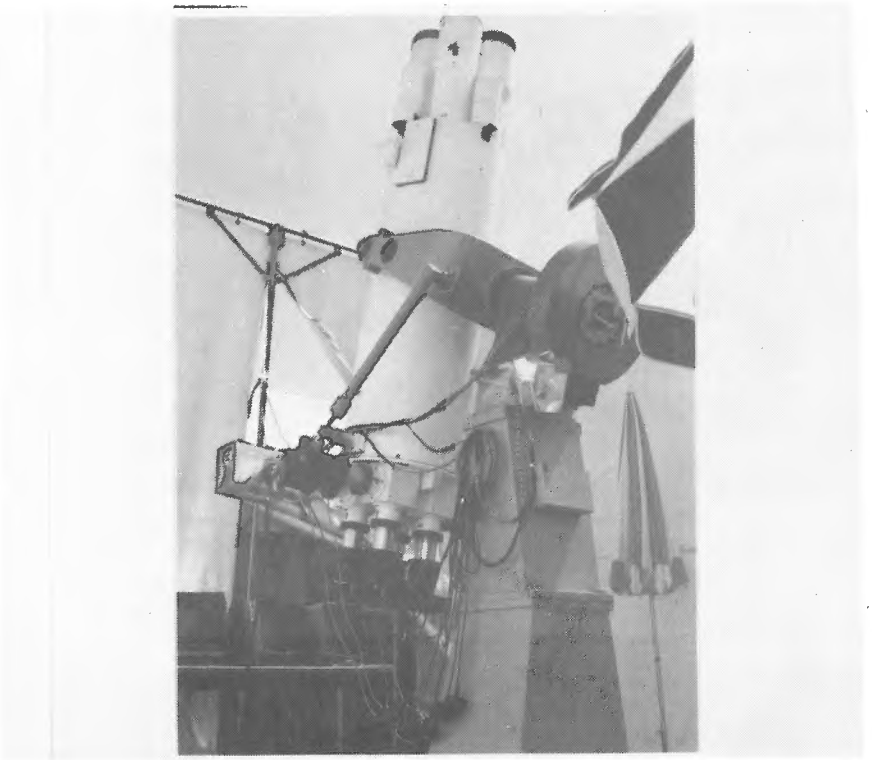

Fig. 9. The telescope fully equipped with eight cameras on the eclipse day.

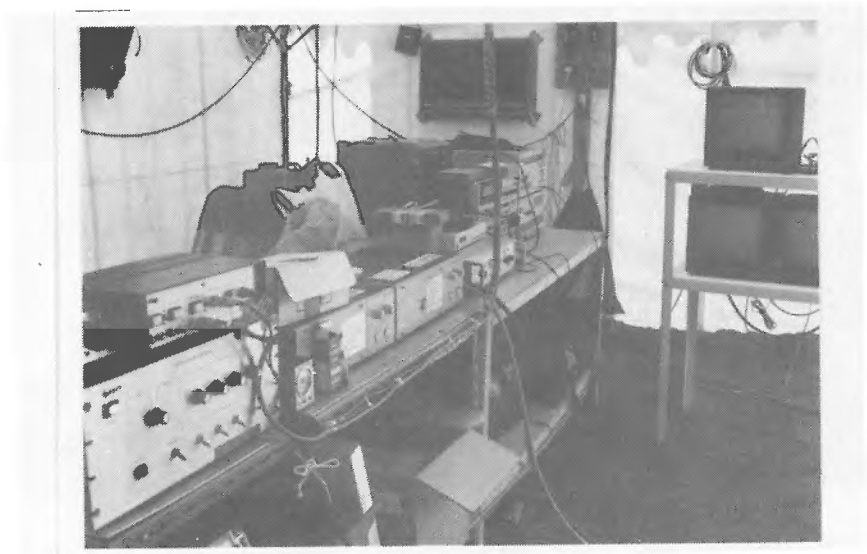

Fig. 10. The observing instruments set-up in the tent on the eclipse day.

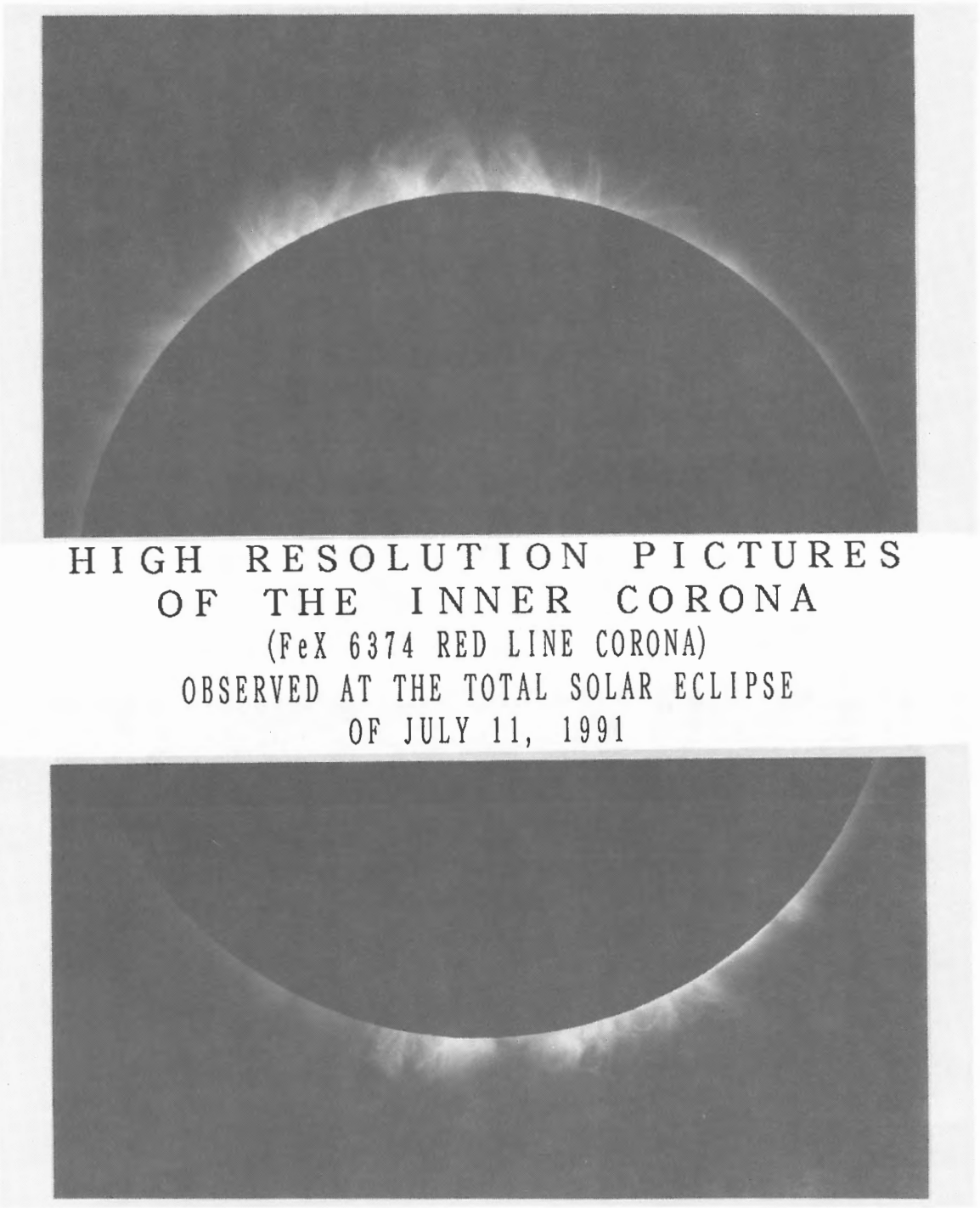

Fig. 11. Composite picture of FeX 6374 corona. the upper half shows the east limb, and, the lower, the west limb.

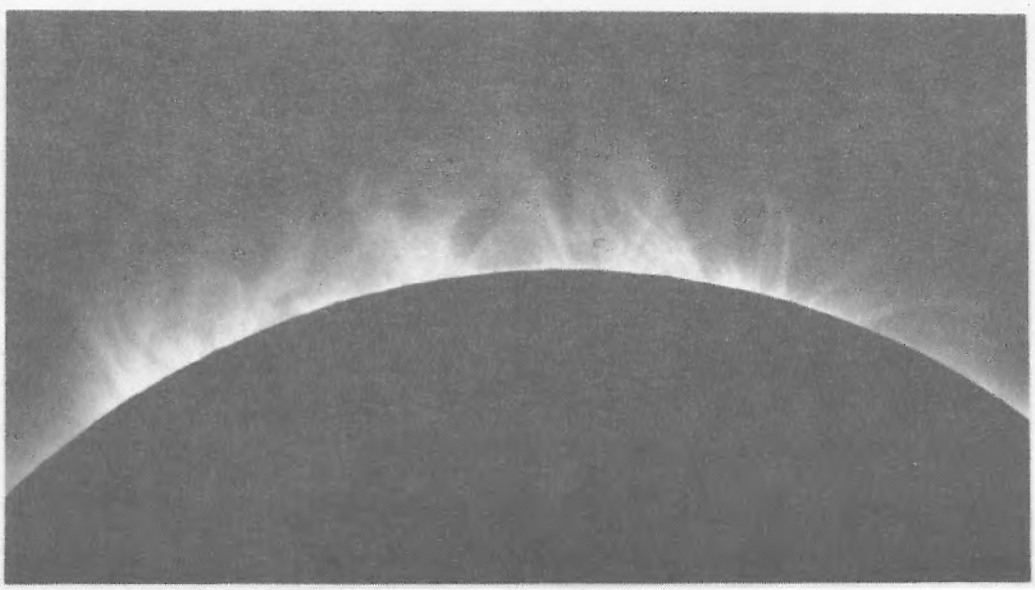

内部コロナの微細構造

（ＦｅＸ６３７４輝線 による単色像）

1991年 7月 11日 皆既日食

メキシコ国ラパス市にて、京都大学理学部附属天文台観測隊撮影

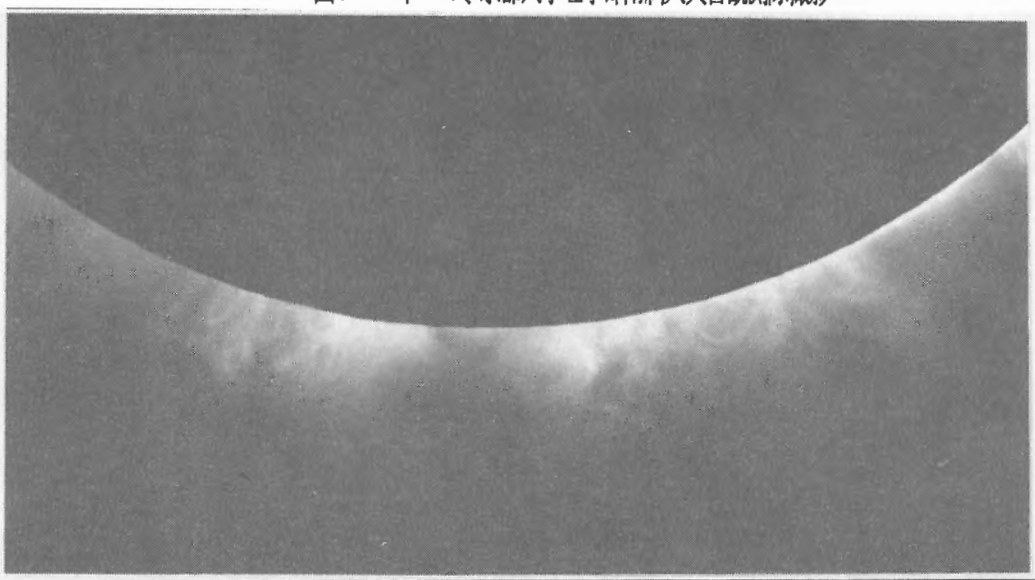

Fig. 12. Enlarged pictures of the central parts of Figure 12. Notice many slender loops

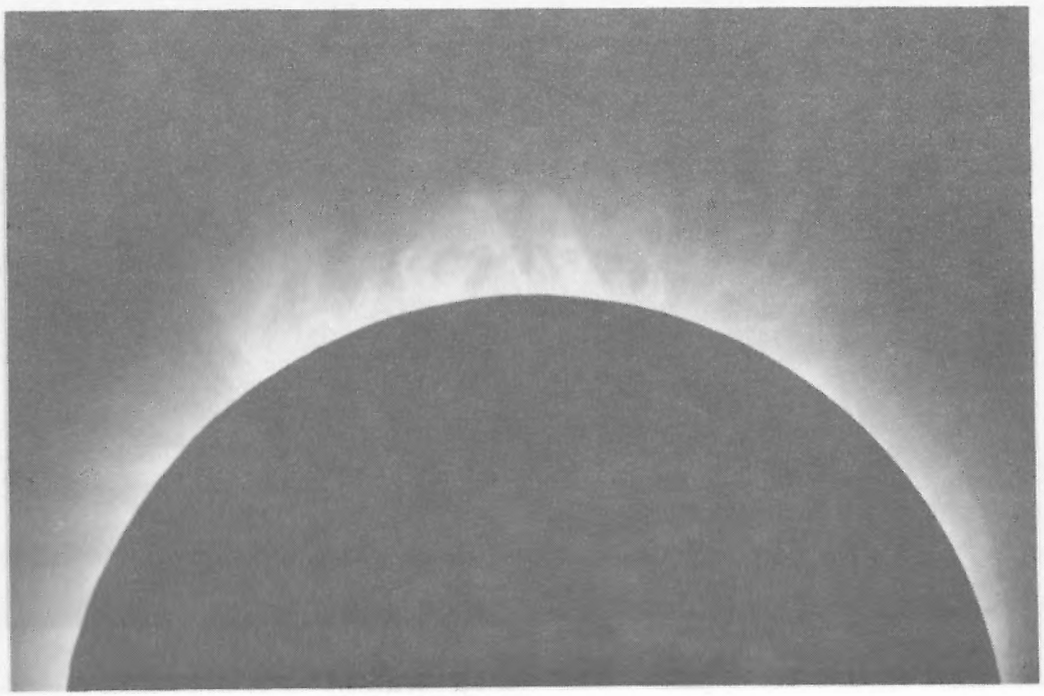

内部コロナの微細構造

（ＦｅＸ６３７４輝線 による単色像）

1991年 7月 11日 皆既日食

メキシコ国ラパス市にて、京都大学理学部附属天文台観測隊撮影

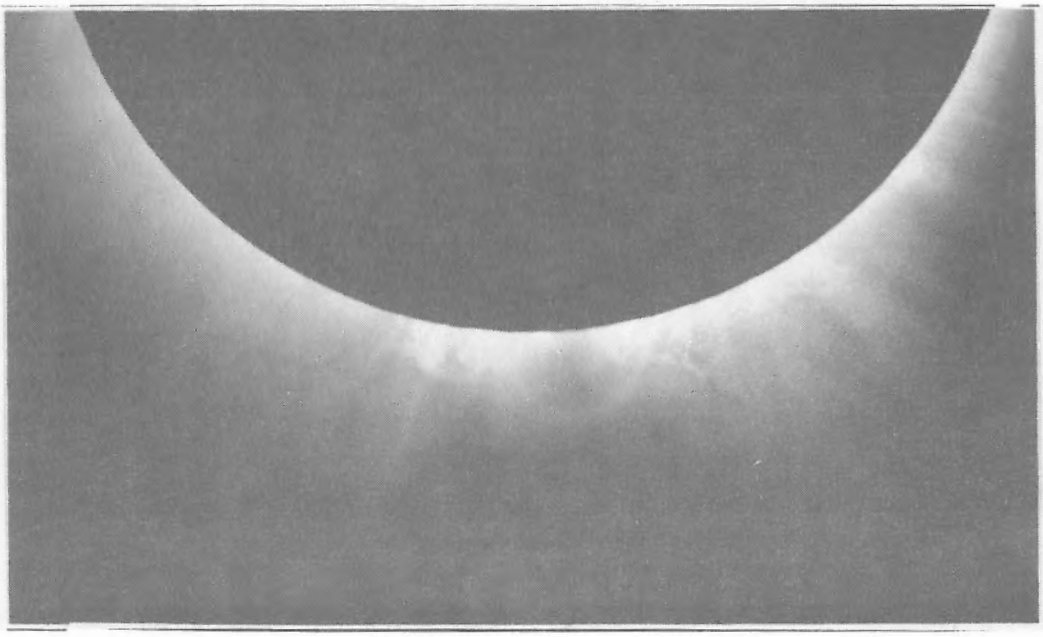

Fig. 13. FeX 6374 images with a longer exposure time. Notice many fine streamers.

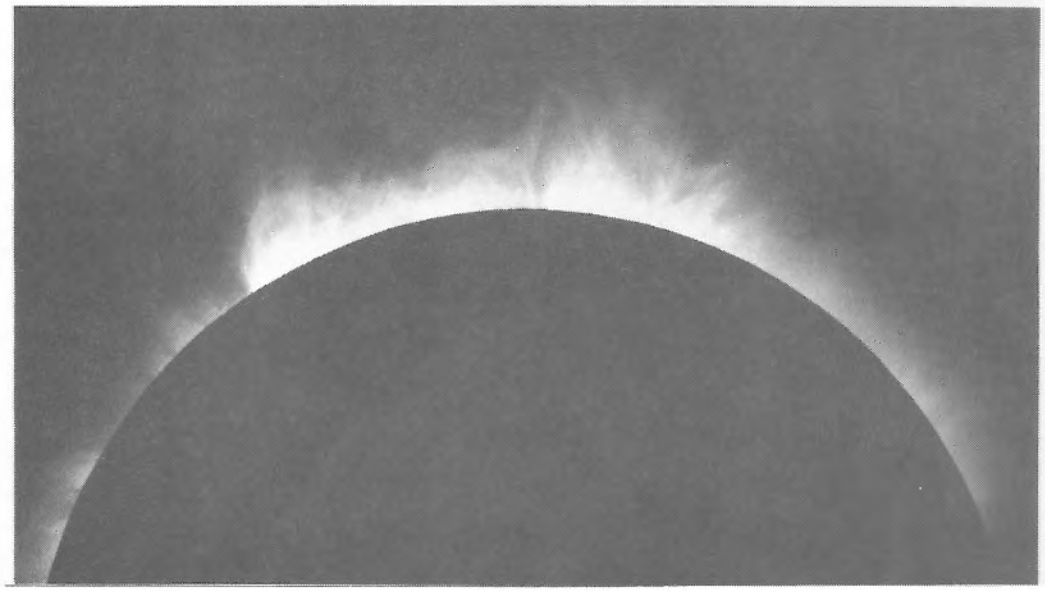

内部コロナの微細構造
（ＦｅＸＩＶ５３０３輝線 による単色像）

1991年 7月 11日 皆既日食
メキシコ国ラパス市にて、京都大学理学部附属天文台観測隊撮影

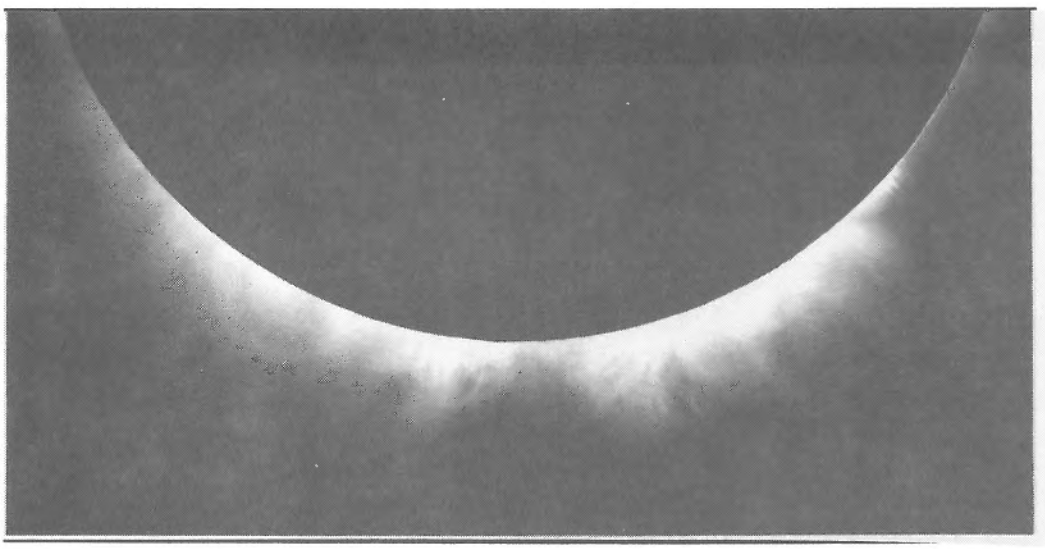

Fig. 14. Composite picture of FeXIV 5303 corona with short exposure time. upper: the east,and the lower: the west.

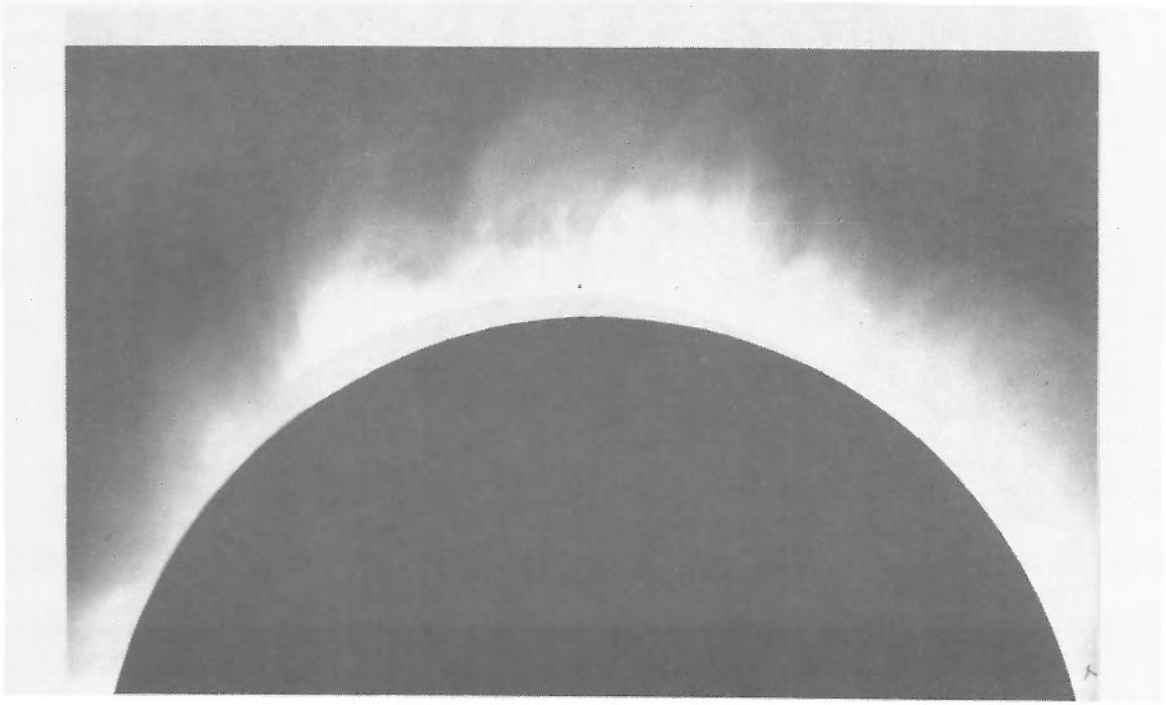

内部コロナの微細構造
（ＦｅＸＩＶ５３０３輝線 による単色像）

１９９１年 ７月 １１日 皆既日食
メキシコ国ラパス市にて、京都大学理学部附属天文台観測隊撮影

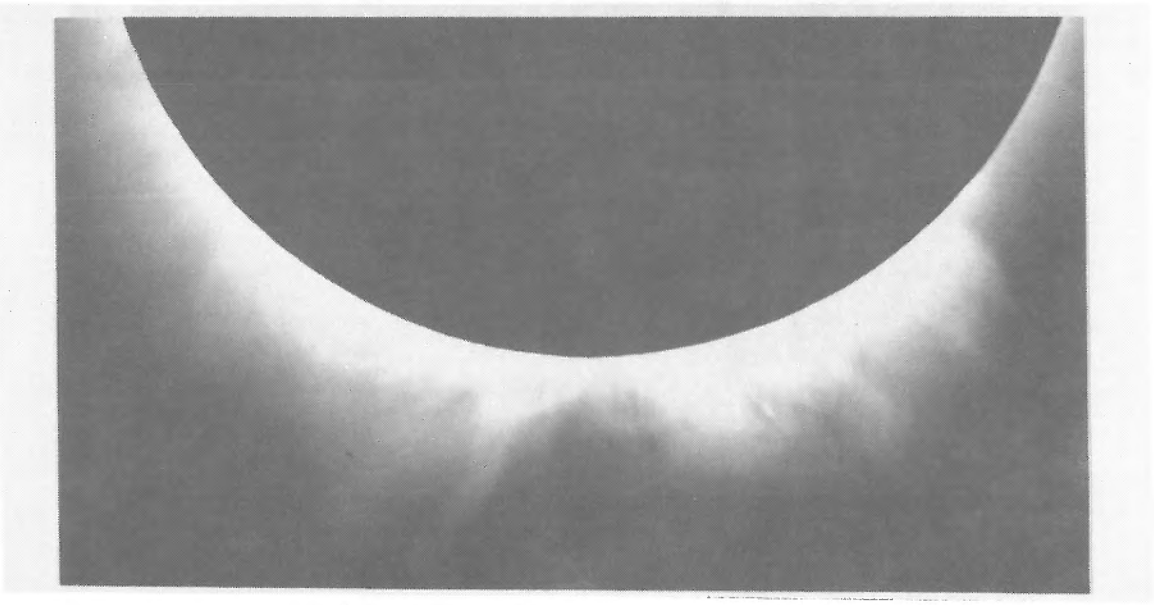

Fig. 15. Same as Figure 15 but with a longer exposure time.

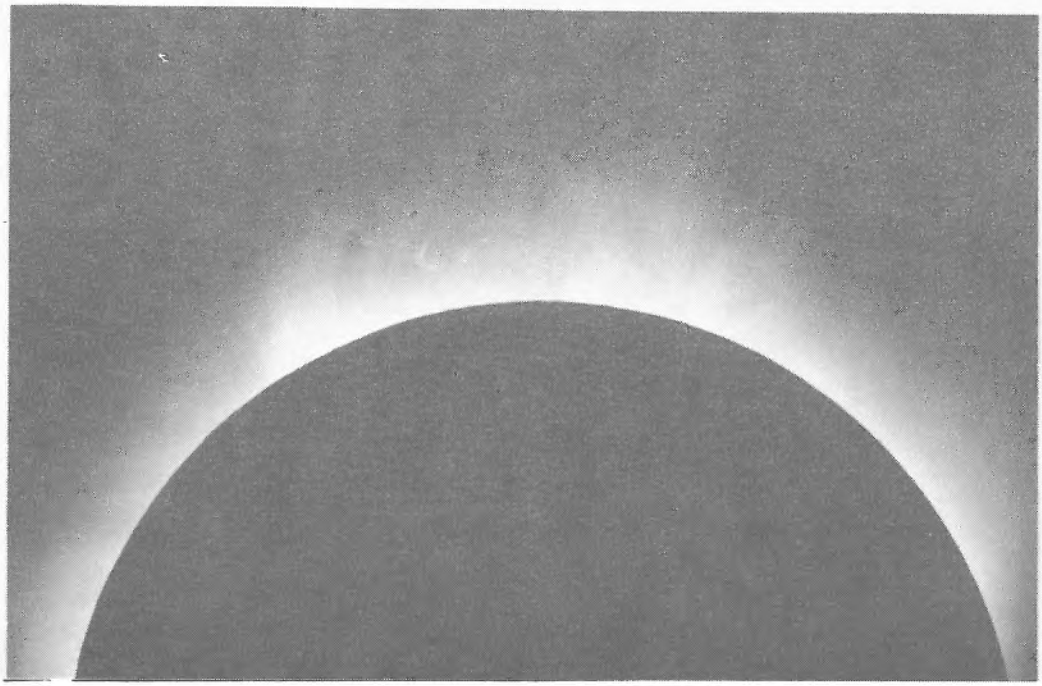

内部コロナの微細構造

（ＣａＸＶ５６９４輝線 による単色像）

1991年 7月 11日 皆既日食

メキシコ国ラパス市にて、京都大学理学部附属天文台観測隊撮影

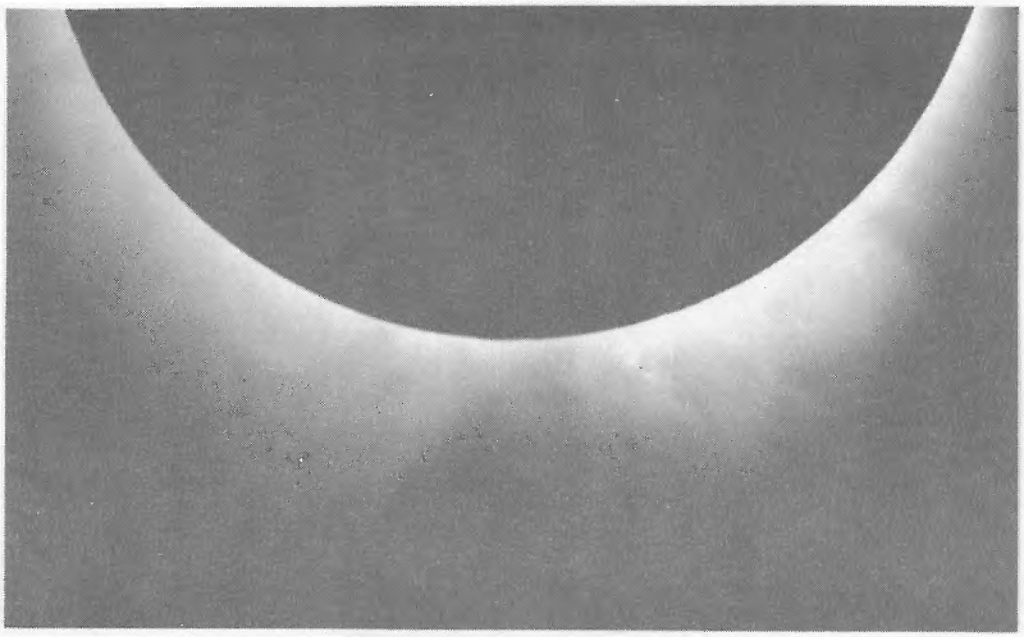

Fig. 16. CaXV 5694Åimages.

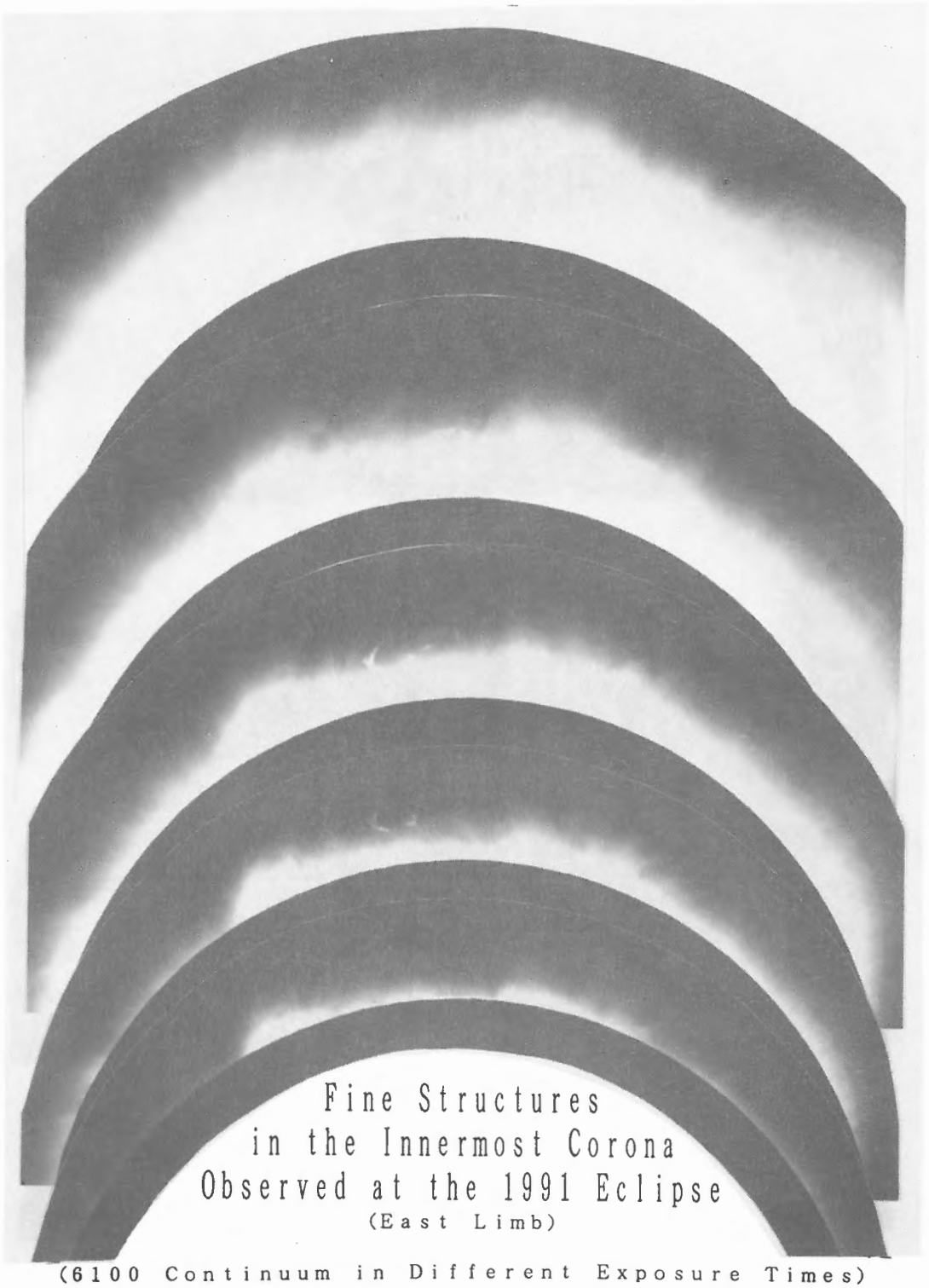

Fig. 17. The 6100Åcontinuum images of the east limb with different exposure times.

Fig. 18. Same as Fig. 18 but for the west limb.

Fine Structures in the Faintest Parts of the Prominence Observed at the 1991 Eclipse

Fig. 19. Enlarged pictures of the Hα prominence on the east limb.

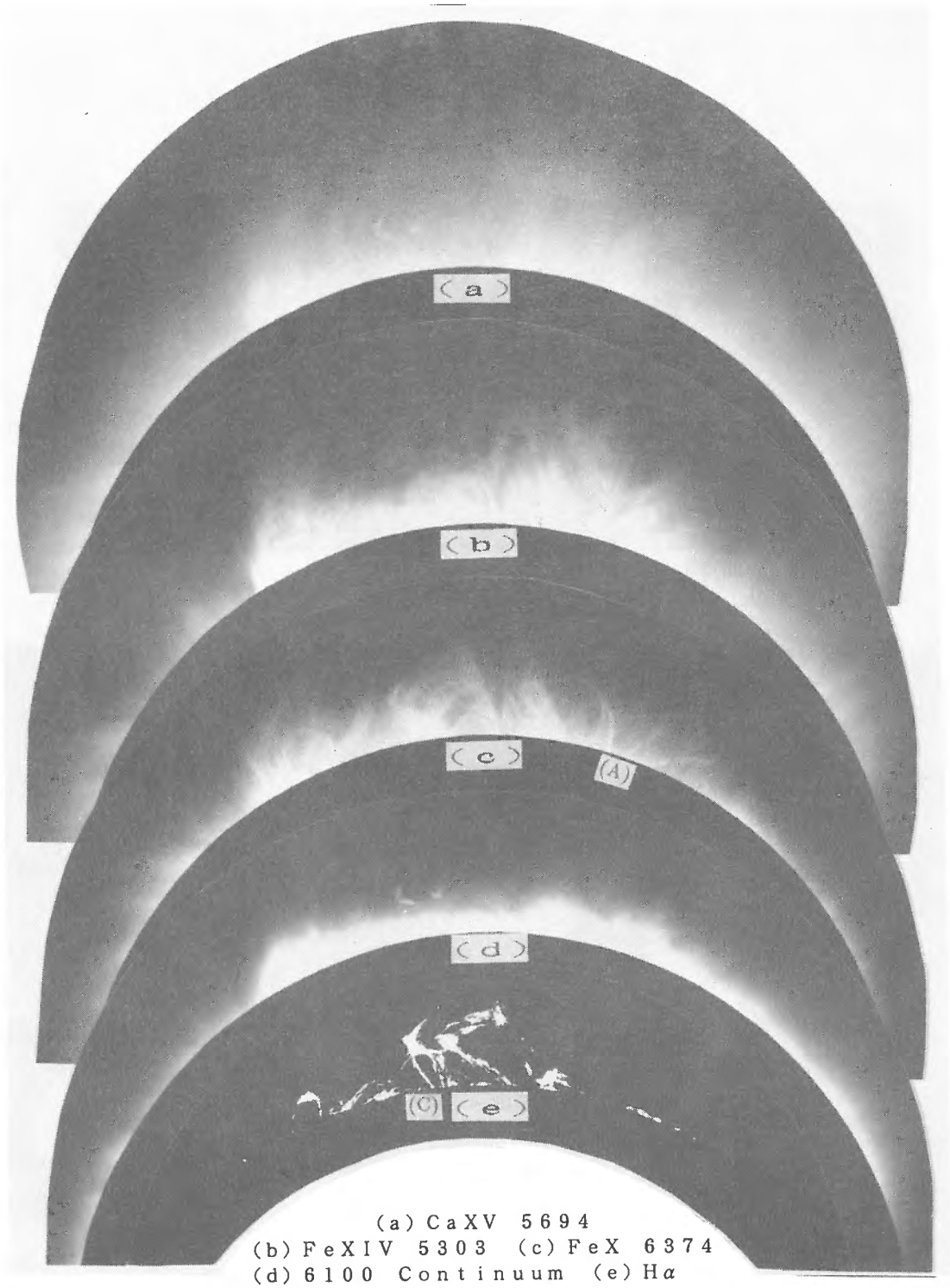

Fig. 20. Comparison among five monochromatic images of different wavelengths for the east limb.

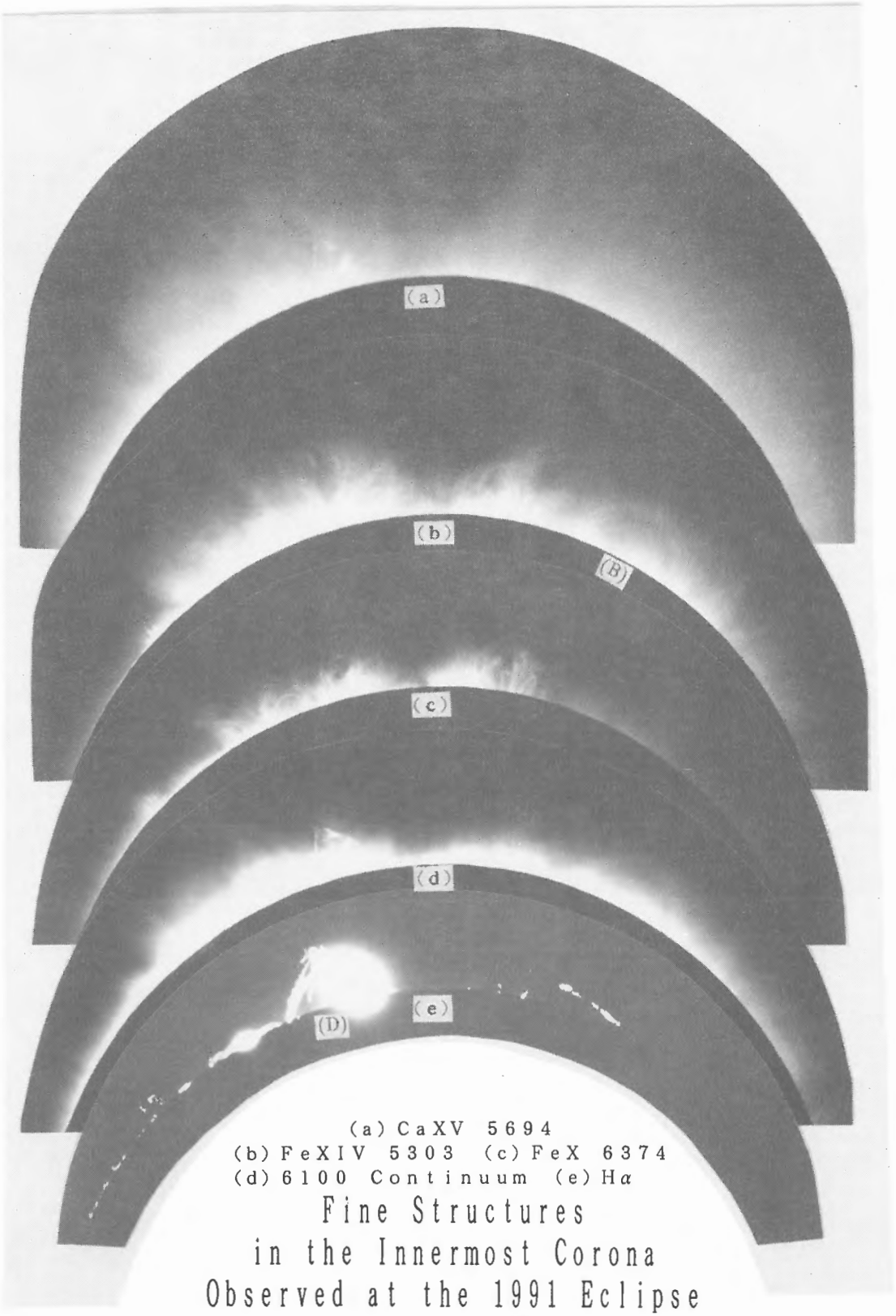

Fig. 21. Same as Figure 20 but for the west limb.

1991年皆既日食観測
ポポカテペトル山のFコロナ観測

磯部琇三（国立天文台）
野口本和（国立天文台）
田辺俊彦（東大・理学部）

Abstruct

Polarization observation of the solar F-corona has been carried out at the total solar eclipse on July 11, 1991, at volcanic ridge of Mt. Popocatepetl (5452m). Although it was clear one hour before the 2nd contact, a slight cirrus ran over the sun. Because of this difficult condition, we had to make some assumptions to obtain maps of two dimensional polarization distribution, which give high polarization regions co-incident with coronal streamers.

1. はじめに

1991年 7月11日の皆既日食の時、Fコロナの観測を行った。Fコロナの赤外観測は多くのグループによって行われていて、４R⊙（R⊙は太陽半径）の所に、赤外強度の強い部分の存在が示されている。可視光での観測を1983年 6月11日にインドネシアでの皆既日食の折に磯部達（1987）が気球を使って行った。４波長（5325A、5965A，7200A，8015A）のデータのうち、３波長のデータは指向性が悪かったために8000Aの一波長分の偏高度分布図しか描けなかった。しかし、この図では４R⊙の所に偏光度の大きい部分が検出されたけれども、偏光の波長分布が得られなく、この超過偏光度が星間塵によるものかどうか決定できなかった。そのため、今回の観測が行われた。

2. 観測

４R⊙近傍のコロナの明るさは、皆既日食では背景光に近い。そのため、背景光を減らすために高高度で観測する必要がある。インドネシアの場合気球を使って28kmの高度からの観測を行った。これが可能になったのは、インドネシア側に気球チームがあったためである。メキシコの場合、それに対応する気球チームがなかったので、日食帯で地上のもっとも高いところ、ポポカテペトル山頂で行うことにした。気球観測と異なり、観測機器を手元において観測できる長所はあったが、大気圧が40％の所で機器を運び、観測者が正常に作業できるまでに順応するのに、３週間近くの日数を要した。

テスト段階では天候に恵まれなかったが、山頂滞在の二晩には晴れたので、間際ではあったが各種の調整をすますことができた。当日は朝から快晴で、皆既外のスカイのデータも順調に得られた。しかし、皆既 1時間前頃から薄いシラスが出始め、皆既中にはコロナの明るさが変動していた。

6分あまりの皆既時間中、後半3分間はシラスの濃さが激しく変動してデータとはならなかった。最初の 1分間はNDフィルターの調整に費やされ、一応使えるデータは 2分のみであった。

3. 結果

望遠鏡の焦点に置かれたCCDカメラで得られた信号がH・VHSビデオレコーダーに記録されている。偏光板は30度毎異なった位置に固定され 2秒間ずつ観測される。16位置 32秒で一回転で、4セットのデータが得られる。四連望遠鏡のそれぞれが消長の異なったものになっている。

解析は各 2秒間のうち、25フレーム分だけ、フレームメモリーで加算して数値化された。快晴中のスカイ画像はゼロ偏光であった。第 0次のデータでは偏光度分布がシステマティックになっていた。そこで、周辺部７R⊙より外側では偏光度がゼロと仮定して計算しなおして求めたのが、図１－３である。残念ながら6000A

のデータは信号レベルが低すぎてまだ十分偏光度分布図が得られていない。

図４は、コロナ写真から描いたコロナの明るさの分布図である。コロナル・ストリーマーのある方向で、図１－３の偏光度が高くなっている。つまり、この部分は、Ｋコロナに相当する電子の散乱によって偏光が高くなっている。幸い、このストリーマーは黄道面から離れた方向にある。我々の求めているＦコロナ成分が本当にあるかどうかは現在までの整約の段階では明らかではない。

今後も整約を進める予定であるが、現在の段階で言えるのは４Ｒ⊙よりはるかに広がったＫコロナ成分の二次元偏光度図を求めた事である。

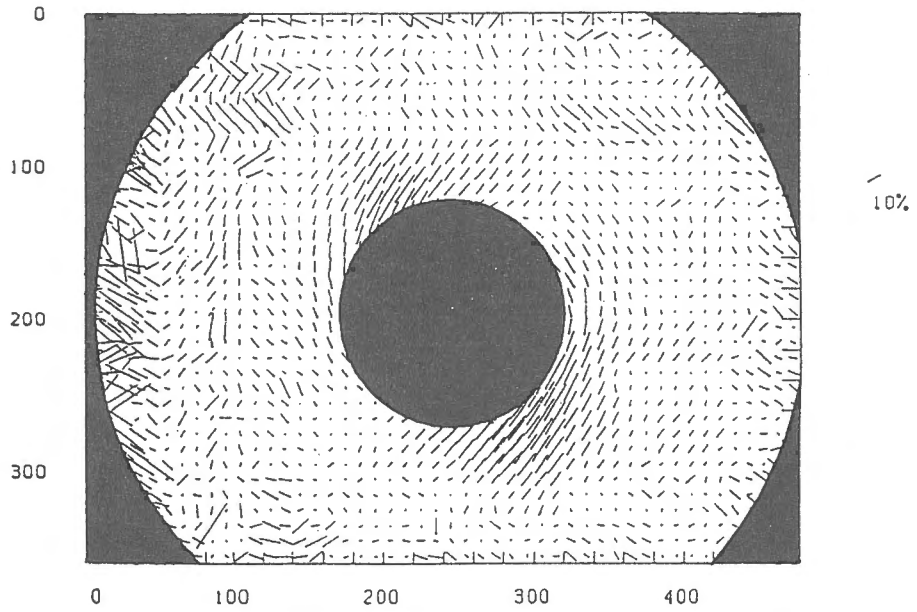

図１．　波長5325Ａにおける日食時の太陽周辺の偏光度分布。
中央の黒丸は太陽半径の3.0倍に相当する。

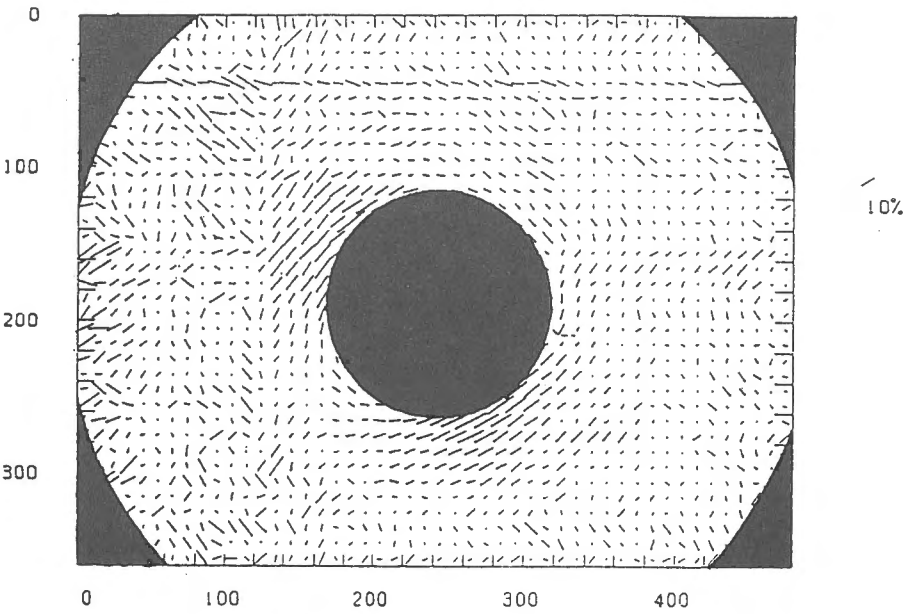

図２．　波長7200Ａにおけるもので他は図１と同じ。

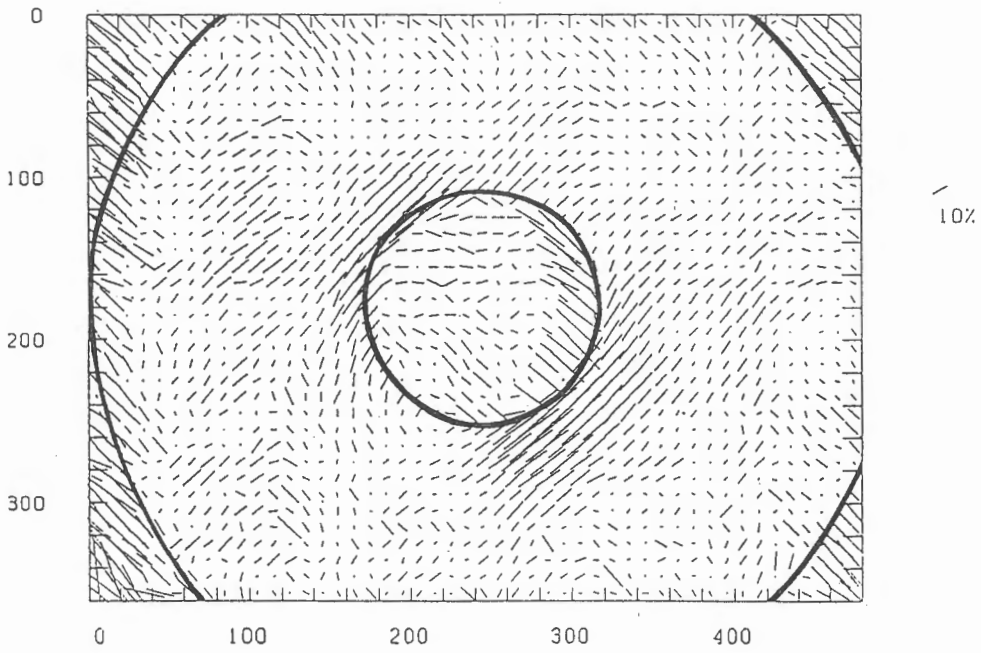

図３．　波長5015Ａにおけるもので他は図１と同じ。

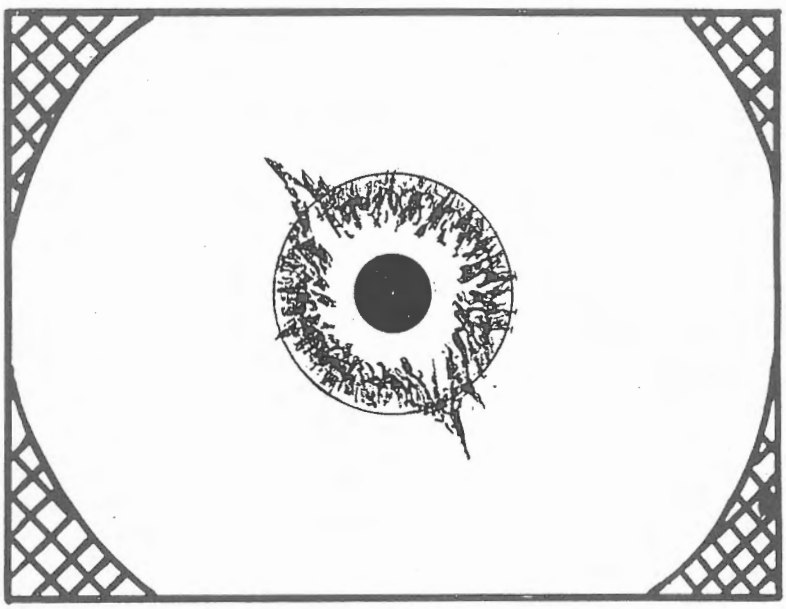

図４．　偏光観測時のコロナの写真のスケッチ。

ポポカテペトル山（Mt. Popocatepetl）
日食観測登山風景

４５００ｍを越えると雪が深くなる
一歩一歩と慎重に歩かなければならない

メデカル・センターで心機能のチェックを受ける野口隊員

日食当日の器機最終調整風景
四連望遠鏡からの信号がモニターＴＶに表示されている

５２５０ｍの観測地点での記念写真
雪の降る中で準備作業を行う

観測に成功し４０００ｍトラマカスに下山後、
補助隊全員と記念撮影

メキシコ日食における接触時刻観測

水路部　小山 薫・奥村 雅之

CONTACT TIME OBSERVATION IN THE 1991 MEXICO SOLAR ECLIPSE

By
Kaoru Koyama and Masayuki Okumura
Hydrographic Department

Abstract

In the total solar eclipse of Jun 11,1991, observation of contact times was made at La Paz in B.C.S., Mexico.

The observation was made by the spectrophotometric method;the spectrograph was composed of an objective prism of a direct vision type, a telescope(f=1200mm, ϕ =80mm), and a 16mm-movie camera.

Registrations were made at a rate of 18 shots per second.

The time signals of 0.1, 1, 10, 60sec were generated by a crystal oscillator and time marks printed on the edge of the film.

The clock rate of crystal oscillator was compared with the Loran-C standard time signals synchronized UTC.

The development of the films was made by a private laboratory in Tokyo and good images of the flash spectra were obtained.

●概　要

水路部は、天体暦の検定を目的とした日食観測を実施した。

具体的には、皆既日食の接触時刻を精密に測定し、太陽と月の相対位置を０．０１″の精度で決めることを目的に観測を行った。

●接触観測（第２、３接触）

接触時前後に月の谷からもれて来る太陽光（ベイリービーズ）をプリズムでスペクトル分散させ、それを１６ｍフイルムに連続撮影することにより、弧の消長を記録する。

望遠鏡は、口径８ｃｍ、焦点距離１２００ｍｍで対物レンズの前に６ｃｍ四方の直視プリズムを取り付けてある。

彩層からの輝線スペクトルと太陽光連続スペクトルと分離するため分散方向は太陽弧と直角にして撮影する。そのため、接触位置によって分散方向を容易に変えることが出来るように鏡筒自体が任意角回転出来る構造になっている。

撮影は、直焦点で１８コマ／秒、タイムマークは水晶時計からの０．１秒毎信号をＬＥＤ発光ダイオードにより直接フイルム上に焼き付けた。

●時　計

観測に使用する水晶時計（ＣⅡ）は、２０～１００ｍｓ／ｄａｙでかつ温度係数も大きいので、常に正確なＵＴＣで検定を行う必要がある。

今までは、ＵＴＣに基づいて短波で放送されている報時信号で検定していたが今回は、ロランＣ電波を利用した位置時刻測定装置（Ｃ１）で検定した。

使用局は、米西岸チェーン９９４０マスター局（４２°４３´Ｎ，１１８°５０´Ｗ、距離１８９１．３ｋｍ、６．３１５ｍｓ）でＵＴＣとの比較精度は±０．５μｓであった。

皆既日食前後の時計比較結果

１８時１５分　Ｃ１－ＣⅡ＝－３６．９ｍｓ

１９時００分　Ｃ１－ＣⅡ＝－３８．１ｍｓ

この間のＣ１とＵＴＣとの比較は、Ｃ１－ＵＴＣ＝０．３５１ｍｓと一定であった。

よってＣⅡのＵＴＣへの補正量は、
１８時１５分　ＣⅡ－ＵＴＣ＝３７ｍｓ
１９時００分　ＣⅡ－ＵＴＣ＝３８ｍｓ
となり１ｍｓの精度で観測時計ＣⅡを検定出来ていた。

●観測位置
世界測地系（ＷＧＳ－８４）で運用されている米海軍航行衛星（ＮＮＳＳ）からの電波を受信し観測点の測地経緯度を決めた。
それによるとＮＮＳＳ受信アンテナ位置は、
２４° ０６′０２．″０７Ｎ
１１０° １８′５１．″１２Ｗ
ＨＴ＝－０．１５ｍ
衛星受信パス数は、３Ｄ計算パス＝３３７パス　標準偏差　０．４ｍ，０．３ｍ，０．９ｍであった。
測量によって観測望遠鏡の位置は、
２４° ０６′０２．″２５Ｎ
１１０° １８′５０．″８２Ｗ
ＨＴ＝－０．２６ｍ
参考までに京都大学の４連型望遠鏡の位置は、
２４° ０６′０１．″６９Ｎ
１１０° １８′５１．″３９Ｗ
ＨＴ＝　０．５３ｍ　であった。
星の定高度法による天文経緯度観測も実施し、測地経緯度との差（鉛直線偏差）を求めた。
結果は、
$\xi = \phi_a - \phi_g$　　＝　５．３″
$\eta = (\lambda_a - \lambda_g)\ \cos\phi = -7.5''$
●観測データの整約
接触時のスペクトル撮影は第２、３接触共成功し、現像したところフイルム中心に濃淡の縞として光球の連続光がシャープに写し込まれていた。
これらの濃度測定は、現在東京大学天文学教育研究センターの協力を得ながら作業を進めている段階である。
最終的には太陽と月の相対位置の決定精度は、０．″０１になる観測データが得られたと思われる。

閃光分光器、16mm撮影機、観測用水晶時計

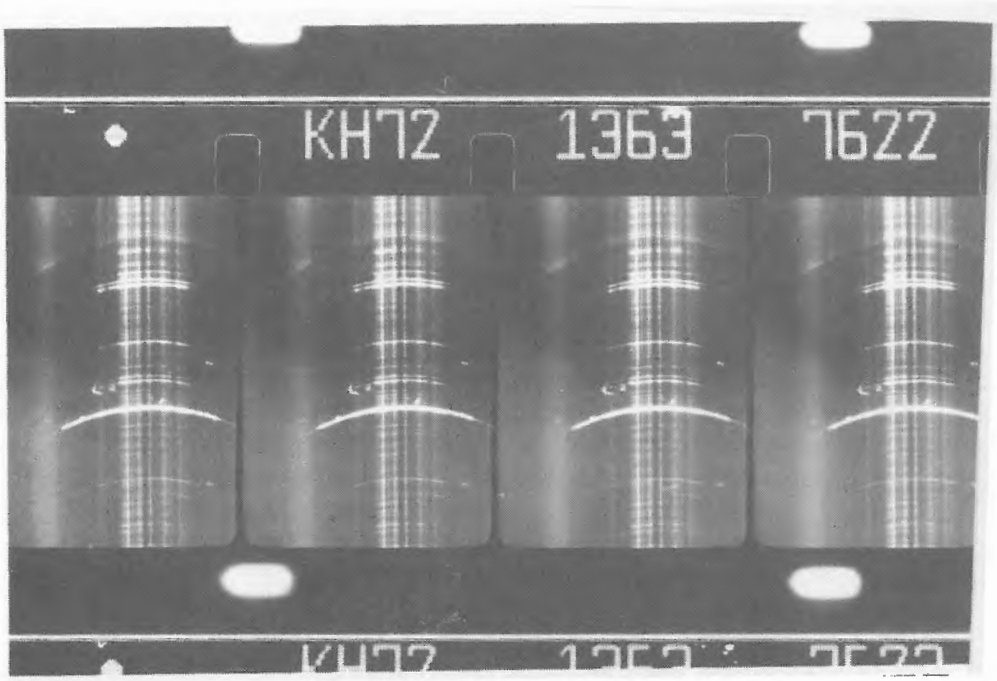

第２接触時付近のスペクトル

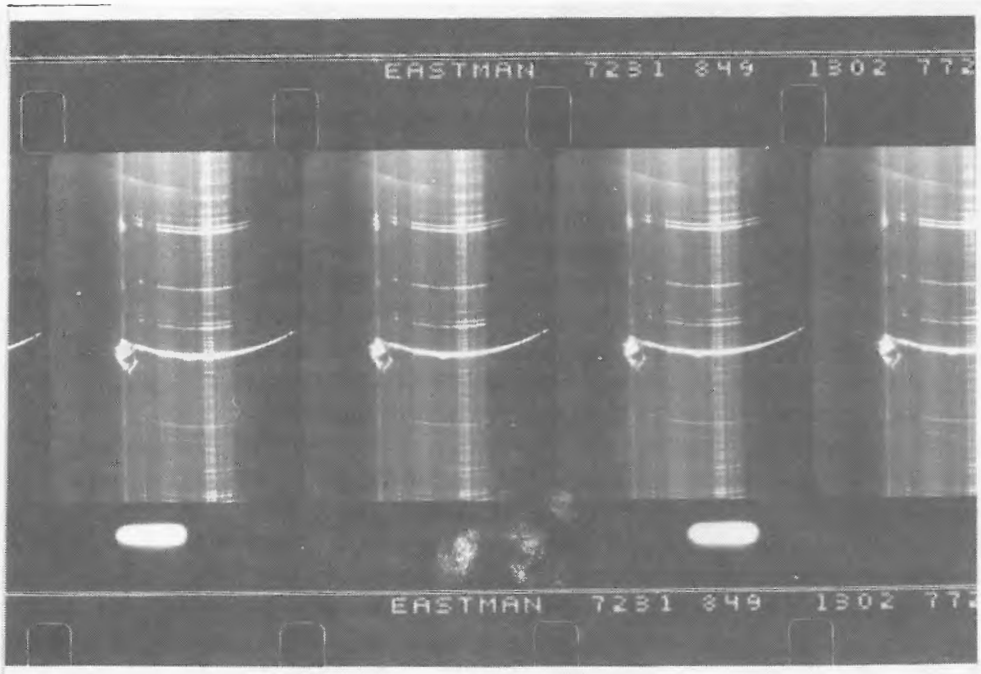

第３接触時付近のスペクトル

On the Coronal and Prominence Structures Observed at La Paz, Mexico, during the Total Solar Eclipse of 11 July 1991

Yoshinori SUEMATSU, Yohei NISHINO, and Hideo FUKUSHIMA

National Astronomical Observatory, Mitaka, Tokyo 181, Japan

Abstract: The coronal images were taken in the light of He I λ10830Å line, λ10000Å-continuum, and Fe XIV λ5303Å line, with the aim of studying the thermal structure of the corona. In addition, spectroscopic observations were made in the wavelength regions of violet (λλ3760-4060Å) and near-infrared (λλ10745-10835Å), to obtain the detailed physical conditions of the corona, especially of its cool part. The data obtained does not show any distinct cool structures other than ordinary prominences. Some preliminary results concerning the corona and prominence structures are given.

1. Introduction

One of the longest total solar eclipse in this century was seen on 11 July 1991 in the restricted area starting near Hawaii Islands, through Mexico and Middle American countries, and ending in Brazil. Solar Physics Division, Naional Astronomical Observatory of Japan (NAOJ), sent an expedition team (Y. Suematsu, Y. Nishino, and H. Fukushima) as member of the Japanese Eclipse Observation Team, to La Paz, Mexico, which was one of the best observation sites, to make observations of the solar corona and prominences during this eclipse. This note describes our observation project of Solar Physics Division, NAOJ, and our preliminary results of this eclipse observation.

The solar corona is generally known to have temperature of million degrees. On the other hand, there exit several features of low temperature in the low corona such as spicules, prominences (10^4 K) and EUV-jets (10^5 K). Since some of these cool features are transient, they should at least in part interact with the hot corona through mass and energy transfers. For instance, the spicules ascend from the chromosphere into the corona, and then some of them fade out and others go back to the chromosphere (Beckers 1972). On the other hand, Wagner et al. (1983) showed that coronal rain prominence forms underneath the bottom of coronal void, using eclipse white-light pictures. Hence it is probable that the materials having temperatures between 10^4 and 10^6 K exist around the well-known cool features or could spread over the entire corona. Shklovskii (1965) had estimated the intensity of chromospheric lines from the million-degree corona.

Some authors reported the existence of cool materials other than well-known features in the corona. In case of eclipse observations, Deutsch and Righini (1964) obtained strange Ca II H and K emission spectrum existing up to one solar radius high in the corona; the intensity ratio of K to H was much larger than 2. They drew the conclusion that the material of 10^5 K existed in the wide region of corona (Cavallini and Righini 1975). Bappu et al. (1972) also obtained strange metallic line emission spectrum, which seemed not to arise from normal prominences, although they have not done any analyses. Outside of eclipses, Leroy (1972) found many small-scale faint features in Hα filtergrams from a

coronagraph while Gnevishev and Gnevisheva (1963) reported such features in He I D_3 filtergrams.

However, many solar physicists have been doubting these evidences for cool materials mentioned above because of their strange properties. Some of these emissions might come from atmospheric or instrumental scattering of the chromosphere or prominences. Our main purpose of this eclipse observations was to confirm the existence or non-existence of cool materials other than ordinary cool features and further to study the origin of such materials if they existed.

We used He I 10830 line for this purpose because this line suffer less atmospheric scattering than visual or violet lines. In order to know the spatial distribution of cool materials, He I 10830 filtergrams were taken with a CCD camera. Moreover, He I 10830 spectra, including famous Fe XIII 10747/10798 line, were taken to know the detailed physical conditions of both cool and hot materials, although this did not yield a good result.

In addition, metallic lines in violet region ($\lambda\lambda$3760-4060Å) including Ca II H and K line were taken because these lines give us much information on the physical conditions of cool materials. Fe XIV 5303 filtergrams were taken in order to study the hot corona and the relationship between the cool and hot structures. As a matter of cource, We were also interested in the thermal structure of the corona, especially of the surrounding regions of prominences and the physical condition of faint parts of prominences.

2. Instrumentation

2.1 3-channel Telescope

The telescope consisted of three tubes mounted on a single equatorial mounting and was designed to obtain three different monochromatic images of the corona.

The two of three tubes had apochromatic lenses of 76 mm diameter (F/7.9), telecentric lens systems, filter boxes, camera lenses, and CCD cameras (TAKENAKA TM-840N, 2/3",768 × 489 pixels). A He I 10830 filter (FWHM of 6Å) was put in one filter box and a 10000Å-continuum filter (FWHM of 200Å) in another box. The solar diameter on the CCD camera was about 5mm. The image data from the CCD were stored on Video Tape Recorder with S-VHS mode as well as on a hard disk of personal computer (NEC PC-9801RA) through a image processor (PIAS-525) of 512 × 512 resolution and 8 bit depth. The image processor automatically integrated digitized video images up to the saturation level.

The third tube consisted of an apochromatic lens of 100mm diameter (F/8), relay lens system, Fe XIV 5303 filter (FWHM of 3.5Å) , and 35mm film-camera (Nikon F3 with 250 exposures camera-back). The solar diameter on the film was about 25mm. We used Kodak TMAX400 emulsion. The exposure of the camera was controlled by a personal computer (NEC 9801note) and the exposure time was changed between 1/2000 and 64 sec. during the eclipse observation.

The connection between the overall instruments is schematically shown in Figure 1. The telescope was pointed to east solar limb before mid-totality, and to west limb after mid-totality.

2.2 Spectrograph

The spectrograph was designed to observe the violet ($\lambda\lambda$3760-4060Å) and near-infrared ($\lambda\lambda$10745-10835Å) wavelength region simultaneously. Solar image was focused on a mirror-slit (straight slit) by a cassegrain type telescope (objective of 100mm diameter and combined F/12.4). The spectrograph assembled with the telescope was mounted on a equatorial mounting.

The width and the length of the slit was 30μm and 15 mm, respectively, for the chromosphere and low corona, while the width was changed to 200 μm during the observation for high corona. The direction of slit axis was always in the north-south in the sky: the slit was put tangentially to the solar east or west limb. In order to examine linear polarization of light, a Gran-Taylor prism, which is effective for both infrared and violet wavelength region, were put in front of the mirror slit. The prism was rotated around its axis in 60 degrees step. The optical diagram of the spectrograph is shown in Figure 2 and its some characteristics are given in Table 1.

We used a CCD camera (National CD-55) with cooling device for the infrared observation. On the other hand, a film-camera (Nikon F-3 with 250 exposures camera-back) was used for the violet. A personal computer (NEC PC-9801RA) was employed to control the exposure of both the CCD and film-camera, the rotation of polarizer, and the fine positionings of spectrograph-slit. The telescope-spectrograph was moved so as that the slit was set to the extreme east solar limb around the second contact time, and higher above the east limb (up to 100 arcsec) with time by one and half min. before the third contact time, and then the telescope was manually pointed to the west just above the lunar limb until the third contact.

We used Kodak TMAX400 emulsion for the violet observations and changed exposure times from 1/15, 1, 4, 8 sec. to 180 min., in this order, synchronizing with the rotations of the polarizer, for the east corona, while kept them 8 sec. for the west corona.

For the cooled CCD camera, we were obliged to select the exposure times of 1/15 sec. and 180 min. for the east corona and store the data on a VTR. This CCD did not work for the west corona.

White-light slit-jaw images, which were also linearly polarized because of the Gran-Taylor prism, were also recorded on a VTR through a CCD camera (Sony XC-77RR) with a neutral density filter and f55 mm camera lens (Micro Nikkor).

The diagram for the connection between the spectrograph and other related instruments is shown in Figure 3.

3. Observational Data

Raw data obtained during this eclipse are summarized as follows.

For the east corona:

(1) 6 frames of digitized image and video images through He I 10830 filter
(2) 6 frames of digitized image and video images through 10000Å-continuum filter
(3) photographic images through FeXIV 5303 filter
(4) photographic spectra through the polarizer in the violet wavelength region
(5) 1 frame of video spectra of He I 10830
(6) slit-jaw white-light images on video through the polarizer

For the west corona:

(1) 10 frames of digitized image and video images through He I 10830 filter
(2) 10 frames of digitized image and video images through 10000Å-continuum filter
(3) photographic images through FeXIV 5303 filter
(4) 6 photographic spectra through the polarizer in the violet wavelength region
(5) slit-jaw white-light images on video through the polarizer
Some examples of data are shown in Figure 4.

In addition to these data, we also obtained some data for intensity calibrations after the eclipse. For the filtergrams, solar disk center images were taken with the combinations of several different neutral density filters. We used a step-wedge filter for the spectra. Furthermore, we took dark and flat images for the CCD data calibrations.

The photographic data were firstly processed with a usual manner; microphotometric scannings and then density-intensity conversions using characteristic curves. On the other hand, it is relatively easy to handle the video data through the CCD cameras because these are easily digitized using the image processor and processed with computers. We firstly made subtraction of dark currents and corrections of CCD pixel sensitivities.

4. Preliminaly Results and Discussion

During this eclipse, we could observe three outstanding streamers: the two was extending in the north-east direction and the other in the south-west, and prominent coronal plumes in the north-west quadrant. There existed two large prominences: one was at the east limb and another at the west. We are now processing quantitative analyses of the data. The followings are rather qualitative results obtained from the glance of the data. Some results about the coronal plumes are given in a separate note in this volume (Fukushima).

In Fe XIV 5303 filtergrams, we can see many fine-scale structures such as loops, threads and rays. In the filtergrams of long exposures, we can even perceive the coronal streamers as in white-light pictures, although they are very faint. The most interesting in the east corona is twin cavity structure underneath the east streamer; two cavities are neighboring each other. The east large prominence is sitting inside one of these two cavities. The 1966-eclipse showed such twin cavity structure too: two adjacent cavities were enclosed by a helmet-streamer structure and each cavity had a prominence (Tandberg-Hanssen 1979). In the west corona, a coronal hole is seen and a thread at the south edge of this coronal hole seems to be twisted. We cannot see the distinct cavity above the west large prominence.

At this point, we can not detect any cool structures other than the ordinary prominences in the limit of the detector sensitivity for He I 10830 line and for Ca II H and K line; about 10^{-2} of ordinary prominence intensity for He I 10830 filtergram and 10^{-4} for Ca II H and K line spectra. To make matters worse, the coronal parts of Ca II H and K line spectra are contaminated by the atmospheric scattered lights from the prominences: false emission lines are seen in the neighboring regions of prominences. This negative result might not always mean that cool materials other than the ordinary prominences do not exist in the corona at all. Our detector sensitivities were not so good for this purpose or one could easily find such cool materials in other eclipses. In this sence, we will need further investigations in future.

The faintest prominence of our observations is in the south-west quadrant, whose intensity is about a few hundredths of ordinary prominence in He I 10830. This prominence

is of nearly-horizontal bar shaped and shows largely shifted line spectra in Ca II H and K, corresponding to the velocity of 100 km s^{-1}. However, the prominence is hardly seen in higher Balmer or metallic lines. This might imply that the temperature of this prominence is higher than that of ordinary ones (eg. Alikayeva 1975). We are trying to find out some Fe XIV 5303 structure related to this prominence.

We can see tilting line spectra in the violet at the most top of the east prominence, which is located near the south inner edge of the helmet-cavity structure in Fe XIV 5303 line. This tilting probably indicates the rotational motion of the prominence matter. At the leg part of this prominence, between the prominence body and the chromosphere, we have largely-shifted Ca II H and K line spectra, corresponding to the line-of-sight velocity of several tens km s^{-1}.

In the violet spectra, besides chromospheric/prominence lines we can detect three coronal lines; Co XII 3800.7, Fe XI 3987.1, and Cr XI 3998.0, which are formed in the plasma of about one million degrees. With these lines as well as the Fe XIV 5303, we can know the irregular temperature structure in the corona.

Acknowledgements

We gratefully thank Dr. H. Kurokawa, Kyoto University, the chief of the Japanese Eclipse Observation Team (JEOT), for his kind and helpful coordination between COMES and our team. We are also grateful to Messrs. K. Koyama and M. Okumura, the members of JEOT, Hydrographic Department of Japan, for providing us the precise eclipse parameters, and to Dr. S. Isobe, the member of JEOT, NAOJ, for giving us useful information on Mexico. We wish to express our hearty appreciation to COMES, especially, Ing. Osegera and Dr. Bohigas, and to Japanese Embassy of Mexico, for their kind and helpful cooperation in Mexico: we could not succeed the observation without their practical assistances. We are obliged to Profs. Y. Yamashita, T. Hirayama, and E. Hiei for their useful suggestion and encouragement. Finally but not least, our thanks go to all members of Solar Physics Division, NAOJ, especially Messrs. N. Tanaka, K. Sano and H. Miyazaki, and all other members of JEOT, for their usefull assistances during this eclipse project.

References

Alikayeva, K.V.: 1975, Solar Phys. **41**, 89-95.
Beckers, J.M.: 1972, *Ann. Rev. Astron. Astrophys.*, **10**, 73
Bappu, M.K.V., Bhattacharyya, J.C., and Sivaraman, K.R.: 1972, Solar Phys. **26**, 366.
Cavallini, F. and Righini, A.: 1975, Solar phys. **45**, 291-299.
Deutsch, A.J. and Righini, G.: 1964, Astrophys. J. **140**, 313.
Gnevishev, M.N. and Gnevisheva, R.S.: 1963, in J.W. Evans (ed.) *The Solar Corona*, New York, Academic Press, p. 241.
Leroy, J.L.: 1972, Solar Phys. **25**, 413.
Shklovskii, I.S.: 1965, *Physics of the Solar Corona*, Pergamon Press.
Tnadberg-Hanssen, E.: 1979, in E. Jensen, P. Maltby, and F.Q. Orrall (eds.), 'Physics of Solar Prominences', *IAU Colloq.*, No. 44, p. 139.
Wagner, W.J., Newkirk, G., and Schmidt, H.U.: 1983, Solar Phys. **83**, 115-119.

Table 1. The Characteristics of Spectrograph

Telescope	ϕ 100mm, F/12.3, cassegrain	
Polarizer	Gran-Taylor, aperture of □ 20mm rotate in 60° step	
Slit	Mirror of □ 40mm with slit 30 μ m × 15mm	
Slit Monitor	CCD camera with ND filter Data are recorded on VTR (S-VHS)	
Grating	□ 52mm, 1200 grooves mm^{-1}, blaze wavelength = 10000 Å	
Collimator	□ 60mm, f500mm, off-axis paraboloidal	
Order	1st	2nd
Camera Lens	ϕ 50mm, F/6	ϕ 50mm, F/8
Wavelengths	10744 - 10834 Å	3763 - 4061 Å
Dispersion	10.3 Å mm^{-1}	8.5 Å mm^{-1}
Resolution	4", 0.3 Å	2", 0.15 Å
Detector	CCD camera with evacuation, cooling and long-exposure device	35mm film camera (Nikon F3) 250 exposures
Recorder	VTR(S-VHS) and image digitizer (512 × 512, 8bit)	emulsion (Kodak TMAX400)

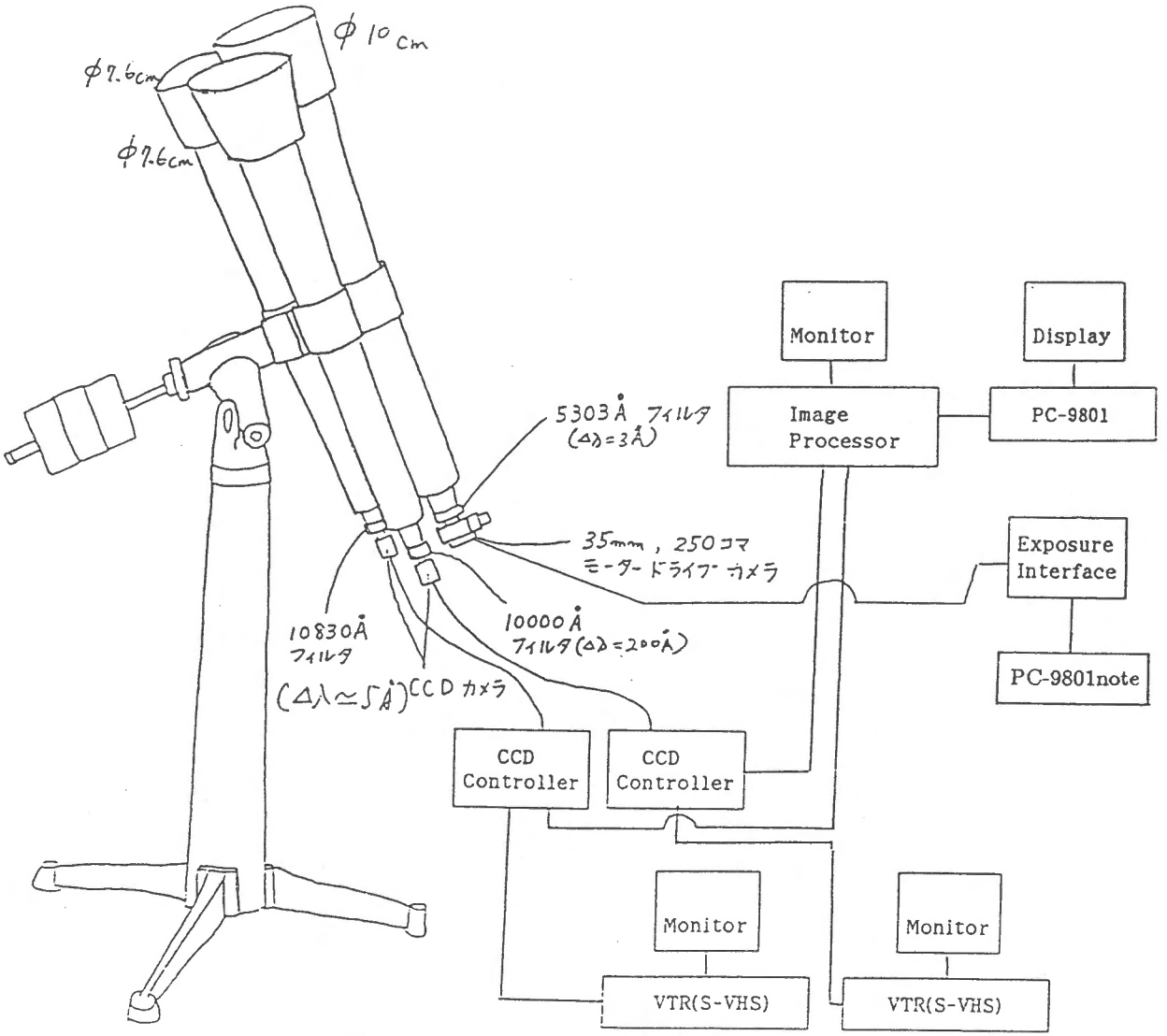

Fig. 1. 3-Channel Telescope

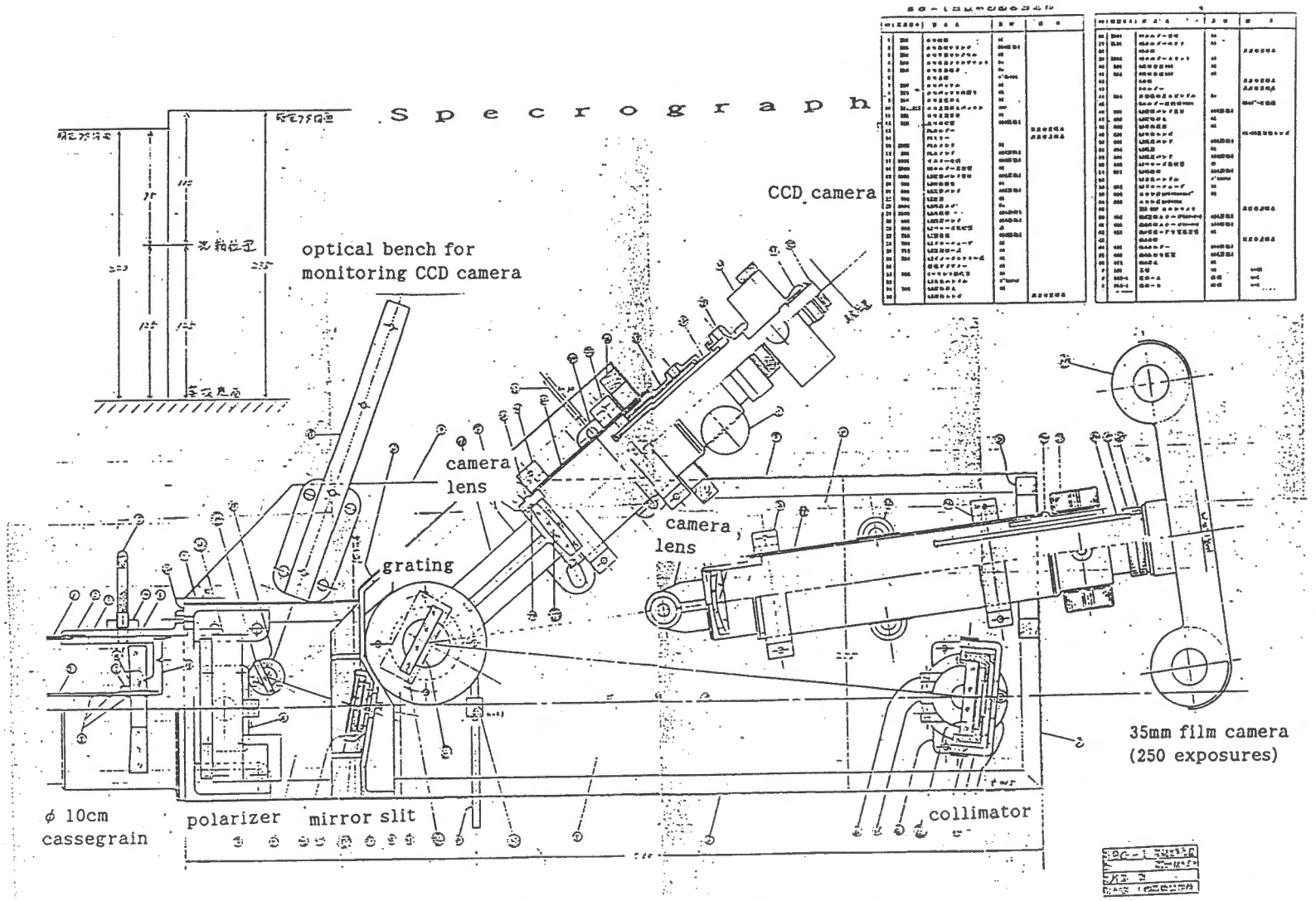

Fig. 2. Optical Diagram of Spectrograph

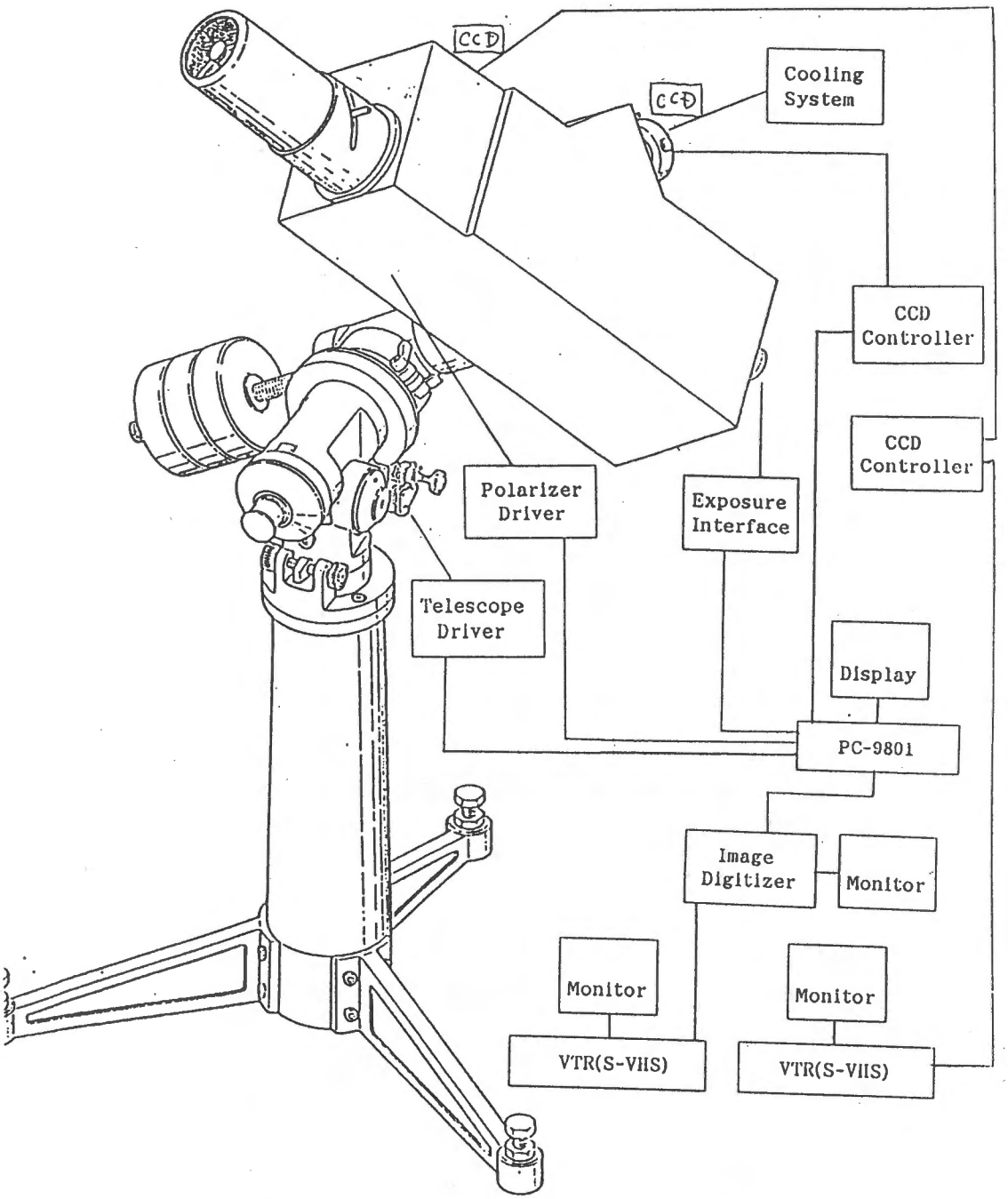

Fig. 3. Connection between the Spectrograph and Other Instruments

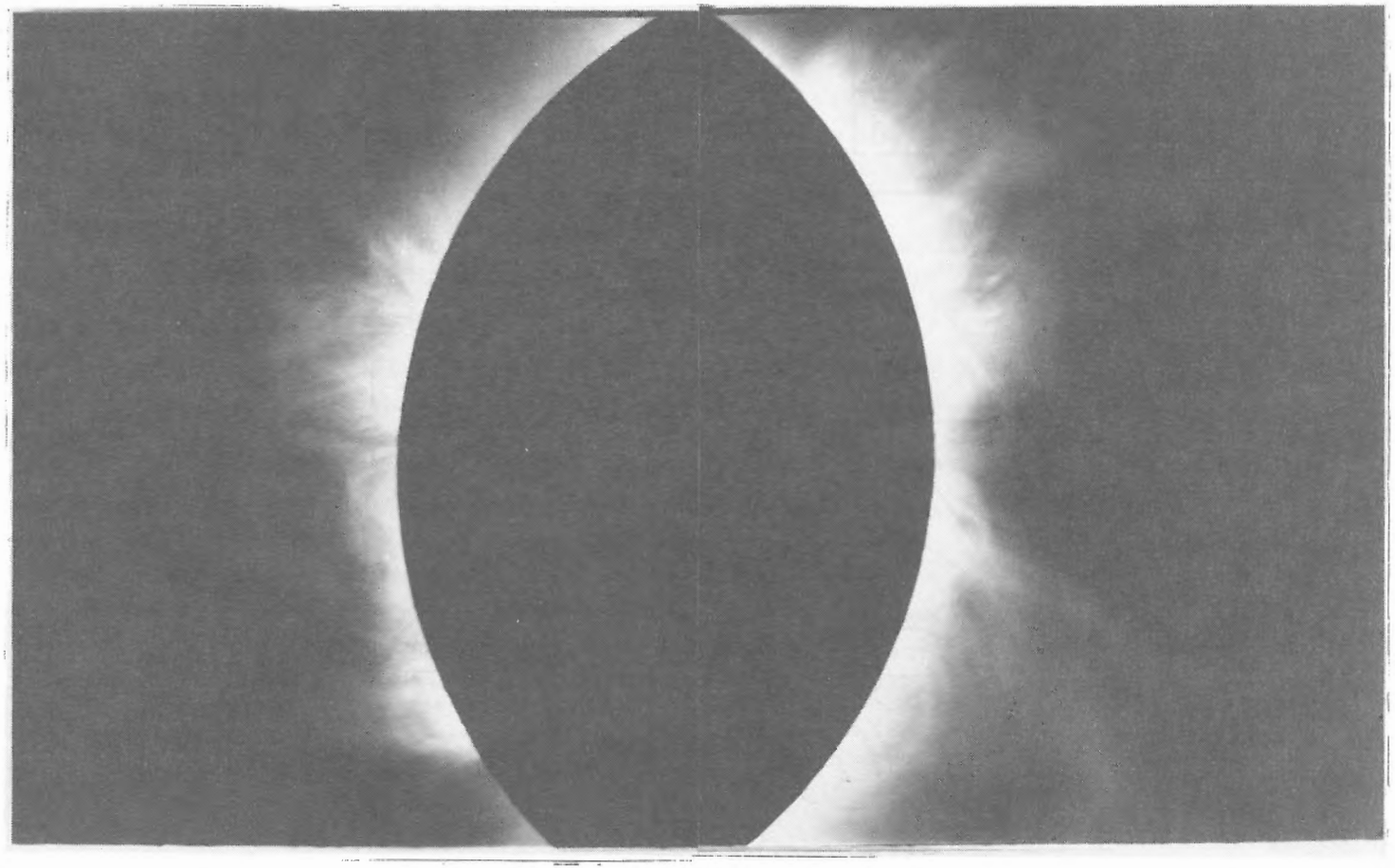

Fig. 4(a) An example of Fe XIV 5303 filtergram for the east corona (left) for the west corona (right)

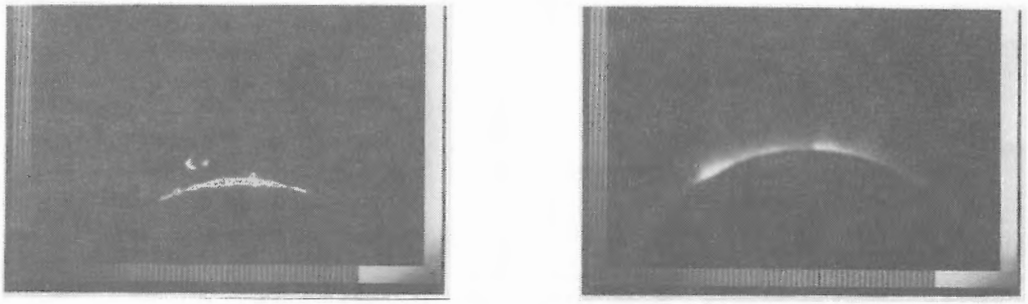

Fig. 4(b) An example of He I 10830 (left) and 10000Å-continuum (right) filtergram

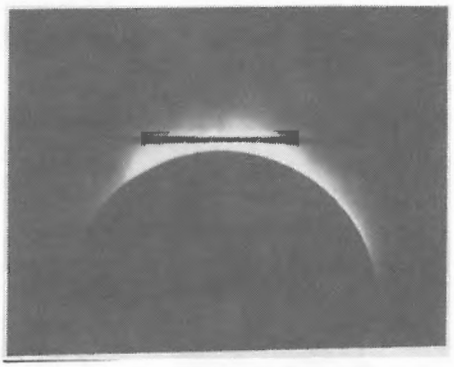

Fig. 4(c) An example of slit-jaw white-light image

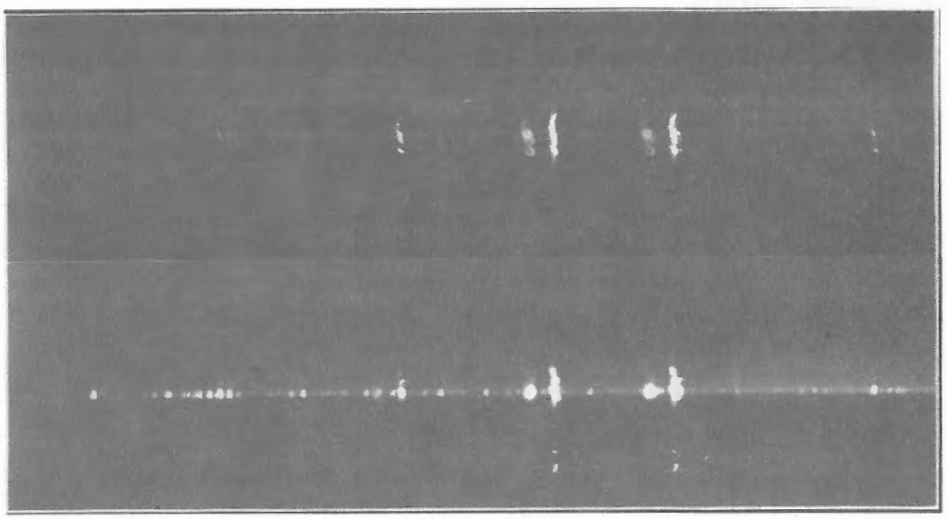

Fig. 4(d) An example of violet spectra ($\lambda\lambda$3760-4060Å) for the east corona (upper) and for the west corona (lower)

左より分光望遠鏡、西野、ボヒガス氏、末松、福島

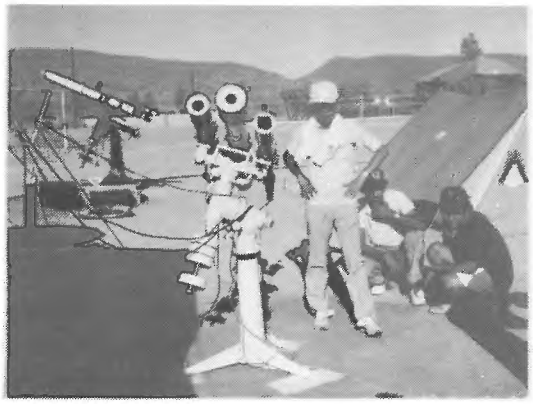

三連望遠鏡、後方は水路部の望遠鏡

砂と熱気を防ぐためにパソコン等はテント内に置いたが、クーラーを入れていても日中３５℃以上になる

日食当日、スタンバイＯＫ

南パハカリフォルニア大学構内に開設された国際色豊かな観測村

夕方涼しくなると、ＴＶ取材や見学者が次々とやって来る

1991年 7月11日 メキシコ皆既日食 Kコロナの流線構造について

The Structure of the Coronal Rays(Streamlines) at the Eclipse on July 11, 1991, in La Paz, B. C. S., Mexico

福島英雄, 末松芳法, 西野洋平
H. Fukushima and Y. Suematsu, Y. Nishino

国立天文台太陽物理学研究系 日食観測隊
A Group for the obsarvation of the Eclipse,
National Astronomical Obsarvatory, Tokyo, Japan

Abstract

Prominent coronal ray structures were observed during the total solar eclipse of July 11, 1991, at La Paz, Mexico. White-light coronal pictures were analyzed to study the width-variation of the streamlines as a function of distance along them. It is found that most of the streamlines expand linearly with distance: its expansion rate is 20～50 arcsec per solar radius. When the widths are extrapolated to the solar suface, we obtain the values of 15～40 arcsec. These values seem to indicate that the coronal streamlines are strongly related to the enhanced unipolar magnetic fields from part of supergranulation network whose typical dimension is 40 arcsec.

はじめに

1991年７月11日（U.T.）に，ハワイからメキシコを通りブラジルにかけて，最大皆既継続時間が約７分もある皆既日食が起こった．国立天文台太陽物理学系では３名の日食観測隊を編成し，メキシコ，カリフォルニア半島先端近くのラ・パス（La Paz）にて，コロナの観測を行った．

おもな観測目的と結果については，末松芳法他が報告しているが，パソコン制御による自動観測であったので，さらに欲張り，当初の観測目的とは別に，ノー・フィルタでのKコロナ全体像の写真観測も行った．皆既日食当日は，快晴の天候に恵まれ，シーイングも良好であり，計画していた観測は，ほぼ成功した．

このKコロナをねらった写真には，プロミネンスから外部コロナまで写っており，数本の長いストリーマは画角からはみだしている．モノクロ，カラーフィルム共に比較的鮮明な写真が得られた．

今回の日食時のコロナの形の特徴は，北東および南西方向に長いストリーマが伸び，北東方向では２個のストリーマが重なり合っている．まるで，極小期のコロナの形を傾けたようである．また，西から北の方向には非常に細かい筋構造が見られ，西側には明るい活動型プロミネンスがあり，その上方には特に明るい筋構造が長く伸びている．一方，南東側には，あまり目立った筋構造は見られない．

この様な顕著な筋構造は，どのような太陽磁場分布と対応しているのか，興味のあるところである．

目的

西から北の方向にかけて見られる流線構造は，太陽活動極小期に極域で見られるポーラー・プルーム（Polar Plumes）と良く似ている．従って，今回の皆既日食時には大きなコロナホールが極域ではなく，筋構造が目立った領域にあったことが予想される．

この流線構造は，大部分のものが明るい筋であるが，中には暗い筋もある．もし，筋の視線方向の幅が見かけの幅と同じ程度なら（この可能性はかなり高い），明るい筋では回りより電子密度が高く，暗い筋では低くなっているはずである．これらの筋構造と太陽表面現象との関係を調べることは，コロナへの質量供給の過程を調べる上で興味深いことである．

この目的の手始めとして，西から北の方向に伸びた目立った流線の位置と幅の高さ変化を求めてみた．

観測方法

高橋製作所製の90型システム赤道儀（電動自動追尾装置付き）にタムロン製の望遠レンズ（f=300㎜，F/2.8）を同架して，35㎜一眼レフ・カメラにて写真撮影を行った．望遠レンズには２倍のリア・テレコンバータ・レンズを装着．テレコンバータ・レンズによる像の悪化を改善するため，絞りは半絞り分しぼり，焦点距離600㎜，F/7として使用．フィルタは使用していない．

この望遠レンズは，ＥＤレンズを使っているため，気温変化によるフォーカスずれが大きく，日食中は気温が短時間のうちに急激に下がるので，そのつどフォーカスを合わせ直す必要がある．しかし，第２接触直前あるいは皆既食中に正確にフォーカス合わせを行っている時間はない．そこで，皆既食中の気温は太陽が欠け始める前の気温より10℃程度下がるだろうと予想し，何日か前の夕方に予想した気温と同じになった時，金星を使って予めフォーカスを合わせておいた．

一眼レフ・カメラ・ボディーは，ニコン，アサヒペンタックスを取り混ぜ５台用意しておき，36コマのフィルムを撮り終えたらカメラ・ボディーを交換するという手順で撮影した．

フィルムは36枚撮りのモノクロとカラー両方を使用し，露出は1/2000から８秒まで連続に一段づつ変えながら撮影．モノクロ，カラーそれぞれ２本づつ，コロナが写った合計４本のネガフィルムを得ることができた．

流線の幅の測定に使った写真は，モノクロ・フィルムであるコダックの ＴMAX 100を使用．現像は，コダックの ＴMAXフィルム専用現像液， ＴMAXデベロッパーにより，液温22℃，７分の処方で行った．露出時間は，1/15秒．カメラは，ニコンＦ３（36コマ・モータードライブ）を使用．撮影時刻は，18時49分10秒（U.T.）．

測定方法

まず，撮影したフィルムの中から流線の幅測定に適した濃度のコマを選び出し，キャビネ・サイズの印画紙にプリント（写真）．その写真から，イメージスキャナを使用してデジタイズし，16ビットの画像データを作成した．シャープ製のＸ68000 というパソコンを利用し，モニタ画面上である程度拡大した画像からx，y座標を読み取り，自作プログラムにて計算処理を行った．

流線構造をモニタ・テレビ画面上で見やすくするため，コントラスト強調とネガ・ポジ反転などの処理が必要であった．

図 3　(fig. 3)

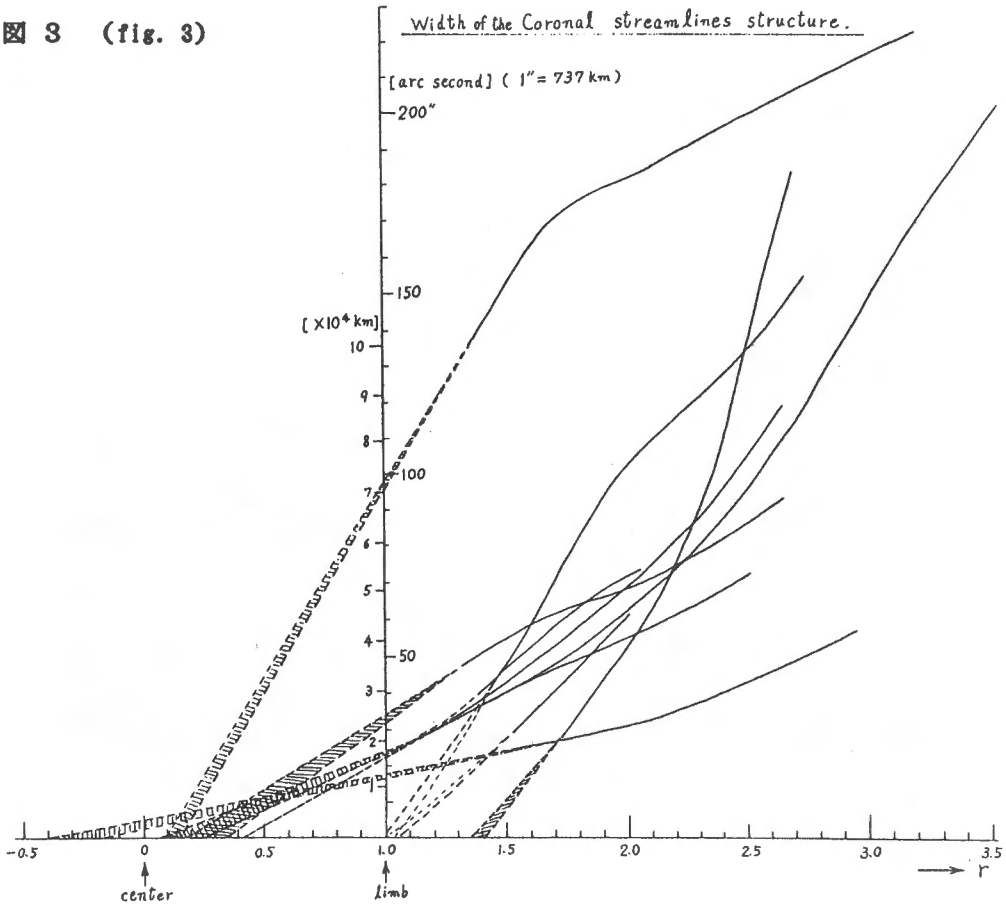

結果

測定したのは図１（Fig. 1）に示す16本の流線，ＡからＮである．流線の幅の高さ変化をプロットしたものが図２（Fig. 2）である．全体の特徴としては，流線，筋の幅は太陽リムから離れるほど広くなっている．これは，流線（筋）構造が磁力線を表していると考えると自然なことである．測定可能な流線の根元の幅は，E_0 を除いて２～４万kmになっている．

図３（fig. 3）は，図２のグラフをスムージングしたもので，この曲線を太陽リムまで延長すると，光球表面上では１～３万kmの幅になっていることが予想される．光球表面上で３万kmというのは，超粒状斑の大きさに対応しているが，ひとつの可能性として，超粒状斑の境界で特に磁場の強い場所が明るい流線構造を作っていることが考えられる．

さらに，図３のグラフの曲線をもとに，太陽リムから内側，太陽中心方向に延長してみると，多くの流線は，幅が０となるところが太陽中心から少しずれており，太陽中心から0.1～0.4ｒ（ｒ＝太陽半径）外側の付近に集中しているようだ．コロナの流線構造が放射状に開放された磁力線に沿ってできているとすれば，単純に考えると，この集束点は太陽中心付近にあると思われるが，どうであろうか？

おわりに

これだけのデータ量だけでは確実な結果を出すことはできないが，過去あるいはこれからの皆既日食時に撮影した写真からも同様な測定をして，数多くのデータを得ることにより，研究していきたいと考えている．

測定に使用した写真 （photograph）

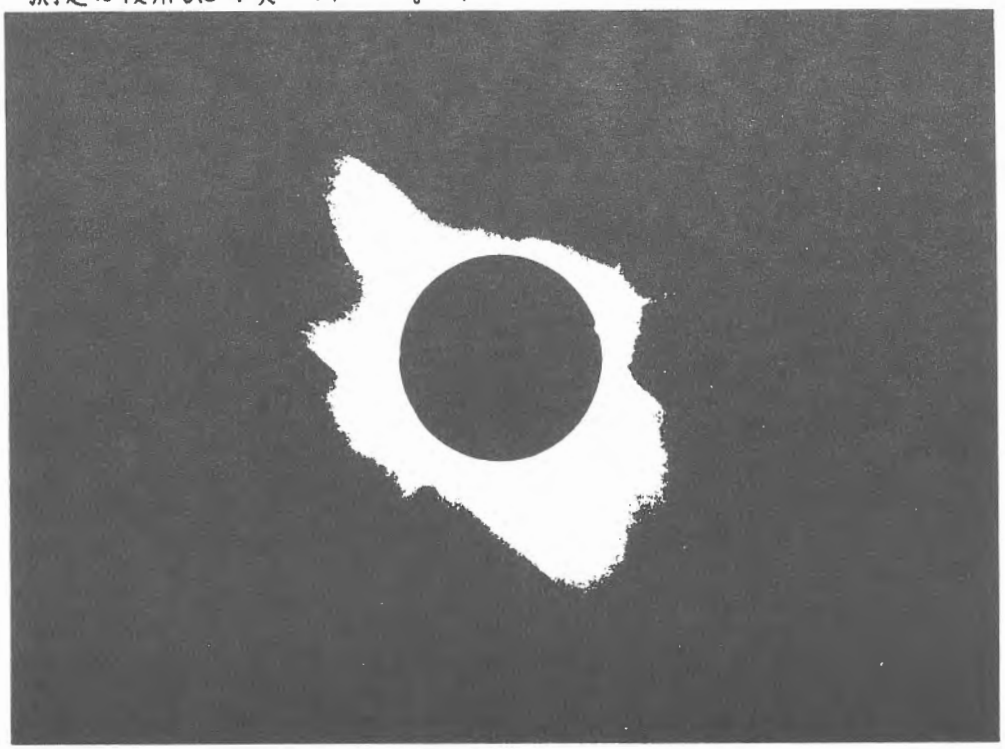

図 1
(fig. 1)

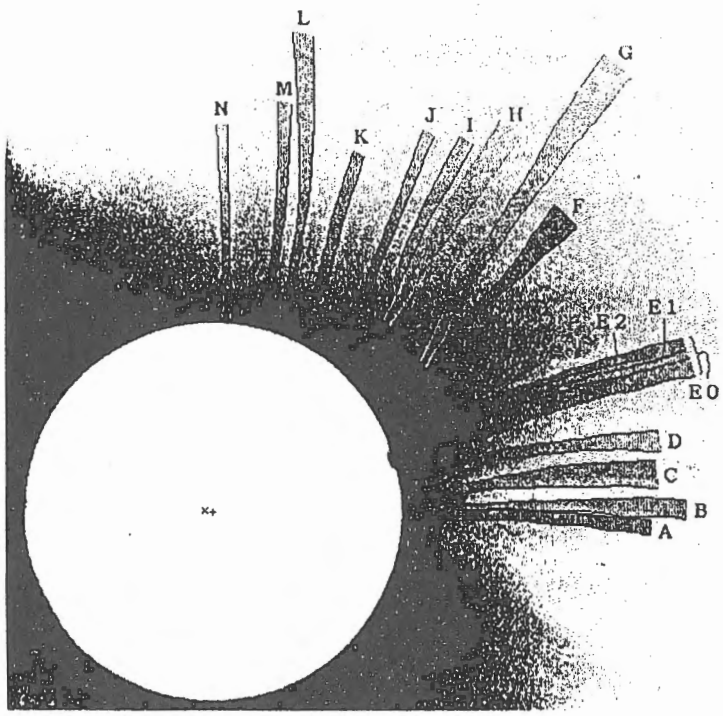

図 2 （fig. 2）

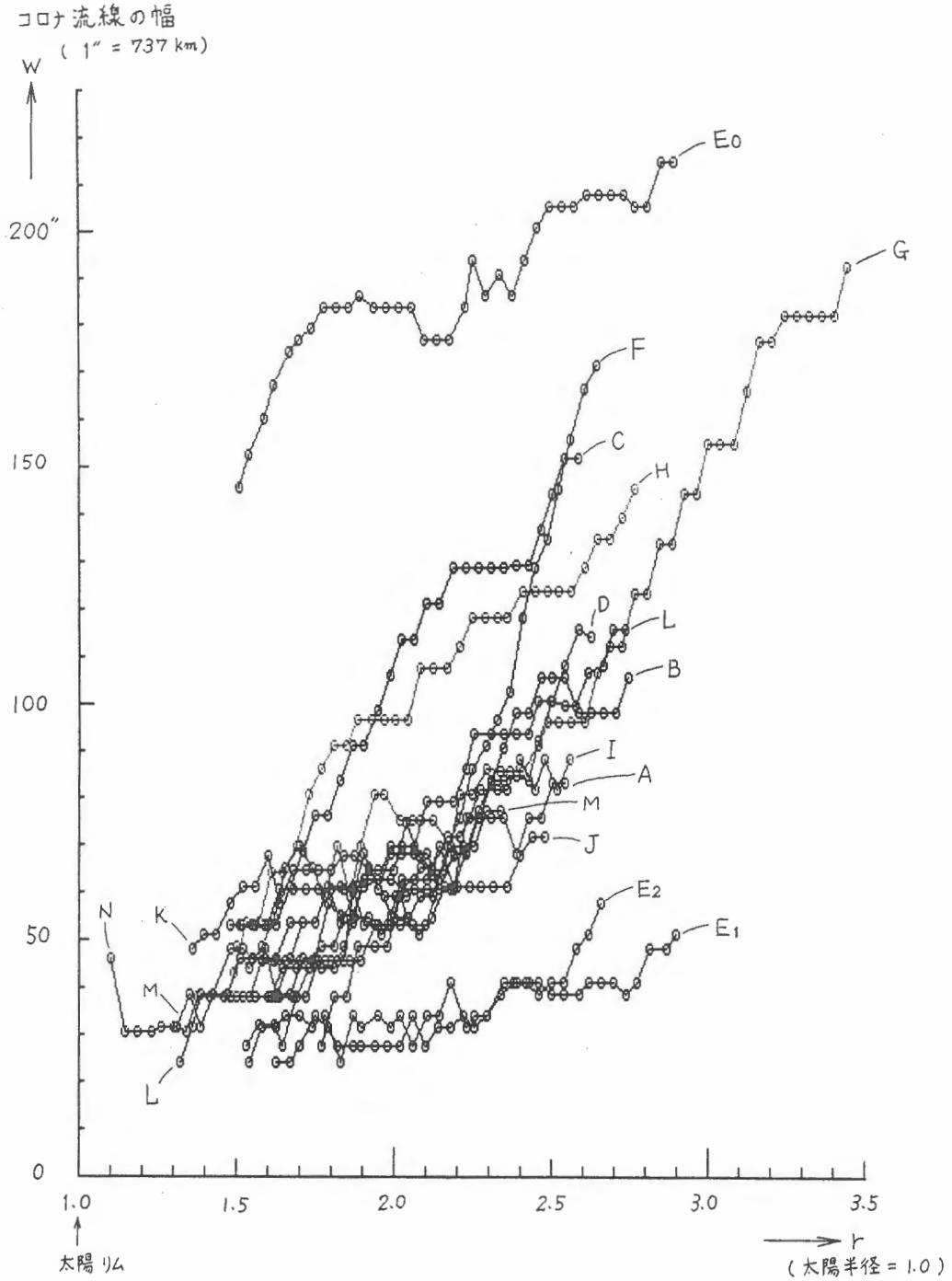
コロナ流線の幅
(1″ = 737 km)
W
200″
150
100
50
0
1.0
1.5
2.0
2.5
3.0
3.5
r
太陽リム
(太陽半径 = 1.0)
E0
G
F
C
H
D
L
B
I
A
M
J
E2
E1
N
K
M
L

Eclipse Observations at Hawaii and Brazil

E. Hiei

There are three merits in the eclipse of 11 July 1991; i) the totality passes over the Mauna Kea Observatories, which can fortunately to take fine structures in the corona with a shorter exposure time by using large telescopes, ii) there is 3 hours' time difference for the observation of the eclipse between Hawaii and Brazil, which is a good opportunity to study the time change of the coronal structures, and iii) the duration is so long as 7 min. that many observing programs on the corona can be made. The observations made at Hawaii and Brazil are described here.

Table 1 shows Principal Investigator, Telescope, Goal of observation, wavelengths used for the observation, and Instruments. Some one thinks that the huge stratospheric cloud of volcanic dust produced by Mt. Pinatubo volcano may arrive across the Hawaii archipelligo several days before the eclipse. In the morning of the eclipse day a few small clouds reached the telescope domes at Mauna Kea just before the first contact, and then the clouds disappeared due to the cooling of partially eclipsed Sun.

The 3.6m and 2.24m telescopes are so powerful that they took more than 6000 useful frames with sub arcsecond resolution. It is interesting to note that incredibly fast time variations in less than 10 seconds time are recorded on several very small coronal features. The polarization observation of the corona with a radially filtered color video movie was successfully carried out. Total 150 positions for a full Stokes Q/U analysis were repeated 42 times during the totality. The CSO and JCMT observations extend to 0.85mm and 1.3mm to the Kuiper data base, which covered the range form 30 to 700 μ. The JCMT observations show a 1.3mm limb lyning approximately 8.5 arc sec above the visible limb.

The eclipse observations in Brazil were made at Tefe and Manicore town near Amazon river. Drs. N. Dzubenko and L. Kurochka, Kiev University, were P.I. of the observations at Tefe, and Drs. B. Artamonov and I. Kim, Moscow University, were P.I. at Manicore. There are four observing programs. i) Multi-station experiment, which is coordinated observation of the corona at Hawaii, Mexico, and Brazil (Sternberg Institute). ii) Velocity field of the corona with Fabry-Perot at emission lines of $\lambda 5303\mathring{A}$ (FeXIV) and $\lambda 7892$ (FeXI) (Sternberg Institute). iii) Polarization of the K-corona (Sternberg Inst. and Georgia Inst.). iv) Coronal structures in continuum and line (Georgia Institute). Total 28 persons (10 Soviet and 18 Brazilians) worked for the eclipse observations. Professor Oscar T. Matsuura, Departmento de Astronomia, IAG-USP, was a responsible person for the eclipse project in Brazilian side.

P.I.	Telescope	Goal	λ	Instrument
Koutchmy	CFHT 3.6m	fine structure, solar wind acceler.	continuum lines	70mm camera monochrome 4frame/s color 1frame/s CCD camera, 20×25cm camera
LaBonte	UH 2.24m	T/ρ inhomogeneities, μ-flare	continuum lines	CCD camera, video
Arnaud	UH 61cm	ρ structure in AR	Fe lines	CCD camera
Deming	IR 3m	chr. structure, mag. field	12.3 μ Mg	Fabry-Perot
Hall	UH 61cm	Interplanetary dust	1.2,1.6,2.2μ	256×256 HgCaTe array data
Fazio G.	5cm	Interplanetary dust	1.6,2.2μ	6.4×6.4 128×128 IR aray
Lamy Ph.	CSO 10.4m	Interplanetary dust(K+F) pol.	1.2,1.6,2.2μ	4×4 128×128 60mm Hasselblad, 35mm Nikon
Zirin	CSO 10.4m	limb, chr. temp. gradient map structure	0.85mm	
Lindsey	JCMT 15m	T/ρ structure photosphere. chr.	1.3mm	

Sketches of the Solar Corona

Hiroyoshi TANABE, Mitsuko AOKI, Takeshi INOUE, Takuya NAGATA,
Haruko SHIBAYAMA and Mitsuko TANABE
(田鍋浩義, 青木光子, 井上　毅, 永田卓也, 柴山治子, 田鍋光子)
(A Group of Japanese Amateur Astronomers in Mexico)

We made sketches of the corona at the total solar eclipse on July 11, 1991 at the tip of Baja California, Mexico. Four of us (H T, M A, T N, M T) observed at Cabo San Lucas (109.9° W, 22.9° N) and two (T I, H S) at La Ribera (approximately 109.5° W, 23.5° N) about 90 km north-east from Cabo San Lucas. At Cabo San Lucas, local time of mid-eclipse was 11h 53m, solar elevation angle 83° , and duration of totality 5m 38s. Duration at La Ribera was 1m 20s longer than that. Sky conditions of both sites were excellent from 1st to 4th contacts.

Figs. 1 ～ 6 are our sketches, which were drawn while watching the corona with naked eyes and/or binoculars. E,W,N,S-directions on the celestial sphere from the sun's center were found with referring to directions of the planets (mainly Venus) indicated in the sketches.

General aspects of the eclipse appeared in our sketches are as follows.

(1) Three prominences, one was large and two were small, could be seen on the limb.

(2) The bright inner corona within 1.5 $R_{\odot}$ was round shaped, but structure of fine stream lines was diverse and complicated from part to part.

(3) Two large and long streamers of the outer corona extending to more than 5 $R_{\odot}$ in SW-direction and to about 4 $R_{\odot}$ in NE-direction, respectively, were seen. Besides them, there were many small streamers in various directions.

(4) During the totality, the planets Mercury, Jupiter and Venus were seen to the east of the sun, however, Mars could not be found.

The brightness of the corona decreases rapidly toward outside, for example, the brightness at 5 $R_{\odot}$ is about 1/10,000 of that of near the limb. Accordingly, we can not take a photograph of the whole corona by one shot without parts of over- and under-exposures. Since the sensitivity latitude of human eye is much wider than photograph, drawing an exact sketch with naked eyes is advantageous for recording whole shape of the corona, especially for the outer corona.

We suggest and recommend amateur astronomers to make a sketch of the corona at the future solar eclipses.

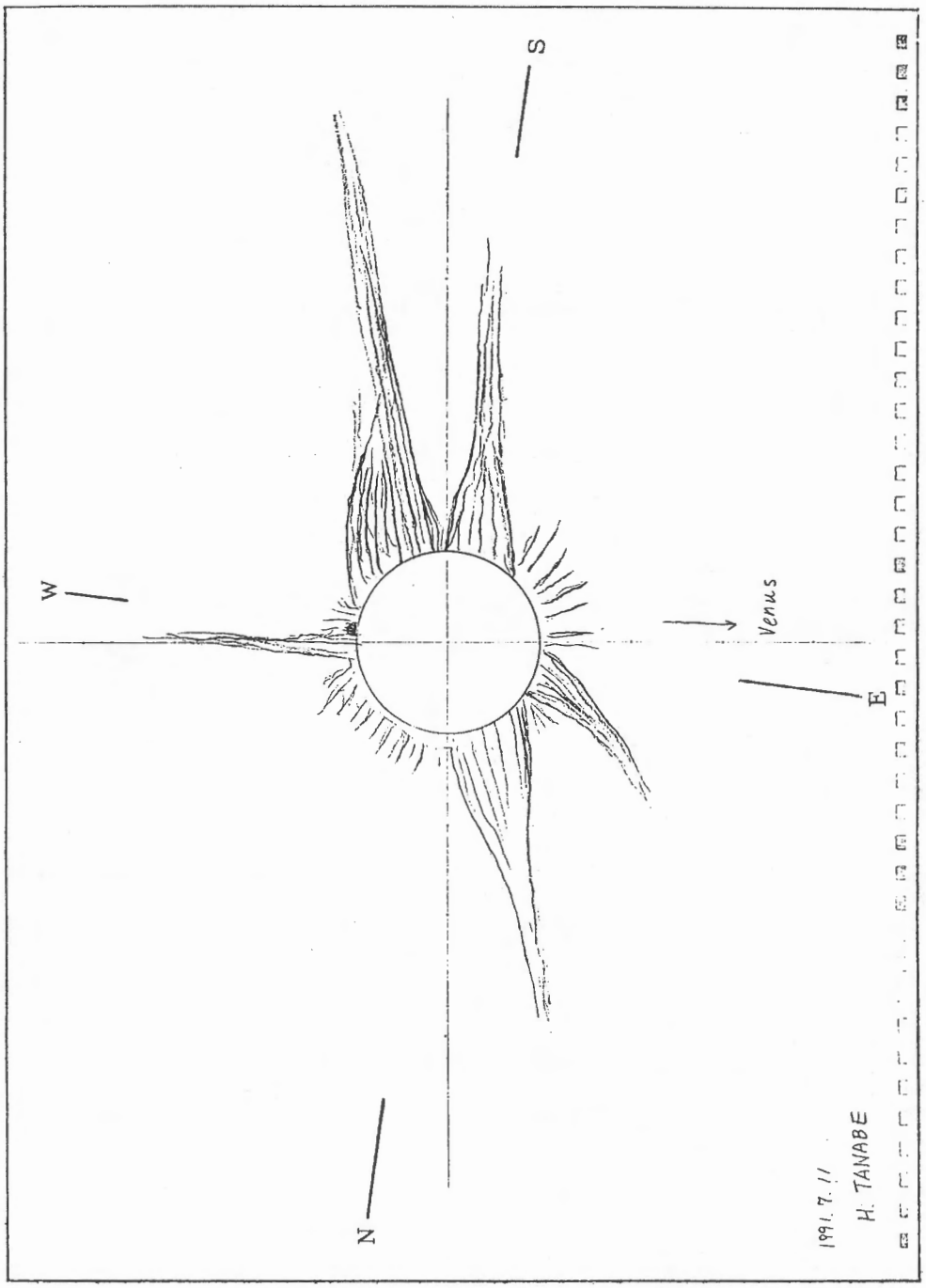

Fig. 1. Drawn by H. Tanabe (1715-8 Takao-machi, Hachioji, Tokyo 193).

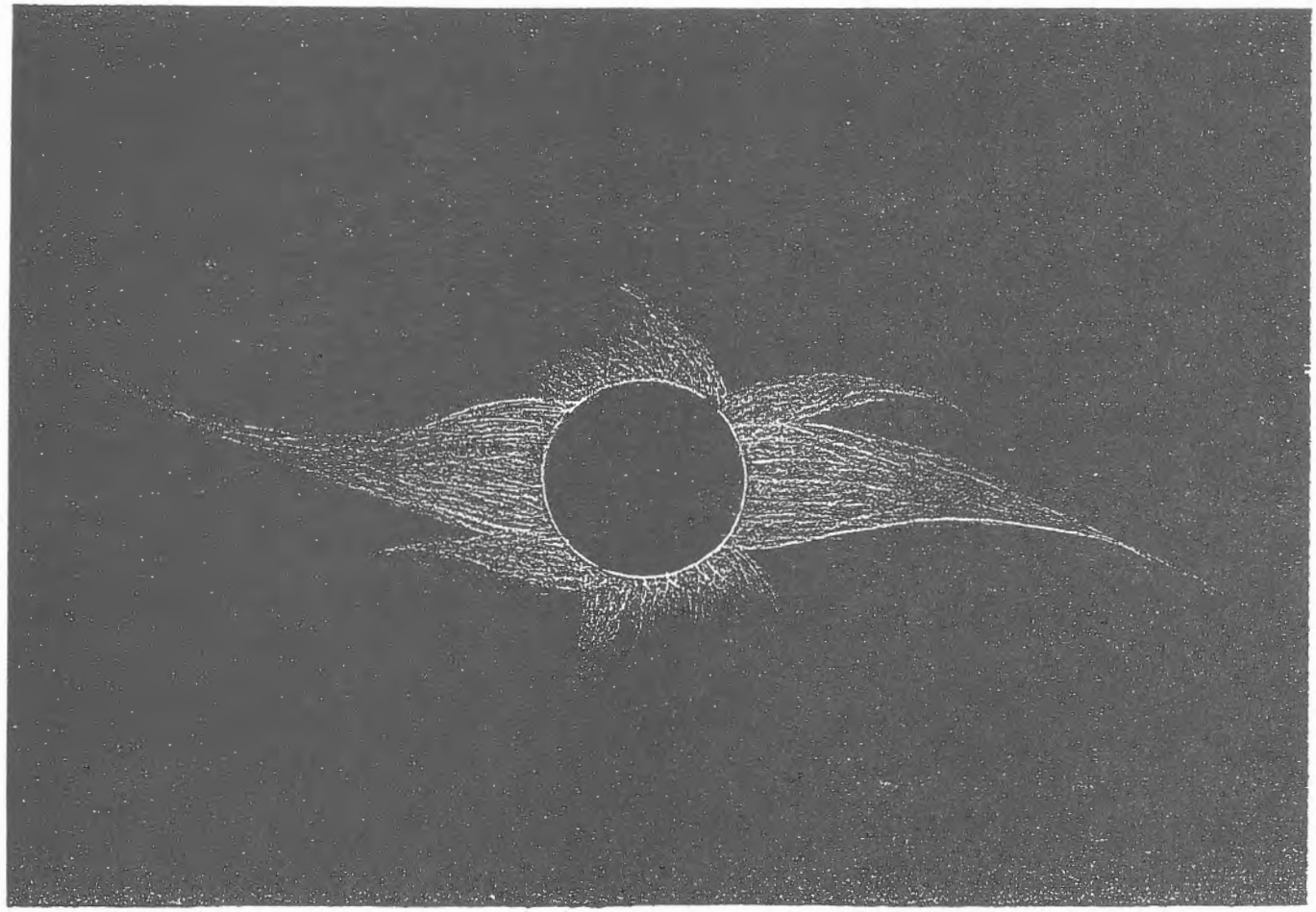

Fig. 2. Drawn by M. Aoki (3-16-8 Takeshirodai, Sakai, Osaka 590-01).

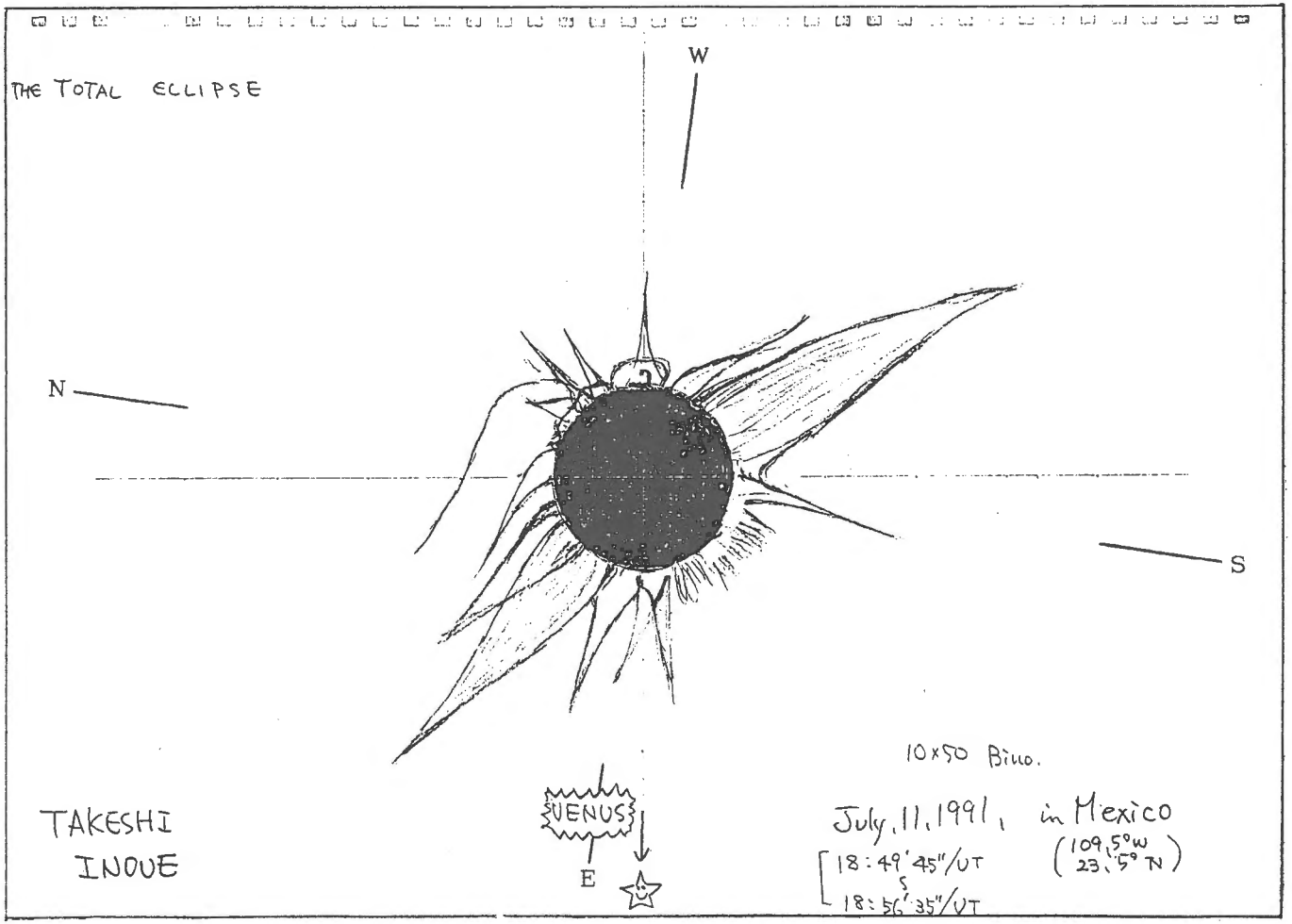

Fig. 3. Drawn by T. Inoue (Mizunoso 2-E, 1-54 Tamen-cho, Syowa-ku, Nagoya 466).

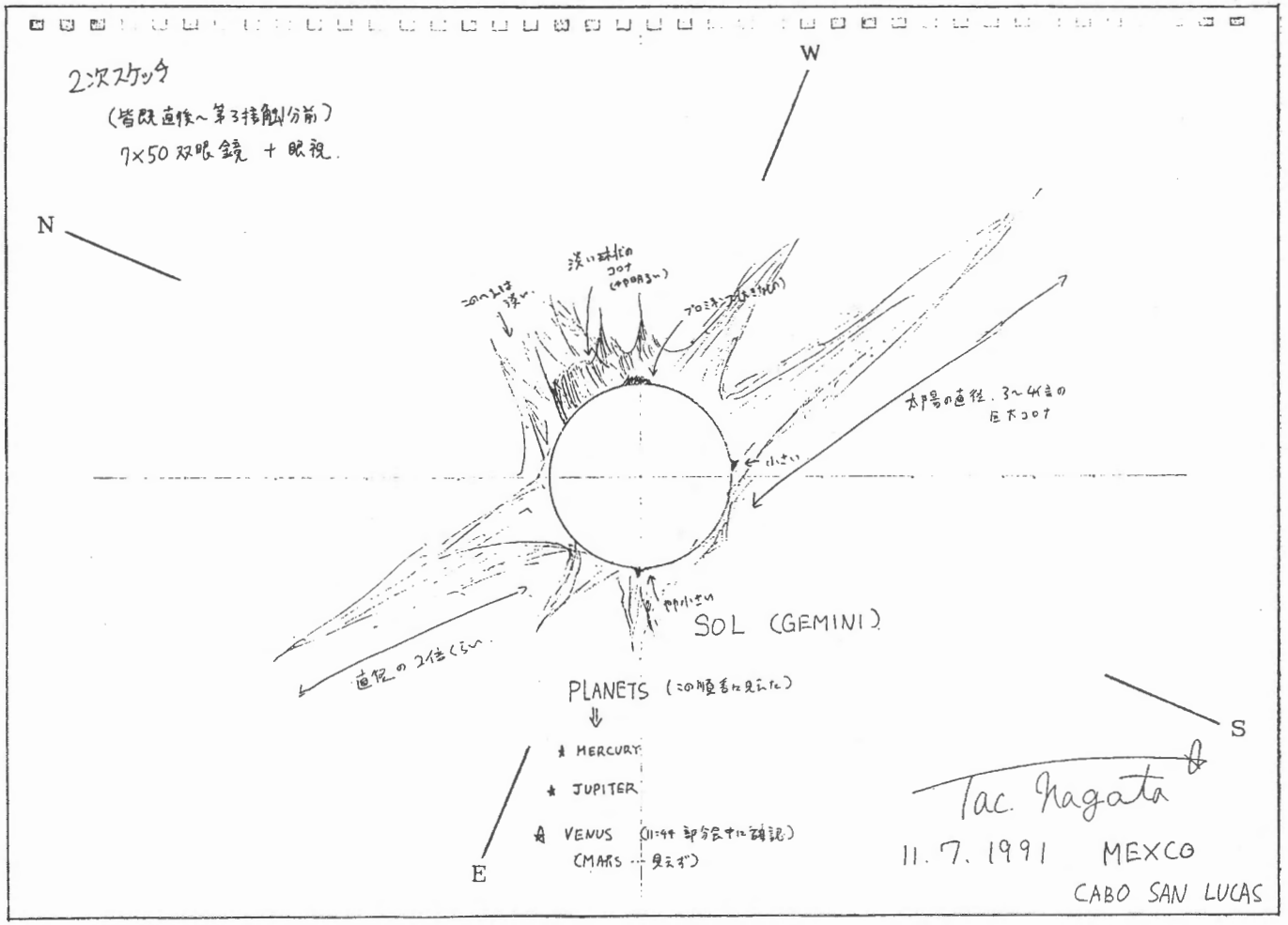

Fig. 4. Drawn by T. Nagata (Tatsukihaitsu 205, 108-2 Hirata, Ichihara, Chiba-ken 290).

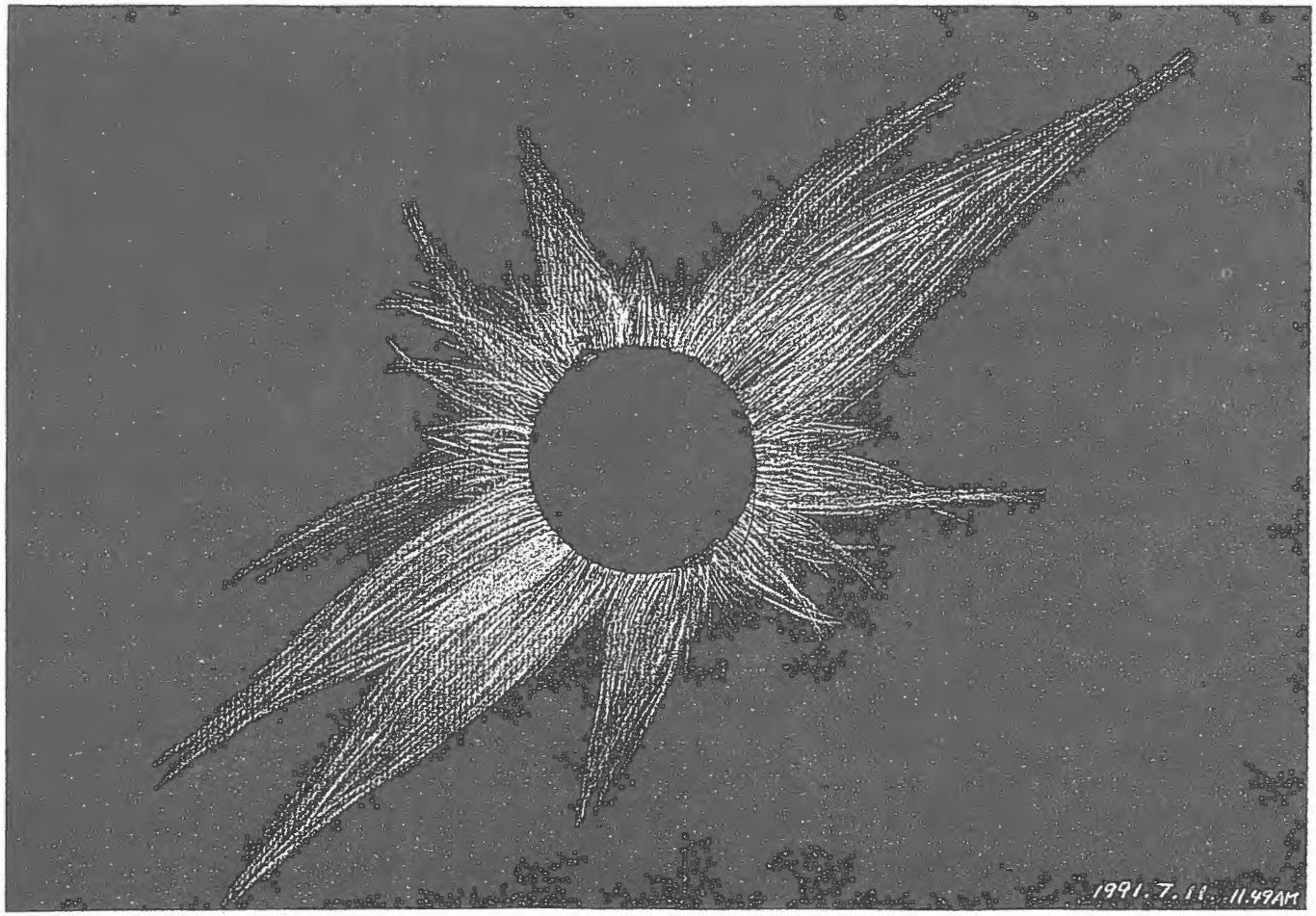

Fig. 5. Drawn by H. Shibayama (25-74 Nagitsuji-Kusakaido-machi, Yamashina-ku, Kyoto 607).

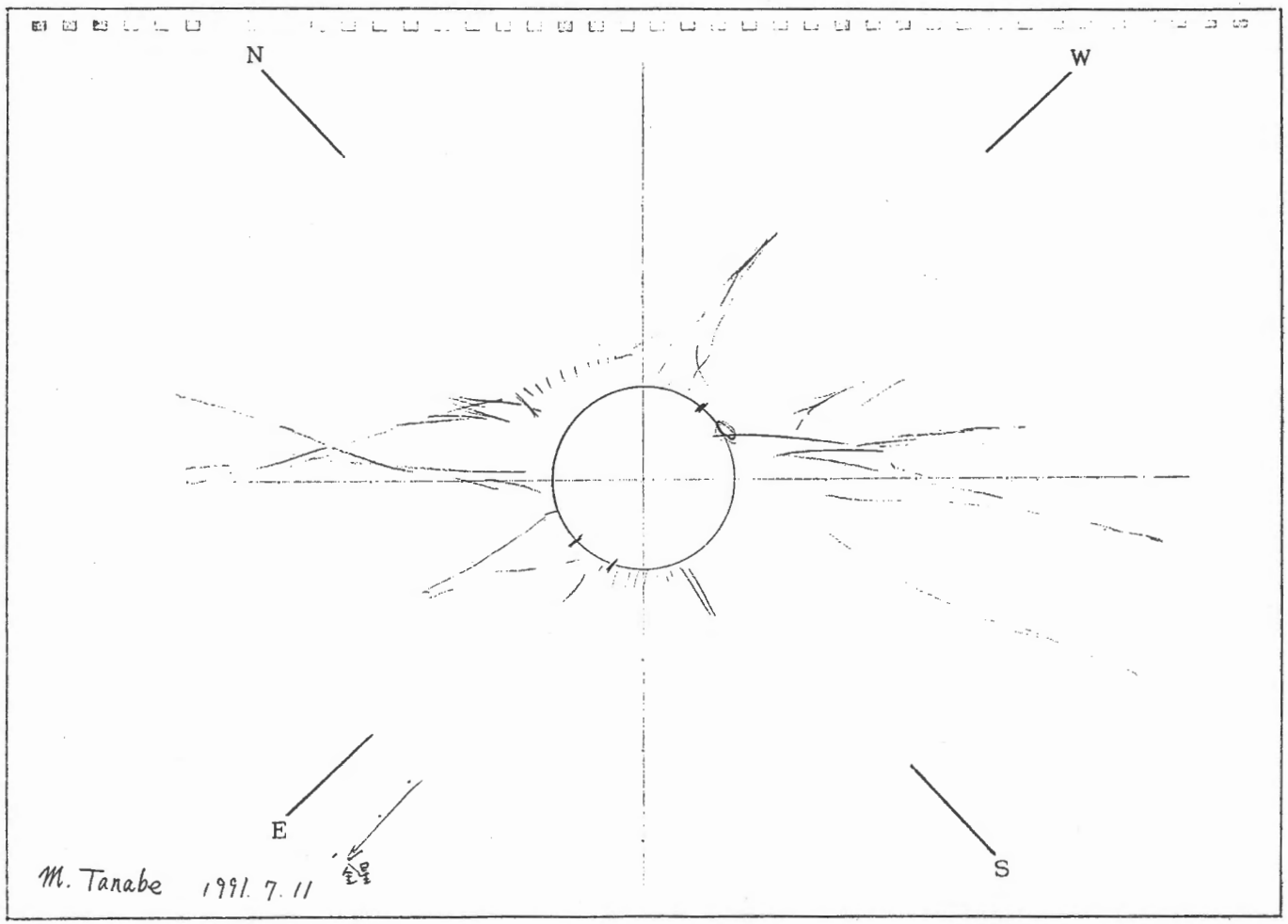

Fig. 6. Drawn by M. Tanabe (1715-8 Takao-machi, Hachioji, Tokyo 193).

1991年7月11日の皆既日食とコロナ面回転反転モデル

斎藤 尚生
(東北大・理)

ABSTRACT

Ten papers of us concerning the solar eclipse on July 11, 1991 are reviewed together with our previous papers related to the rotational reversing model of the coronal sheet.

In the first part of this paper, our studies on the north-south type coronal streamers, which were observed in the eclipse, are reviewed. Possible relations of the NS-type corona with the circular corona and the EW-type corona are discussed in the second part. The microstructure of the corona observed during the eclipse is discussed in the last part.

1. 緒言

今回の１９９１年７月１１日の皆既日食は、外部 corona に関して筆者がこれまで抱いていた沢山の謎を解いたように思われる。今回明らかになった事項をもし大別するならば、第１に、斜めに傾いた南北型corona が予測通り観測されたことであり、第２に、corona に関する３種類の形態学的矛盾が解けたことであり、第３に、corona に関する種々の微細構造が明らかになったことである。

南北型 corona の予測は、単なる気まぐれな思いつきではなく、約20年間の予備的な研究を集積した結果である。そこで第２節では、南北型 corona 発想の経緯を辿ることによって、論理的な積み重ねについての批判を仰ぎ、それによって将来の外部 corona 構造研究の役に立てることを目指そうとする。第３節では、今回の corona が従来の極大期型 corona に関する定説と、どの点で矛盾があり、その矛盾を筆者なりに、どのように解釈したかを述べる。第４節では、 今回の corona の微細構造につき、筆者が判断した解釈について述べる。

この小論は大上段に振りかぶった大 review paper ではない。従って引用も、筆者の考えてきたことを辿ることに主眼を置いたために、おのずと筆者等の論文に weight がかけられている。ここでは簡潔を期するために、詳細については、既に私達がこの日食などについて書いた論文または記事等約10編を読んで頂くことにする。またこの記事は、コロナそのものの専門研究者から、日食を目撃したいわゆる非専門家に至るまで、幅広い読者の眼に触れる可能性がある。従って「参考文献」にも、国際誌に限らず解説記事も併記することとした。

2. 南北型 CORONA

(1) 太陽風磁場や地球磁場観測 data を解析したところ、太陽活動極大期に、太陽圏中性面が黄道面に対して、直立している可能性があることを示唆した(図1. Saito, 1972)。

(2) 太陽活動極小期に東西型 corona が観測されるのは、その時期に太陽圏磁気中性面が黄道面にほぼ平行になり、かつ外部 corona が、中性面に沿って sheet 状に分布するから、地球から coronal sheet を見れば、sheetが東西に伸びて見えるせいであることを提唱した(図2. Saito, 1975)。

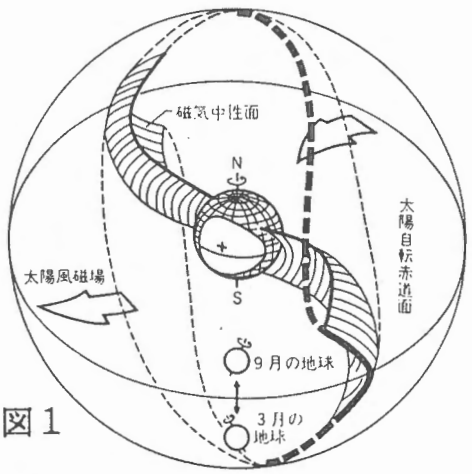

図１

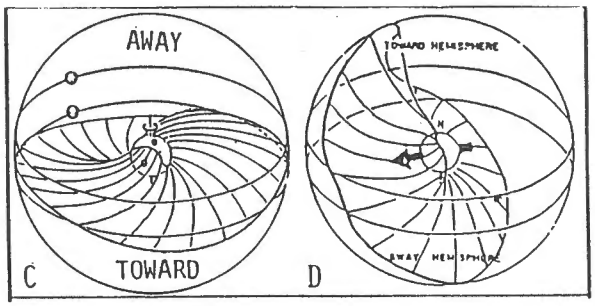

図3

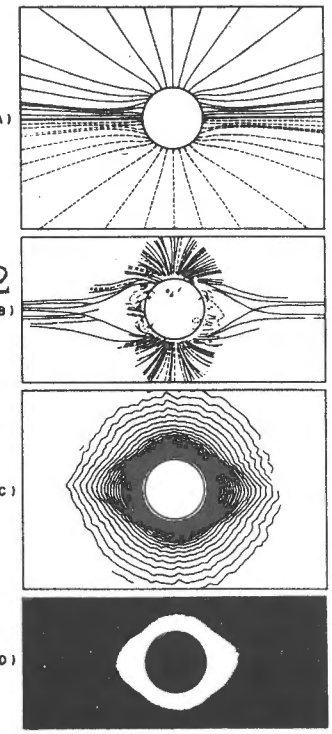

図2

(3) その太陽圏中性曲面は常に基本的には１枚であり、それが one solar cycle の間に回転反転することを提唱した。(1) (2)は二半球 model と名付けられたが、Prof. Alfven がつけてくれた、 balle-rina skirt model という nick name で呼ばれてきた(図3. Saito, 1975)。

(4) この model の当然の帰結として、極大期に直立した中性面に沿う coronal sheet が、自転位相角によっては南北型 corona として、地球から観測され得ること、ただし位相角の関係から、大抵は丸型 corona として観測されてきたという説を称えた(図4 Saito, 1980)。

図4

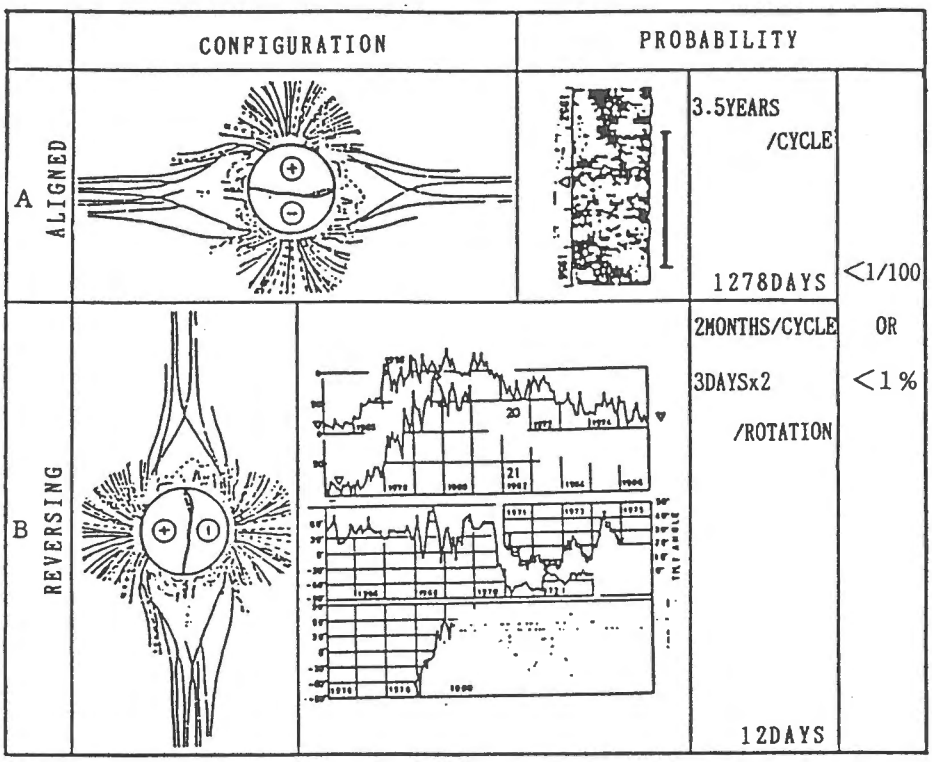

(5) 太陽圏中性面の回転反転が、Cycle Nos. 19～22 に共通した法則であること、どの cycle の極大期にも中性面が直立していること、を示す証拠が沢山出された(図5. Saito et al. , 1989)。

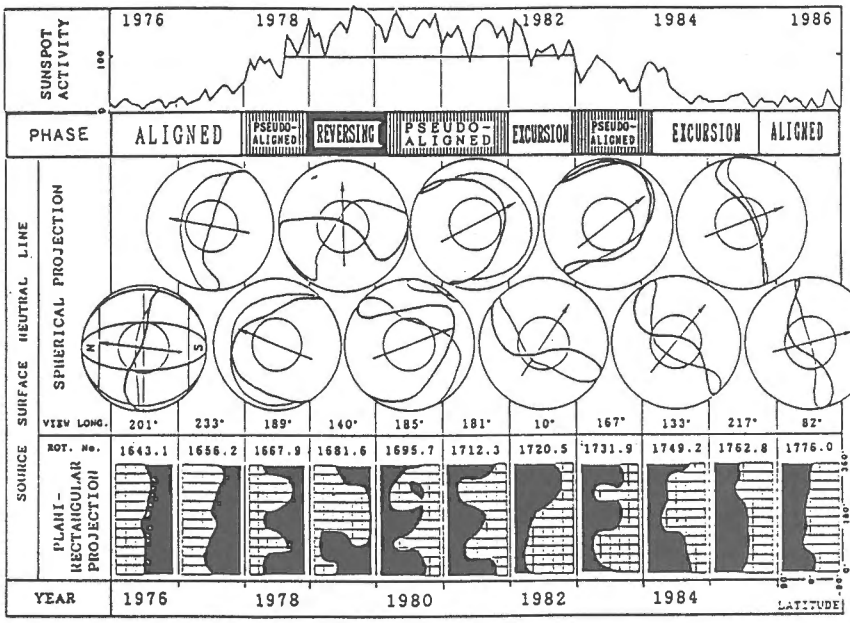

図5

(6) 太陽活動極大期ミッション衛星に搭載したコロナグラフ data を解析した結果、外部 corona の sheet がきれいに回転反転している事実を示し（図6）、かつ1980年 4月5日 にもし皆既日食がおこっていたら、 ほとんど正南北方向に伸びた streamer が観測されたであろうことを示した(Saito, 1991)。

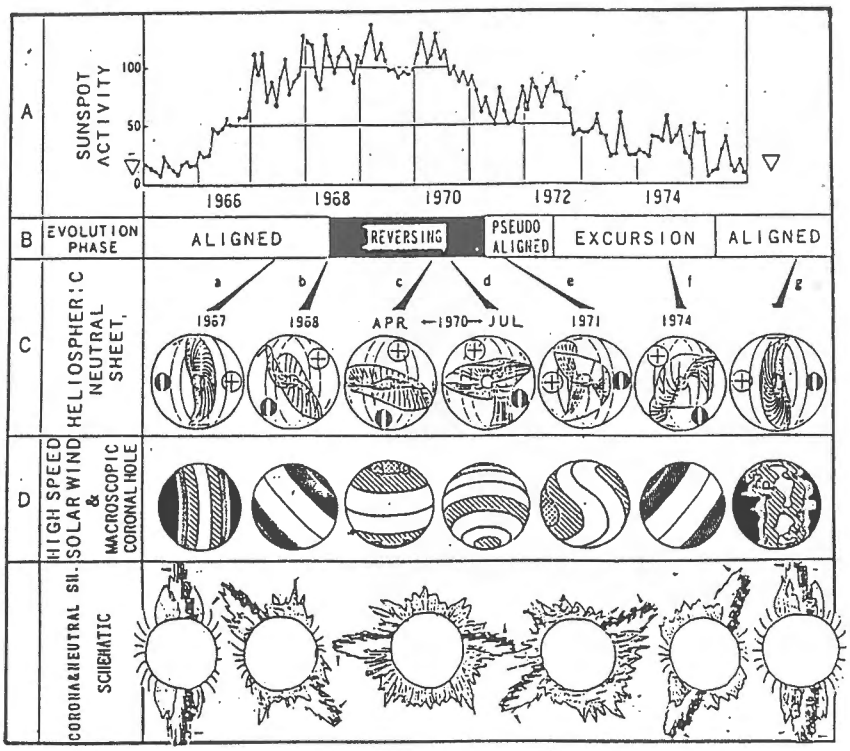

図6

(7) 1991年 7月11日日食の corona に関する予測的解析がいくつかなされた。1989年 7月から、入手可能限界の1991年 3月までの全磁場 data を用いて解析したところ、反転の間の1989年 5月、90年 1月と 6月の３回 corona 面は既に直立し終っていた。日食当日は図7に示すように、反転した瞬間を既に過ぎて、corona 面は緯度的にやや左傾した状態であることが判明し，日食日の一週間前の symposium で、次項の (8)(9)(10)と共に発表された(Saito et al. , 1991)。

(8) 更に自転に伴う中性面の経度的傾きを調べたところ、日食当日は、幸いにも図8に示すように、地球はほとんど中性面内にあり、中性面に沿った corona が、左傾した南北型 streamer として観測される確率がますます高くなった。

図7

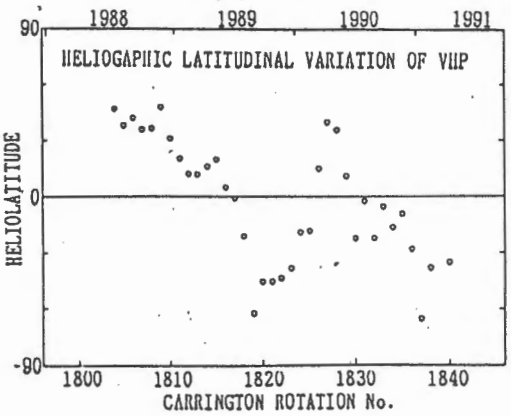

図8

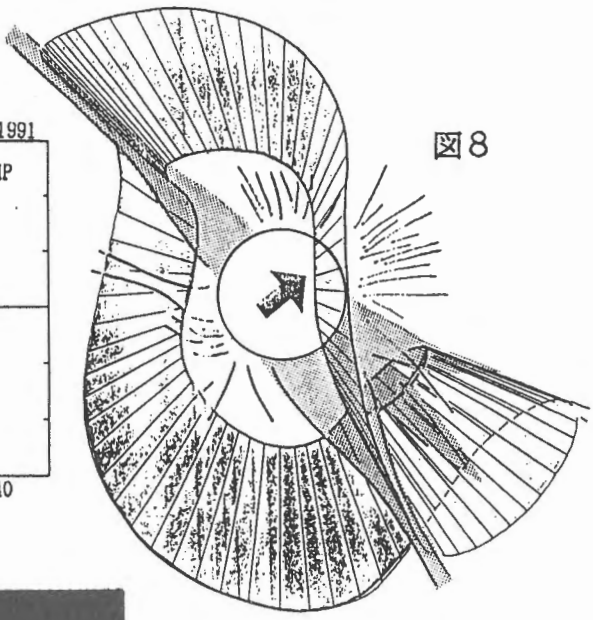

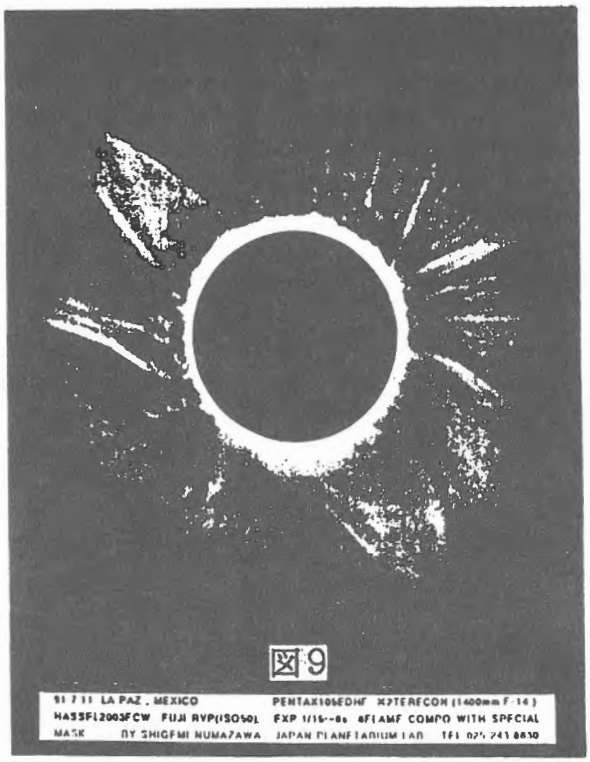

図9

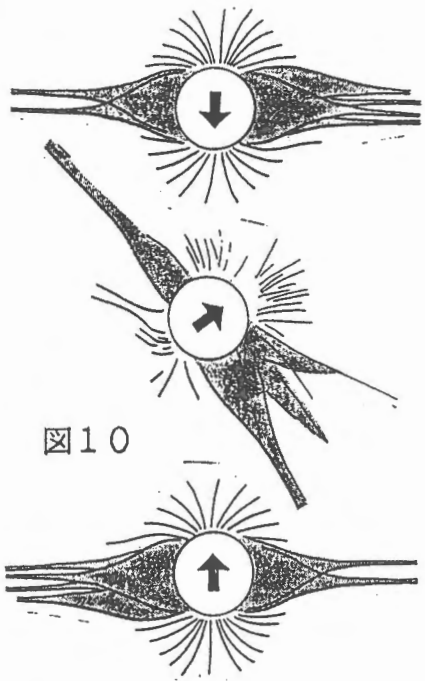

図10

(9) 日食当日は予測どうり左傾した南北型 streamer が現れた。図9は代表として沼沢の撮影による写真を示す。

(10) この極大期の特徴を抜き出し、極大期の corona (図2B参照) と並べると、図10に示すように外部 corona は常に一枚の曲面上に分布し、それが11年でくりりと反転するという corona 面回転反転説を、今回の日食はわかり易く説明したと結論することができる。

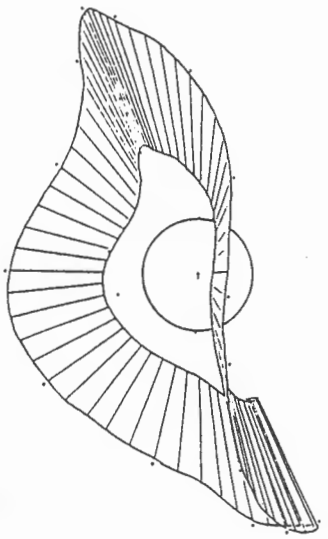

3．従来の定説との矛盾と解釈

(1) 南北型 corona の出現という現実に反して、永年のあいだ広く信じられてきた定説は、「極小期の corona は東西型、極大期の corona は丸型」というものであった。図11は、従来の教科書で度々引用されてきた典型的な丸型 corona を示す。

(2) この定説と、現実に観測された南北型 corona との間の矛盾に対する筆者の解釈は、次のふたつである。第１は、(南北型 corona を予言するときの根拠にもなった) 垂直 corona 面の「自転効果」(図12) であり、第２は「露出時間効果」である。図13に、自転効果の例を示す。即ち太陽が自転して、もし 7月 16日に皆既日食が起こったと仮定したとすると、図8と全く同じ垂直 corona 面も、図13に示すように天球面とほぼ平行になり、丸型 corona が見えた筈である(Saito, 1991)。

(3) 「露出時間効果」と名付けた解釈は次の通りである。今回の日食ですら撮影露出時間を長くかけて撮った写真を見ると、従来の、典形的な丸型 corona と全く変わらないような、丸い corona (図14参照) が撮影されていた。

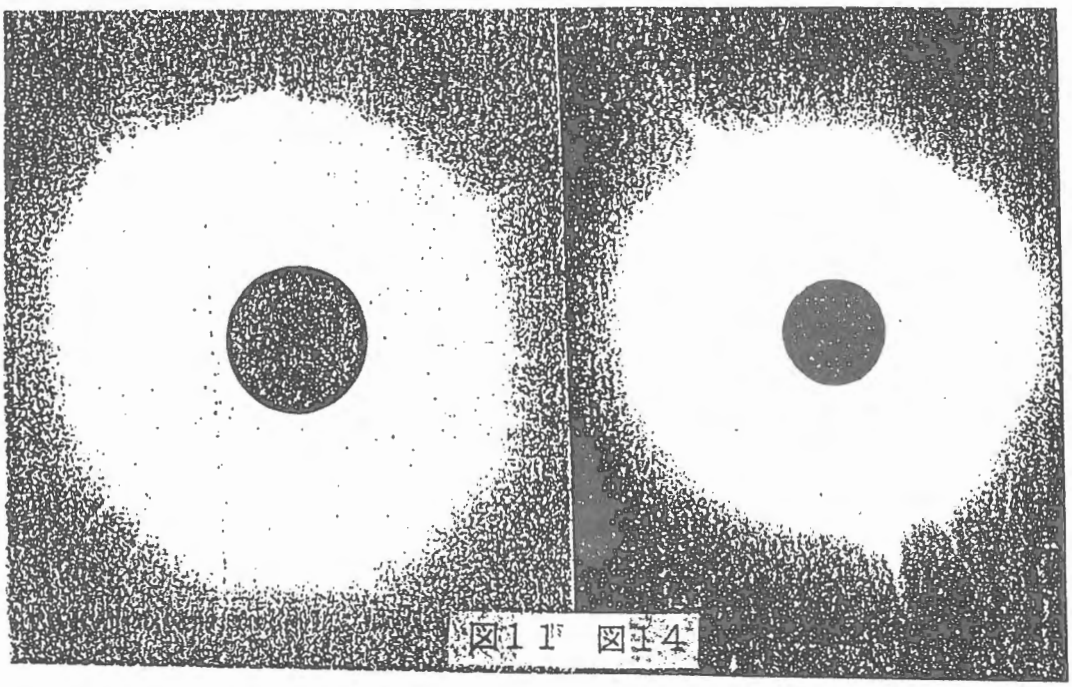

図11　図14

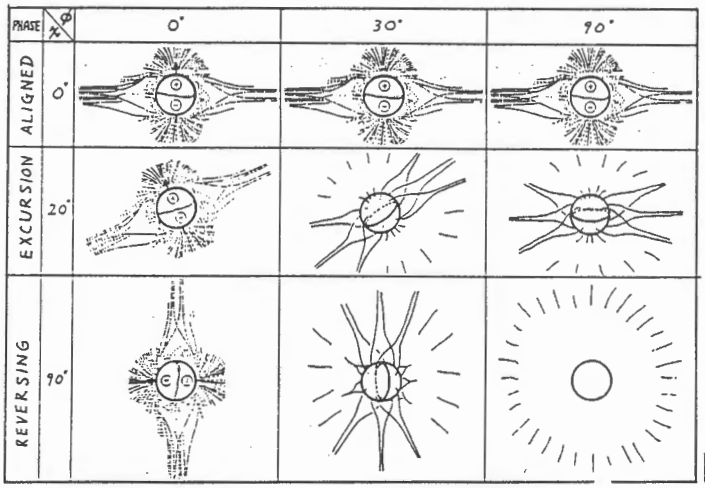

図１２

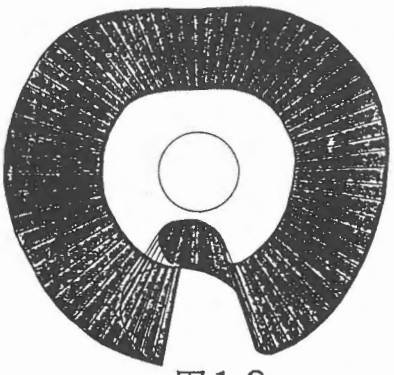

図１３

(4) 次に、極大期の丸型 corona と、東西型 corona に関する矛盾について述べる。
極大期には丸型 corona が現れる、という広く知られた定説があるにも拘らず、一方では外部 corona の形態に関して別の定説がある。それは太陽外部 corona の更に外側は、zodiacal light につながっており（図15参照）、zodiacal light の主軸は、太陽活動に依存せずほとんど不変である、という観測事実である。このことは、太陽の外部 corona は solar cycle phase に依存せず、空間的に常に黄道面即ち地球からみて東西方向に伸びていることを意味する。事実 apolo 飛行士が撮影した太陽 corona の最外縁は、図16に見られるように東西型であることを示している。

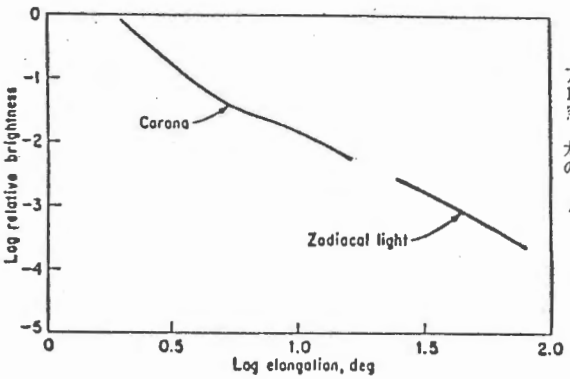

図１５

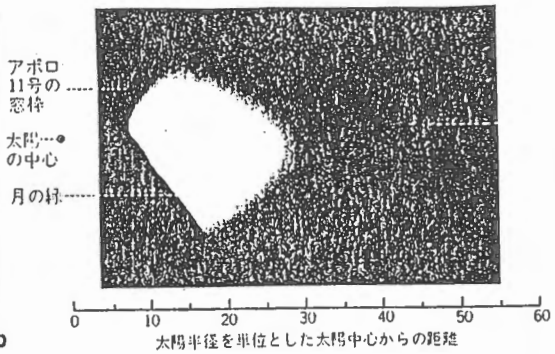

図１６

(5) この、丸型と東西型 corona の矛盾は、長時間露出した color 写真によって今回解決された。即ち須貝が color film を用いて、広角 lens で長時間露出で撮影した写真では、丸型 corona の外側に、赤味を帯びた淡い東西型 corona が広がっていた。図17で、最も外側に示した corona の等濃度線は、その一部を示す。

(6) 従って極大期の南北型および丸型 corona は、太陽磁場の影響を受けている plasma corona であるのに対して、zodiacal light に関係した東西型 corona は、dust corona という名称で区別することにより、電磁的組成的性質を特徴づけることができよう。

(7) 決定的には、今回の日食の外部 corona は、次のような構造を持っていたと言える。即ち露出時間が短ければ南北型、やや長ければその外側に丸型の plasma corona が写り、露出時間が更に長ければ、更にその外側に東西型の dust corona が写っていたのである。

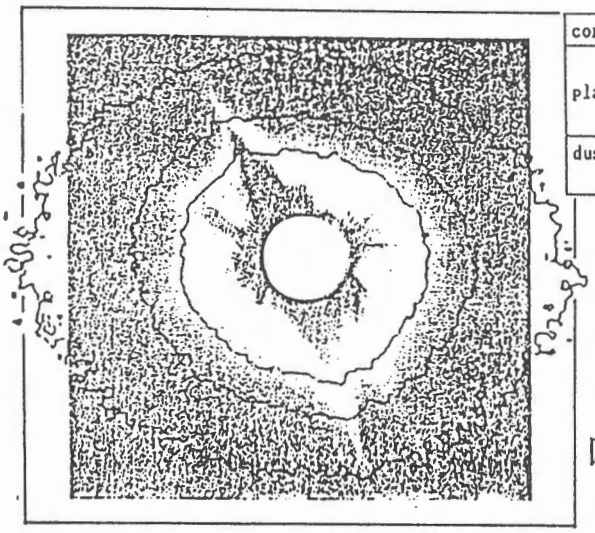

corona	形態	原因	主軸	電流面
plasma	南北型	磁気中性面 corona 面	radial	一致
	丸型	polar plume	non-radial	なし
dust	東西型	interplanetary dust	ecliptic	無関係

図１７

４．CORONA の微細構造

(1) corona は微細構造として、次の要素から成り立っていると考えられる。第１は、流源面中性線（磁気赤道）に沿う、helmet 型 corona 面である（図10および18）。

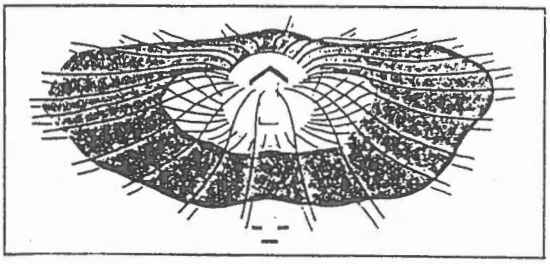

図１８

(2) 第２に、磁極冠から磁力線に沿って拡がる polar plume である。これはやや淡いが球状に外まで広がり、天球上に投影された形として丸型 corona の原因となっている。

(3) 第３に、active region から出ている streamer である。この streamer は、歪んだ磁場を反映して、non-radial である場合が多いが、一般的に外側では、等価中心双極子磁場に沿う傾向にある。

(4) 第４に、coronal sheet の一部分が全体に拡がって、(1)(2)(3) の背景を作っている。これは一般に地球が sheet 面内になく、また sheet 曲面を形成しているためである。(1)(2)(3)(4) が plasma corona である。

(5) 最後に、常に東西型に淡く拡がる dust corona である。

(6) (1) の helmet 低部の corona が乱れていないのは、active region 性でないからであると解釈できる。(1) は丸型 corona からはみ出した大きなツノを形成し、その性質から radial である。

(7) polar plume の根は磁気的に同極性であり、plume 内には電流面を挟み得ない。 従って末松等 (1991)によって指摘された「日心距離が増すにつれて太くなる」という観測事実が、説明できる。

(8) 等価中心双極子が回転反転している途中なので、自転軸より～30° 傾いている。従って自転軸まわりに polar plume が存在する極小期と異なって、磁極まわりの（地球から見て）北西面と南東部分に polar plume が異常分布していることもよく説明できる。

(9) (3) は丸型 corona からはみ出した小さなツノを形成する。

謝辞

本研究に当たっては、国立天文台、京大理、東北大理、そのほかの corona 専門家から貴重な discussion を頂いた。また写真等は専門家諸氏から頂いたと同時に、沼沢茂美、須貝秀夫、髙橋 実、千田広子、福島 円、そのほか多数の方々から貴重な資料を送って頂いた。ここに深く感謝する。

参考文献

Saito, T. , Recurrent magnetic storms in relation to the structure of solar and interplanetary magnetic fields, Rep. Ionos. Space Res. Japan, 26, 245-266, 1972.

Saito, T. , Two-hemisphere model on the three-dimensional magnetic structure of the interplanetary space, Sci. Rept. Tohoku Univ. , Ser. 5, Geophys., 23, 37-54, 1975.

Saito, T. , T. Sakurai and K. Yumoto, The earth's paleomagnetosphere as the third type of the planetary magnetosphere, Planet. Space Sci. , 26, 413-422, 1978.

Saito, T. , K. Yumoto and T. Tamura, Diagnostics of the heliosphere by means of ground-based ULF observation, Mem. National Inst. Polar Res ., Tokyo, Special Issue No.36, 64-72, 1985.

斎藤尚生，太陽に関する巨大斑磁場 model とその惑星磁場成因論への応用，宇宙科学研究所報告特集第15号，69-87，1986.

Saito, T. , Rotational reversing model of the heliospheric neutral sheet, 第７回太陽系科学シンポジウム，25-26，1986.

Saito, T. , and S. -I. Akasofu, On the reversal of the dipolar field of the sun and its possible implication for the reversal of the earth's field, J. Geophys. Res. , 92, A2, 1255-1259, 1987.

斎藤尚生・大木俊夫・赤祖父俊一・Olmsted，３双極子モデルによる太陽磁気圏２２年周期変化の解釈，第９回太陽系科学シンポジウム，33-35，1988.

Saito, T., and T. Oki, Rotation/recurrence relation among solar, interplanetary, and terrestrial magnetic fields,Proc.21th ISAS Lunar Planet. Symp., 52-58, 1988.

Saito, T., Solar cycle variation of solar, interplanetary, and terrestrial phenomena,in Laboratory and Space Plasmas, Ed. by H. Kikuchi, Springer, p. 473-528, 1989.

Saito, T.,and T. Oki, Interaction between the heliomagnetosphere and cometary magnetosphere, in Laboratory and Space Plasmas, Ed. by H. Kikuchi, Springer, p. 531-578, 1989.

Saito, T., T. Oki, S.-I. Akasofu, and C.Olmsted, The sunspot cycle variations of the neutral line on the source surface, J. Geophys. Res., 94, 5453-5455, 1989.

Saito, T. , T. Oki, C. Olmsted, and S.-I. Akasofu, A representation of the magnetic neutral line on the solar source surface in terms of the sun's axial dipole at the center and two equatorial dipoles in the photosphere, J. Geophys. Res., 94, 14993-14999, 1989.

Saito, T. , Y. Kozuka, T. Oki,and S.-I. Akasofu, The source surface and photospheric magnetic field models, J. Geophys. Res., 96, 3807-3810, 1991.

斎藤尚生，見えるかモヒカン刈り型コロナ，スカイウオッチャー7月号，72-75，1991.

斎藤尚生，天文ガイド6月号，1991.

Saito, T. , Y. Kozuka, T. Takahashi, and S. Numazawa, Meridian coronal sheet during sunspot maximum phase, Proc. 24th ISAS Lunar Planet. Symp., in press, 1991.

Saito, T., T. Takahashi, and Y. Kozuka, Reversing of the solar dipole field during the present solar cycle, Proc. 24th ISAS Lunar Planet. Symp., in press, 1991.

斎藤尚生・小塚幸央・竹内　仁・今崎　篤・荻野竜樹・渡辺堯，３双極子モデルによる太陽風流源面磁場の動画表示，第１２回太陽系科学シンポジウム，1-7，1991.

斎藤尚生，モヒカン刈り型コロナが見えた，月刊天文10月号，76-79，1991.

斎藤尚生，7.11皆既日食詳報：モヒカン刈り型コロナ，天文ガイド10月号，152-153，1991.

斎藤尚生，沼澤茂美，小塚幸央，赤祖父俊一，髙橋 実，千田広子，皆既日食資料によるコロナ面回転反転モデルの実証，太陽系科学シンポジウム論文集，1992（印刷中）.

斎藤尚生，小塚幸央，髙橋忠利，黒点活動サイクル No. 22 における太陽圏磁場反転の特性，太陽系科学シンポジウム論文集，1991.

斎藤尚生，須貝秀夫，小塚幸央，プラズマ・コロナとダスト・コロナ,太陽系科学シンポジウム論文集，1991.

Airborne and Rocket-borne Observations of Total Solar Eclipses

Ichiroh TOHMURA
Osaka Prefectural College of Technology
Neyagawa, Osaka 572, JAPAN

Abstract

An overview of airborne and rocket-borne observations of total solar eclipses is given. Most of them were performed in far-infrared(IR) wavelength region which reveals the physical state of the upper photosphere and the lower chromosphere, or in near-IR radiation from the outermost corona of the sun. From far-IR observations, spicular or non-spicular inhomogeneities in the photosphere and/or chromosphere have been suggested, while an excess of radiation was reported from near-IR observations. Finally, a rocket-borne EUV observation of the chromosphere-corona transition region with high spatial and temporal resolution during a total solar eclipse is proposed by the author.

1. Eclipse Observations in Far-Infrared Region

The most prominent feature discovered from far-IR observations will be the inhomogeneity in the upper photosphere and/or lower chromosphere. At first, Beckman et al.(1975) observed the 1973 African eclipse using the Concorde supersonic aircraft. They reported that narrow but intense 'spikes' near the solar limb extend from 5 arcsec inside to 4 arcsec outside the white-light limb at λ =400, 800, and 1200 μm.

In order to verify this finding, Clark and Boreiko(1982) performed a rocket-borne observation at λ =400 μm during the 1979 northern-American and southern-Canadian eclipse. They found no such 'spikes' as reported by Beckman et al.(1975) but suggested non-spicular inhomogeneities in photosphere and/or chromosphere from the comparison between their observed light curve and calculated ones from solar model atmospheres. The answer to this problem seems to be still unclear.

On the other hand, 'limb extension' in λ =30 - 800 μm was reported by Roellig et al.(1988). They observed the 1988 eclipse using the Kuiper Airborne Observatory to find that the solar limb seen in this wavelength range extended beyond the visible limb, especially at 400 μm and 800 μm by ~5 arcsec. Their result provided an important restriction to the modeling of spicules.

2. Eclipse Observations in Near-Infrared Region

Eclipse observation in this wavelength region is considered to reveal the distribution of interplanetary dust around the sun. The existence of excess of IR radiation at ~4 solar radii from the sun was firstly reported by Peterson(1967) at 2.2 μm during the 1966 total solar eclipse and later was confirmed by McQueen(1968) with a balloon-borne coronagraph. Peterson(1971) obtained similar result while Rao et al.(1981) detected no such 'IR excess'.

Mizutani et al.(1984) performed a balloon-borne observation at 1.25 μm, 1.65 μm, 2.25 μm, and 2.8 μm during the 1983 Indonesian eclipse. They recorded emissions in excess of the strong coronal background emission at ~4 solar radii from the sun. Further extension of this observation was carried out during the 1991 Hawaiian-Mexican eclipse(Isobe, 1991).

3. A Research Proposal : Rocket-borne Eclipse Observation in EUV

Few eclipse observation in extreme ultraviolet(EUV) wavelengths, which is highly important to the physics of the chromosphere-corona transition region (C-C TR), have been reported. Therefore, here we propose a rocket-borne observation of total solar eclipses in EUV region.

Our proposed observation is as follows; in order to study the fine structure of the chromosphere-corona transition region, which will enlighten the physics of outer solar atmosphere(especially the heating problem of the chromosphere and corona),

(1) flash or curved-slit spectra (or narrow-band filtergrams) shall be taken during total solar eclipses using a rocket-borne telescope and spectrograph in EUV wavelength region such as Lyman alpha, CII,CIII, OIV, or SiIII lines,
(2) with high spatial and temporal resolution(at least, spatially ~1 arcsec and temporally ~1/60 sec),
(3) using high-speed CCD camera which is optimized for solar observation.

It is believed that the structure of the C-C TR is one of the most important problem because it is closely related to the structure of the chromosphere and hence also to the mechanism of the chromospheric and coronal heating(e.g. Rabin and Moore, 1984; Antiochos, 1984; Antiochos and Noci 1986). Dere et al.(1987) obtained the evidence for discrete subresolution structures in the C-C TR from the NRL High Resolution Telescope and Spectrograph(HRTS) during the Spacelab-2 mission.

Our proposed observation is expected to extend the results by Dere et al.(1987). With its high spatial resolution it will show us the horizontal fine structure of the C-C TR and with the temporal one, the vertical fine structure. Such high-resolution observation requires a newly-developed equipment, or the high-speed CCD solar camera proposed by Hanaoka(1991).

This observation will surely provide us useful tools to answer the questions about the physics of the solar outer atmosphere.

References.

Antiochos(1984) *Astrophys. J.*, **280**, 416.
Antiochos and Noci(1986) *Astrophys. J.*, **301**, 440.
Beckman et al.(1975) *Nature*, **254**, 38.
Clark and Boreiko(1982) *Solar Phys.*, **76**, 117.
Dere et al.(1987) *Solar Phys.*, **114**, 223.
Hanaoka(1991) *appeared in this proceeding.*
Isobe(1991) *appeared in this proceeding.*
McQueen(1968) *Astrophys. J.*, **154**, 1059.
Mizutani et al.(1984) *Nature*, **312**, 134.
Peterson(1967) *Astrophys. J. Lett.*, **148**, L37.
Peterson(1971) *Bull. Am. Astron. Soc.*, **3**, 500.
Rabin and Moore(1984) *Astrophys. J.*, **285**, 359.
Rao et al.(1981) *Nature*, **289**, 779.
Roellig et al.(1988) *Bull. Am. Astron. Soc.*, **20**, 689.

Lyman α Observation from a Rocket

E. Hiei

Lyman α observation at the total solar eclipse is one of a promicing way for the determination of the cooler matter surrounded by million degree plasma, and velocity field of solar wind. Outside of the eclipse Kohl et al. (1982) observed Ly α in the corona by using a coronagraph, flown by a rocket.

Figure 1 shows a rough sketch of the instrument for the observation. The size of the instrument depends on the size of a rocket for the observation. If we use a grating with 2400 grooves/mm, then a linear dispersion is 8 A/mm. A pixel size of MCP of 30 μ corresponds to 0.24$\AA$, which can detect a velocity shift of solar wind with a few ten km/s. If a solar wind move up perpendicularly to the line of sight, there is no shift in wavelength. However, Doppler dimming appears in this case and there may even detect the velocity field perpendicular to the line of sight direction.

References

Kohl et al. *Ap.J.* **254**, 361, 1982.
Kohl et al. *Ap.J.* **256**, 263, 1982.

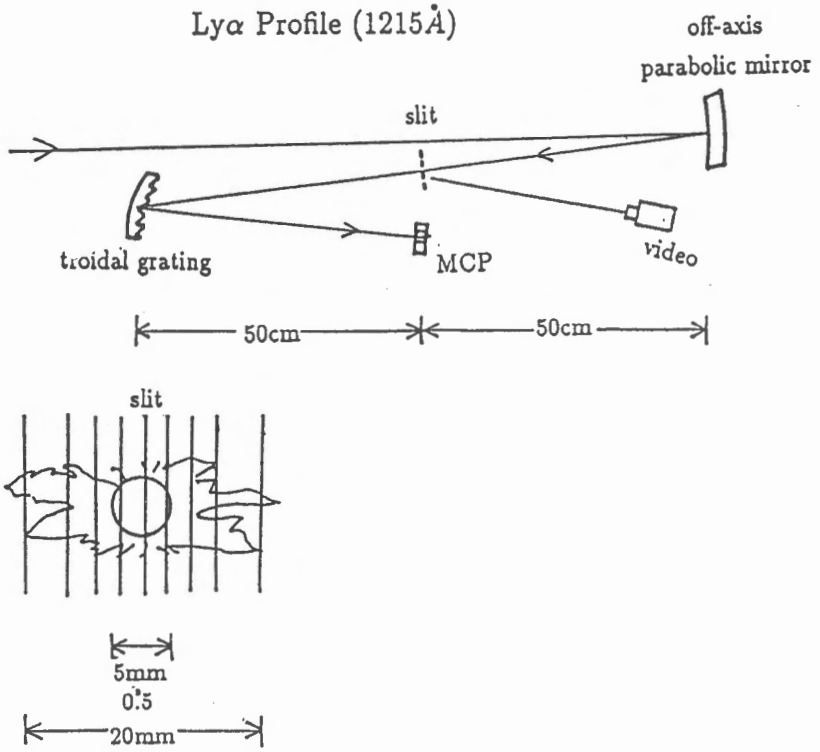

Observations of Contact Times at Total Solar Eclipses

Teruo KANAZAWA
Maritime Safety Academy
Wakabacho 5-1, Kure-shi,
Hiroshima 737, JAPAN

Abstract

Observations of contact times at total solar eclipses have been conducted by the Hydrographic Department of Japan to check and improve astronomical ephemerides. Flash spectra of the second and the third contacts of a total solar eclipse are recorded by a 16mm movie camera together with time marks from a calibrated clock. Density of the film along the position angle of the sun is measured and transformed into intensity of light, and contact times along each position angle are determined. Applying corrections of the effects of lunar surface height at each position angle, we obtain relations between the centers of the sun and the moon. Precision of the observation reaches 0.01".

1. Introduction

Hydrographic Department of Japan (JHD) has been publishing astronomical ephemerides (Japanese Ephemerides) since 1943. Observations of the sun and the moon are necessary to check and improve ephemerides. But, observation of the position of the sun is difficult than that of the moon because of the brightness of the sun. Total solar eclipses give us good chances to measure relative positions between the sun and the moon precisely, because the sun and the moon locate nearly the same direction and the brightness of the sun is lost.

The observations of the solar eclipses carried out by JHD are listed in Table 1. Some earlier observations are conducted in spite of bad conditions as they occurred in Japanese territory. Others are chosen by their good conditions and these can be grouped into 5 saros series. They are shown as a-e in Table 1.

2. Method of observation

Because the light from the sun is still quite bright at annular eclipses as well as the first and the forth contacts of total solar eclipses, precise observations are limited at the second and the third contacts of total solar eclipses. The method described below has been adopted since the observation of the 1970 solar eclipse.

At the second contact of a total solar eclipse, the sun becomes a thin arc and the arc shrinks from its both ends. As the surface of the moon is not smooth, the mountains of the moon's limb cut the sun's arc and make Baily's beads. The ruggedness of the moon's surface reaches a few seconds of arc and it is essential to correct these effect in observing contact times.

Table 1. Solar eclipse observations carried out by JHD.

Date				Observation site
1948	May 9	A		Rebun-to (Japan)
1955	June 20	T	a	Vietnam
1958	Apr. 19	A		Amami O-sima, Takara-jima, Aoga-sima (Japan)
1958	Oct. 12	T	b	Suvorov (North Cook Is.)
1962	Feb. 5	T	c	Lae (Papua New Guinea)
1963	July 20	T		Abasiri (Japan)
1965	May 30	T	d	Manuae (Cook Is.)
1970	Mar. 7	T	e	Mexico
1973	June 30	T	a	Mauritania
1976	Oct. 23	T	b	Australia
1980	Feb. 16	T	c	Kenya
1983	June 11	T	d	Indonesia
1991	July 11	T	a	Mexico

A: Annular eclipse, T: Total eclipse,
a-e: the same saros series.

Chromosphere is another disturbing source in observing contact times. It lies just outside of photosphere and emits many emission lines. In order to observe the edge of the sun precisely these emission lines of the chromosphere should be avoided.

Considering these conditions, we adopted a method to disperse the light of the sun into a spectrum with a prism and record its change with a 16mm movie camera. An example of the spectrum (so called flash spectrum) is shown in Figure 1. The continuum light comes from parts of the sun's arc which are not obscured by the moon's mountains and many emission lines from the chromosphere appear as the same shape of the sun's arc.

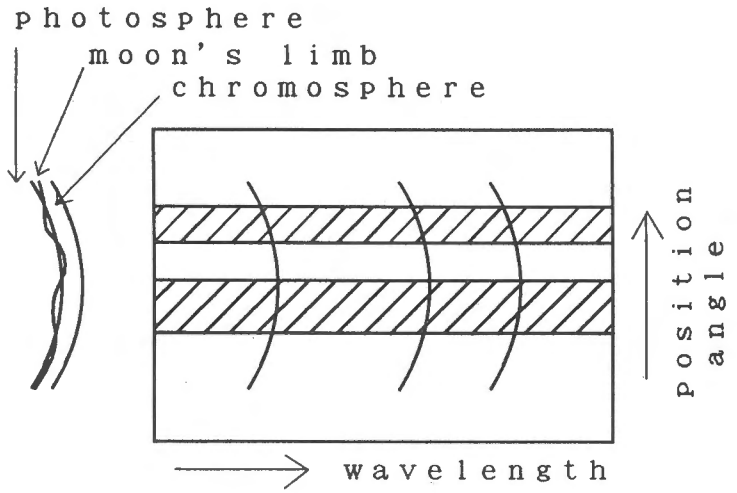

Figure 1. Flash spectrum.

3. Equipments

Equipments to record the flash spectrum consist of a prism, a telescope and a 16mm movie camera which are supported on an equatorial mounting. We don't need a slit before the prism because the sun's arc is so thin that we may consider the light parallel. Figure 2 shows the schematic diagram of the equipments. The prism is an objective direct version type of 60mm x 60mm in size and consists of a SF2 prism put between two BK7 prisms. It passes the light of 486nm in wavelength strait. The aperture and focal length of the telescope are 80mm and 1200mm, respectively. The dispersion of the spectrum is 7nm/mm at 486nm. The movie camera is a Bolex H16's type which is driven with an electric motor. The telescope tube is supported by two rings with bearings and can be rotated around its optical axis in order to make the direction of the dispersion perpendicular to the direction of the sun's arc.

Time signals are sent from a crystal oscillator and recorded on a edge of the film with a light emitting diode stimulated by these time signals. Time marks are recorded every 1/10 second, 1 second, 1 minute and 1 hour. Differences of the lengths of these time marks are used to identify the time. The time signals of the crystal oscillator are calibrated by using the standard time signals broadcasted on the short wave. As the speed of the moon's motion is the order of 1" (second of arc) in 1 second of time, we need precision of 0.01 second in time to attain precision of 0.01".

4. Observation

An arc of 0.01" at moon's distance is about 20m. So, we

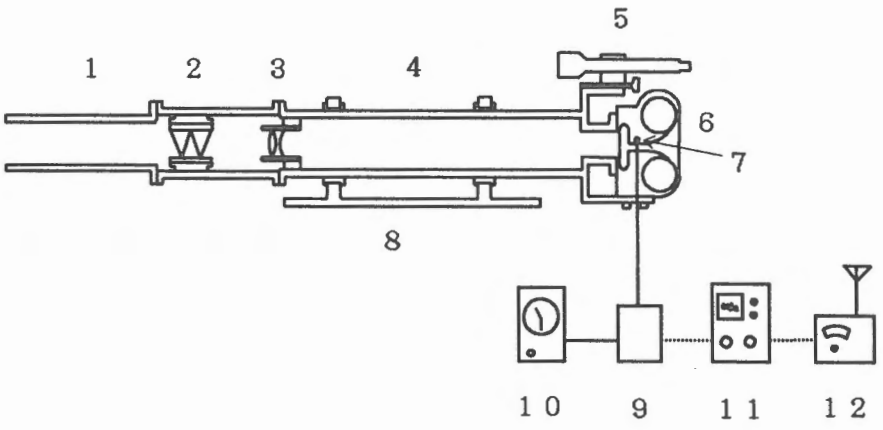

1. hood
2. prism
3. lens
4. body
5. guide telescope
6. 16mm movie camera
7. light emitting diode
8. mounting attachment
9. an electronic circuit
10. quartz oscillator
11. synchroscope
12. short wave radio receiver

Figure 2. Observing facilities.

must know the location of the observation site on the surface of the earth with 20m of precision to get the relative positions between the sun and the moon with 0.01" precision. Since the late 70's Navy Navigational Satellite System is applicable to this purpose.

The observations of the second and the third contacts are carried out by operating the 16mm movie camera for about a minute at each contact time. Additional shots are taken within a few hours after totality to obtain the characteristic curve of the film, that is, the relation between the density of the film and the intensity of light. To make this, the hood in Figure 1 is replaced by a slit and a collimation lens. The intensity of light is changed in a very wide range by the combinations of the width of the slit and insertion of one of neutral density filters in front of the 16mm camera.

5. Data reduction

The density of the film is measured with a microphotometer. We select 461.5nm of wavelength to be measured where the emission lines of chromosphere seem sufficiently weak. We measure along a strait line perpendicular to the direction of the dispersion with a rectangular slit of 100 microns x 20 microns. The length of 100 microns corresponds to the wavelength of 0.7nm and the 20 microns corresponds to position angle of 0.2 degrees of the moon's limb. The position angle of each frame must be identified by the density profiles of prominent valleys and mountains of the moon's limb. Then change of the density at each position angle can be traced from one frame to another.

The characteristic curve is drawn from the shots taken with a slit and one of neutral density filters. The density is transformed into the intensity of light by using this characteristic curve. The intensity change along the radius at the edge of the photosphere is shown schematically in Figure 3. In order to keep consistency of the radius of the sun, inflection point of this intensity change curve is used to determine the contact time at each position angle. Because background scatter of light increases rapidly as the sun's arc gets long, the measurement of this method is limited for about 20 degrees of position angle at each contact.

Figure 3. Intensity curve at the edge of the sun.

The corrections for the ruggedness of the moon's limb are obtained from Watts'charts (Watts, 1963). These charts delineate heights of the moon's limb at given position angles as function of libration of the moon. Heights of the moon's limb are drawn as equal height contours of every 0.2 degrees. Resolution of position angle is 0.2 degrees and 1800 charts cover the whole

limb. As values of libration of the moon at a solar eclipse are given, we consult these charts one by one and get the height of the moon's limb through an interpolation of the contours with a precision of a few hundredths of a second of arc.

Applying these corrections of the height of the moon's limb, contact times of the moon's datum with the defined edge of the sun's photosphere at every 0.2 degrees of position angle are obtained. Then the relative positions between centers of the sun and the moon are calculated. It is easily observed from the geometry of the two circles that the precision of determining the relative positions between the centers of the sun and the moon reaches 0.01" in the direction perpendicular to the sun's arc and 0.1" in the direction parallel to it.

When the observation is made near the central line of totality, the position angles of the second and the third contacts occur about 90 degrees and 270 degrees, respectively. In this case east-west component of the relative positions between the centers of the sun and the moon is well determined than that of north-south component. As the observation site gets away from the central line of totality, the position angles of contacts approach to 0 degrees or 180 degrees, and these observations contribute to determine north-south component. In some cases of our recent observations, an observation near the northern or southern limit of totality were added to the observation near the central line of totality to make geometrical conditions better.

Obtained results are compared with the predictions from ephemerides. Differences between them are typically a few hundredths of a second of arc (Mori and Kubo, 1971). This means that the accuracy of the ephemerides are in balance with that of observations.

6. Future improvement of the observation method

In order to observe relative positions between the sun and the moon, the principle of our method, that is, to record the flash spectra of the second and the third contacts of total solar eclipses and measure the changes of the continuum light from the photosphere seems to be the best at present. On the stand point of technical advances, 16mm movie camera are going to become obsolete to record images and video camera or some devices utilizing CCD (charge coupled device) and computers are in fashion. We are ready to adopt these techniques if they satisfy our needs of resolutions in space and time and of keeping absolute time records. Positioning method on the surface of the earth will be replaced by Global Positioning System (GPS).

Even if the resolution of the measurements may improve in future, precision of final results is limited by the corrections of lunar limb about which we depend on Watts charts at present. More precise information of the lunar limb is necessary to improve overall precision of the results. If observations may give more precise results, efforts to improve ephemerides should be done to keep pace with the advancement of observations.

References

Mori, T. and Kubo, Y., 1971: Report of Hydrogr. Res., Vol.7, 39.
Watts, C. B., 1963: Astr. Pap. Amer. Eph., Vol.17, 1.

Temperature Structure of Active Region Coronal Loops

Yoichiro Hanaoka

Nobeyama Radio Observatory, National Astronomical Observatory

Observations of the active region coronal loops made at EUV and X-ray wavelengths during the Skylab mission showed the loop structures both at transition region temperatures and at coronal temperatures. The structures of the cool matter($< 1 \times 10^6$K) are much different from those of the hot one($> 1 \times 10^6$K). However, temperature structure of a single loop remain unresolved.

Foukal(1975) analized the data taken with the S055 instrument on board the Skylab, which is used to get spectroheliograms in the wavelength range of 300-1400 A. He obtained the results that an active region coronal loop has a density which is 3-4 times higher than surrounding coronal matter, and that it has a cool core surrounded by a hot sheath. The calculated density of the cool core is not so different from that of the hot sheath. Foukal(1976) concluded from the 22 observations with the S055 that the hot-sheath/cool-core structure is general in coronal loops. Since the intensity scale height of the cool loops is much higher than the hydrodynamic scale height, cool matter is unstable; it must flows down and the matter is supplied from the hot sheath across the magnetic field lines. Levine and Withbroe (1977) confirmed the hot-sheath/cool-core structure also from the S055 observations, and concluded the diameter of the cool loops is several hundred kilometers.

However, Cheng(1980), Cheng et al.(1980), Sheeley(1980) and Dere(1982) obtained the different results, also from the Skylab observations but with the S082A instrument, which is used as a photographic spectroheliograph. They concluded that the hot loops are compact but the cool loops are extend, and they are independent loops. This inconsistency may be explained by the assumption that developing loops or transient loops have cool cores, but quiescent loops do not (Webb 1981, Pneuman and Orrall 1986); but it is not decisive. We can not reject a possibility that this discrepancy is caused by the instrumental effect, because the authors who used the same instrument obtained similar results. Therefore observations with different methods are required to solve this problem. At the eclipse of February 16, 1980, high resolution monochromatic photographs of the coronal loops are taken in emission lines of Fe X 6374(1×10^6K) and Fe XIV 5303(2×10^6 K) and in continuum(Hanaoka et al. 1988). The observed active region coronal loops have the cool-core/hot-sheath structure, and this result is consistent with Foukal's(1975 and 1976). However the derived density of the cool loops is much higher than that of the hot loops, and that the cool loops are too fine to resolved in the monochromatic picture, as suggested by Levine and Withbroe (1977) and Dere (1982).

To solve this discrepancy, it is expected that the higher resolution pictures of cool loops are taken.

References

Cheng, C.-C. 1980, *Astrophys. J.*, **238**, 743.

Cheng, C.-C., Smith, J. B., and Tandberg-Hanssen, E. 1980, *Solar Phys.*, **67**, 259.

Dere, K. P. and Mason, H. E. 1981, in Solar Active Regions, ed. F. Q. Orrall (Colorado Assoc. Univ. Press, Boulder), p.130.

Dere, K. P. 1982, *Solar Phys.*, **75**, 189.

Foukal, P. 1975, *Solar Phys.*, **43**, 327.

Foukal, P. V. 1976, *Astrophys. J.*, **210**, 575.

Foukal, P. V. 1978, *Astrophys. J.*, **223**, 1046.

Levine, R. H., and Withbroe, G. L. 1977, *Solar Phys.*, **51**, 83.

Sheeley, Jr., N. R. 1980, *Solar Phys.*, **66**, 79.

Sheeley, Jr., N. R. 1981, in Solar Active Regions, ed. F. Q. Orrall (Colorado Assoc. Univ. Press, Boulder), p.17.

Webb, D. F. 1981, in Solar Active Regions, ed. F. Q. Orrall (Colorado Assoc. Univ. Press, Boulder), p.165

太陽周辺の塵 － Fコロナ

磯部琇三（国立天文台）

Abstruct

Solar corona is composed of K corona (continuum light scattered by high temperature electrons), E corona (emission light emitted by ionized atoms), and F corona (light with solar spectra scattered by interplanetary dust grains). There are questions how far those dust grains reach to the sun and what are compositions of dust grains. Infrared and optical observations show enchancement of infrared emission and optical polarization at 4R$_\odot$ (R$_\odot$ is solar radius measured in angle), which give a possibility to answer the questions.

1. はじめに

1967年のインドネシア日食において、Peterson (1967) がFコロナの近赤外線観測を行ない、黄道上４R$_\odot$（R$_\odot$：太陽半径）の位置に赤外線放射の増大があることを見つけ、その後、何回かの皆既日食において、その存在が確かめられてきた。図１は、Mizutani et al (1984) によるものである。この観測は筆者達のグループと同じゴンドラに観測装置を乗せ、高度27kmから行なわれたものである。

惑星間塵は太陽の光を吸収・散乱する。吸収した光のエネルギーによって、塵は温められ赤外線を放射する。この場合、塵の温度がもっとも高くなる太陽にもっとも近い所にある塵粒子からの赤外線の強度が強くなる。一方、可視光の観測では、塵粒子の散乱光を見ており、４R$_\odot$部分の塵粒子による散乱光の分離には間接的な方法を使わなければならない。しかし、赤外線観測による塵粒子の吸収という性質とは異なる散乱の性質を可視光観測では明らかにできるので、塵粒子の組成を決める上では重要なものであると言える。

2. 塵粒子の運動

惑星間塵は、地球や他の惑星のように太陽のまわりを回転している。しかし、太陽による重力作用は質量（半径の３乗）に比例し、太陽の光による圧力は断面積（半径の2乗）に比例するので、半径の小さい惑星間塵は、単純なケプラー運動からはずれてくる。この効果を Poynting Robertson 効果とよんでいる。Mukai and Yamamoto (1979) はこれらの効果を考慮して、惑星間塵の振舞いを数値計算し、惑星間塵がら線状に太陽に近づき、４r$_\odot$の近傍で昇化し始めて半径が小さくなる。その結果、放射圧の効果が強くなって、円運動に導き、その部分での惑星間塵の量が増大することを示した。（図２、図３）

地球近傍にある惑星間塵が太陽近傍にまで達する時間は、１万年のオーダーである。惑星間塵は多分小惑星の衝突により、常に新鮮なものが供給されている。

これまでの計算では、塵粒子の運動は平面（黄道面）内だけで行なわれてきた。それは、赤外線による観測が、一次元の強度分布を求める方向でおこなわれていた事による。我々の観測（磯部等、1992）のように二次元分布が得られると、塵粒子の黄道面からのはずれが問題になってくる。

惑星間塵は太陽からの紫外線、風、宇宙線によって、電荷を持っている。Satheethと磯部(1992)は表１のような結果を得ている。太陽からの距離と塵の電荷ポテンシャルの差によって重力(F_g)、放射圧(F_r)、ポインティングロバートソン効果(F_{PR})、とローレンツ力の効果(F_L)が比べられている。太陽に近いとローレンツ力が効いてきて、図４のような分布になることが期待されている。（目下、詳細な計算を行なっている）

Fコロナの黄道面からの広がりとこれらの値を比較して塵粒子の性質を求める基礎データが得られる。

3. Fコロナの観測結果

1983年 6月11日にインドネシア・ジャワ島を通る皆既日食の折に偏光測光装置をつりさげた気球によって、27kmの高度での観測を行なった。地上からの観測では、目的の４R$_\odot$のコロナの表面輝度が皆既日食時でも地球大気の散乱光とほぼ同じレベルであるので、この大気の影響をできる限り小さくするために

高高度からの観測が必要であった。

この観測においても、 5325A, 5965A,7200A,8015A の４波長で試みたが、残念ながら望遠鏡の指向方向が５分角程度ずれたために明るい内部コロナの光によって受光器の４Ｒ⊙に相当する部分かつぶされてしまい、8015A のデータのみが有効に観測できた。

図５に偏光分布が示してある。太線で示した黄道上の分布を示したのが図６である。この図から明らかなように４Ｒ⊙の所で偏光度の増大がみられる。(Isobe et al 1987)

インドネシアの観測を基にして、1991年 7月11日に磯部等(1992)はその論文の中に示したような結果を得ている。この場合２節で書いた事が重要になってくる。

4. 偏光分布の計算

図７のように地球から４Ｒ⊙の方向を見ると、太陽コロナの電子による散乱光のＫコロナの成分（添字Ｋで示す）、惑星間塵の地球と太陽にある比較的半径の大きいものによる散乱光のＦコロナの成分（添字Ｌで示す）、および、太陽半径の４倍の所（４ｒ⊙）にある比較的半径の小さいものによるＦコロナの成分（添字Ｓで示す）を足したものを観測することになる。Ｋ成分の偏光度はほぼ100%で、Ｋ成分とＦ成分の強度比は太陽近辺から徐々に減少し、３Ｒ⊙近辺で逆転する。Ｌ成分は散乱角が小さいので偏光度は0%である。Ｓ成分の４Ｒ⊙近辺の散乱角は90度に近いので、塵粒子の半径によって偏光の波長分布は図８のようになる。一方、半径と散乱角を変数とした強度の波長分布は図９のようになる。その結果観測される偏光の波長依存性は図10のようになることが期待される。ここでは5000Ａにおけるｋ成分とＦ成分の強度比が等しい場合に対して示してある。ｍの値はＬ成分に対するＳ成分の比である。

ここに示した例はシリケイト粒子の場合である。いろいろなタイプの粒子に対して同様な図が描けるので今回の観測によって４波長の観測データが得られれば惑星間塵の組成を明らかにする大きな手がかりがえられる。

5. 結果

1983年と1991年の観測を比較すると太陽の活動期とそうでない時期の間にＦコロナの分布に変化があるように見える。この場合、本項で示した計算を時間依存性を考慮して行う必要が出てくる。塵の組成の決定までにはまだステップを踏まなければならない。

References

1. Isobe, s., Hirayama, T., Baba, N., and Miura, N. 1987, Publ. Astron. Soc. Japan, 39, 667.
2. Isobe, S. et al. 1992, 本集録。
3. Mizutani, K., Maihara, T., Hiromoto, N., and Takami, H., 1984, Nature, 312, 134.
4. Mukai, T., and Yamamoto, T., 1979, Publ. Astron. Soc. Japan, 31, 585.
5. Peterson, A. W. 1967, Astrophys. J. Letters, 148, L37.

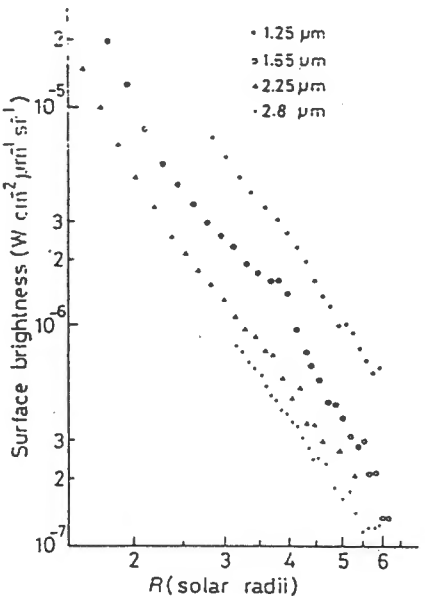

図１．　1983年6月11日のインドネシア日食観測で得られた赤外強度分布。

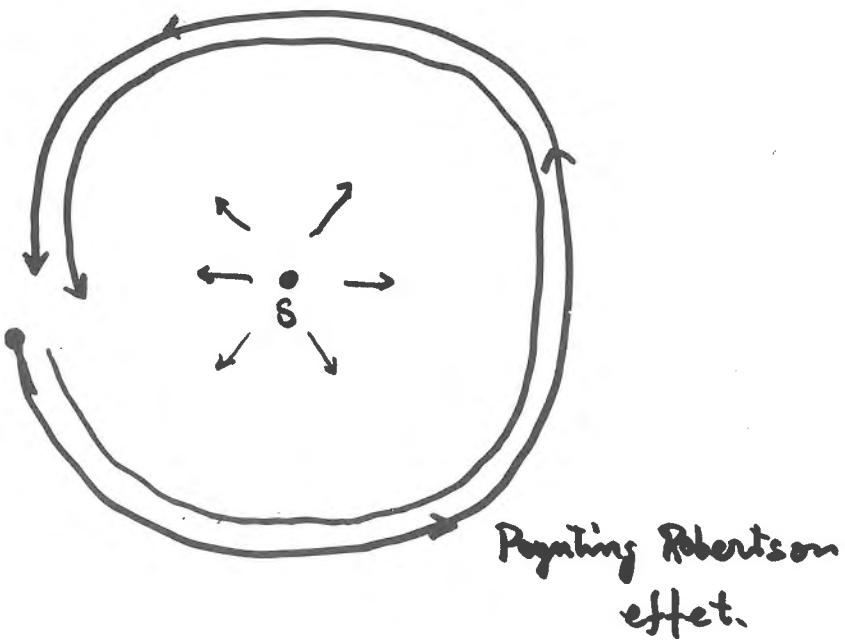

図２．　惑星間塵は太陽の放射圧による３ポインティング・ロバートソン効果で、ら線状に太陽に近づく。

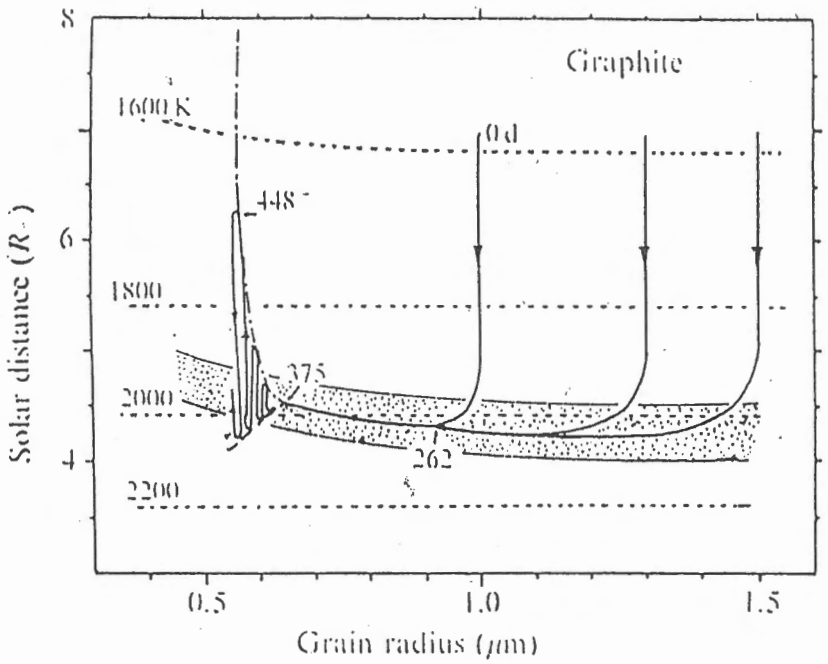

図３．　それぞれのサイズの塵粒子が線運動しながら太陽に近づくにつれて温度が上昇して、昇華し、半径が小さくなって、４ｒ⊙の所をまわる。

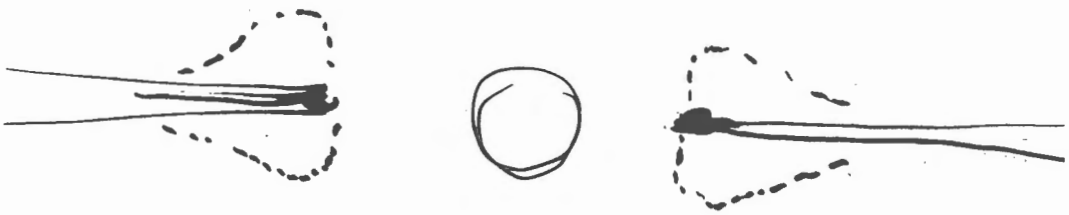

図４．　惑星間塵にローレンツ力が働いた時に期待される時の分布。

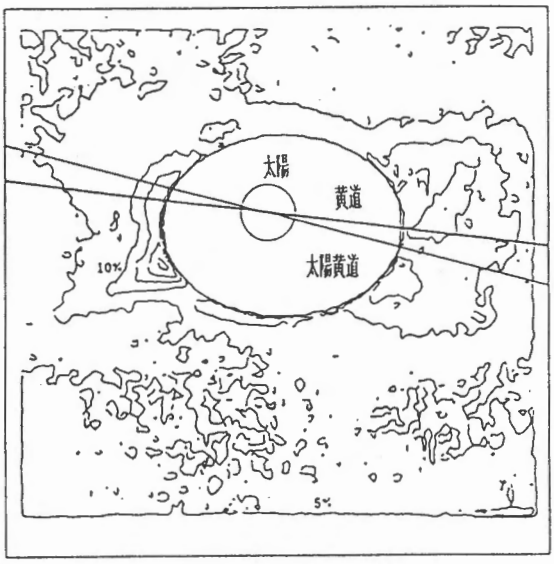

図５．　波長8015Ａにおける偏光分布

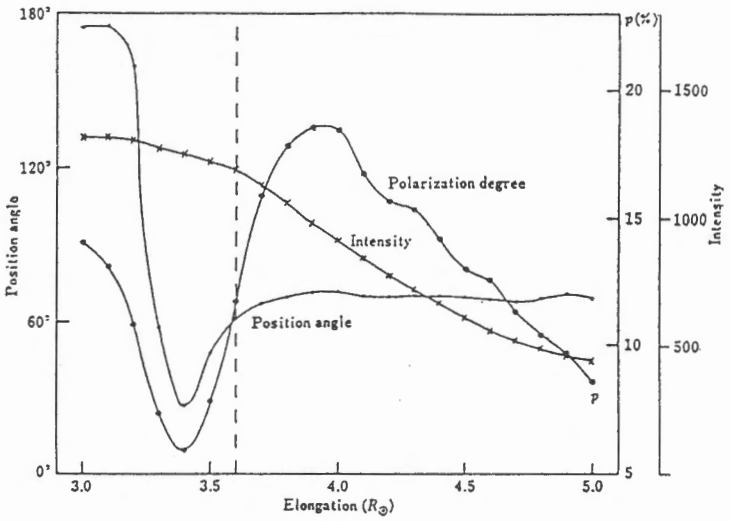

図６．　黄道面に沿った偏光度などの分布

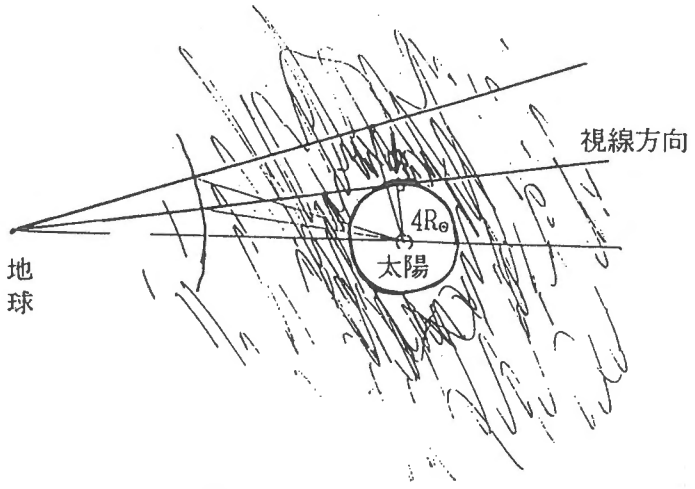

図７．　太陽のまわりには塵はない。
４Ｒ⊙近傍に多量に存在している。

$$n(a) = n(0) \exp\left[-5\,(a/a_0)^3\right] \qquad \theta = 85^\circ$$

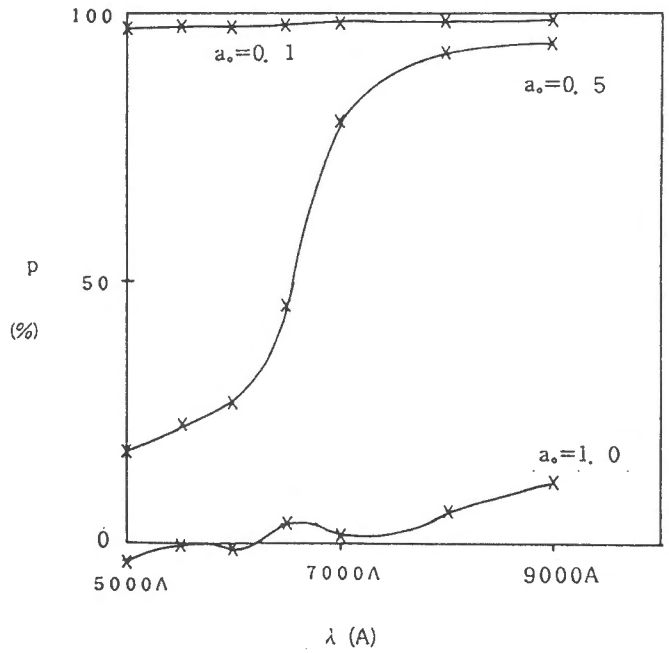

図８．　散乱角85°の場合の角a_0の値に対する偏光の値の波長分布。

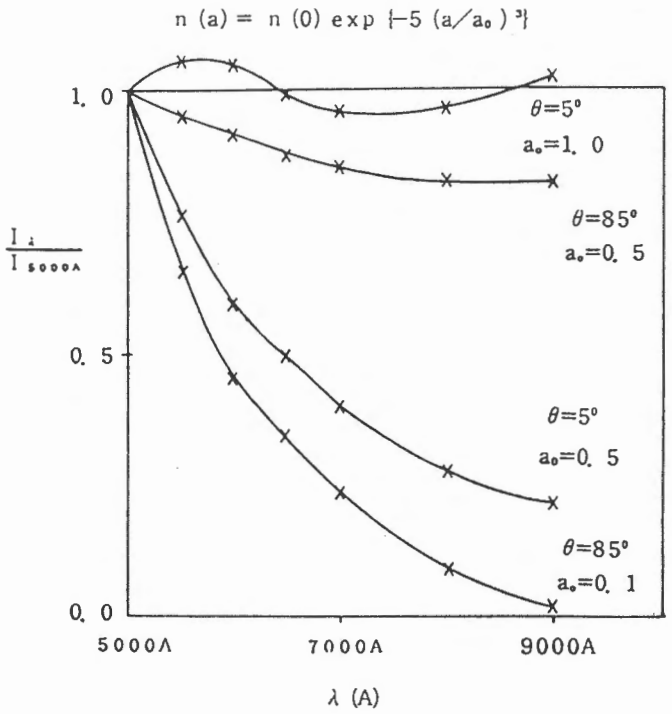

図９．　各散乱角、各ａ₀値に対する強度の波長分布。

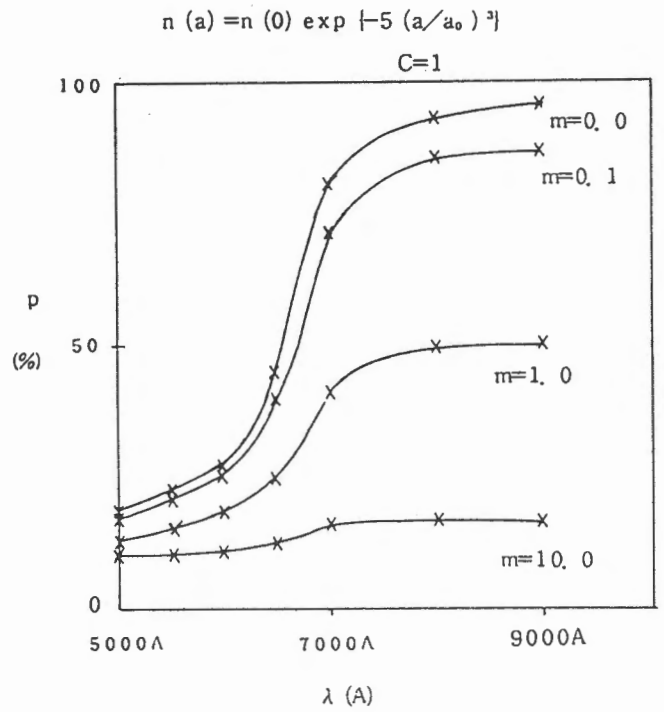

図１０．各ｍの値に対する偏光度の波長分布。

Table I

COMPARISON OF THE FORCES ACTING ON A DUST PARTICLE AT 1A.U. AND AT $4R_\odot$

	$r = 4R_\odot$ $\Phi = 10$ V				
Force	Grain Size(μm)				
	0.1	0.3	0.5	1.0	10.0
F_g	$-1.6*10^{-11}$	$-4.3*10^{-10}$	$-2.0*10^{-9}$	$-1.6*10^{-8}$	$-1.6*10^{-5}$
F_r	$9.7*10^{-11}$	$5.3*10^{-10}$	$1.1*10^{-9}$	$4.1*10^{-9}$	$4.1*10^{-7}$
F_r/F_g	6.05	1.23	0.55	0.25	0.025
F_{PR}	$-6.5*10^{-14}$	$-3.6*10^{-13}$	$-7.4*10^{-13}$	$-2.7*10^{-12}$	$-2.7*10^{-10}$
F_L	$\pm1.4*10^{-11}$	$\pm4.2*10^{-11}$	$\pm6.9*10^{-11}$	$\pm1.4*10^{-10}$	$\pm1.4*10^{-9}$
F_L/F_{PR}	$2.14*10^{2}$	$1.17*10^{2}$	$9.40*10^{1}$	$5.12*10^{1}$	5.12
	$r = 4R_\odot$ $\Phi = 15$ V				
F_L/F_{PR}	$3.22*10^{2}$	$1.76*10^{2}$	$1.41*10^{2}$	$7.69*10^{1}$	7.69
	$r = 4R_\odot$ $\Phi = 20$ V				
F_L/F_{PR}	$4.29*10^{2}$	$2.34*10^{2}$	$1.88*10^{2}$	$1.03*10^{2}$	10.3

日食における太陽風速度場測定の可能性について

国立天文台　一本潔

A method to detect the lateral motion of the solar corona is studied. Since the emission of the K-corona is produced by the scattering of photospheric light by the coronal electron, a coronal motion against the photosphere results a wave length shift of the K-corona spectra. A simple model calculation shows that a radial motion of 100km/s produces 0.1-0.4% intensity variations in the K-corona spectra. It can be one of the target in the next solar eclipse.

一般に天体の視線方向の運動は、線スペクトルのドップラー偏移から求めることが出来るが、ここでは視線方向と垂直な方向の太陽コロナの運動を求める可能性について検討する。基本的な考え方はつぎのとうりである。K-コロナのスペクトルはコロナを形成する電子が光球の光を散乱することによって形成されており、その強度分布は光球スペクトルの形を反映している。従ってコロナが光球から遠ざかるような運動をしていれば、K-コロナのスペクトルは光球のそれに対して全体として波長がシフトしているはずであり、もし何等かのスペクトル構造を使ってそのシフト量を測ることが出来れば、コロナの光球に対する相対速度が求まるはずである。しかしよく知られているように、K-コロナのスペクトルにおいて、光球の線スペクトルは高温電子の熱運動によってほぼ完全にかき消されているので、波長シフトを求めるための手がかりは非常に微弱な信号となることが予想される。K-コロナに残る僅かな光球スペクトルの構造を使ってコロナの速度を求めるには、どの程度の観測精度が要求されるだろうか？太陽光スペクトルのデータを用いてシミュレーションを行ってみた。

図１の上は６０００Ｋのプランク関数に、ＳａｃＰｅａｋのスペクトルアトラスを重ね、２００万度の電子の熱運動に相当するガウシアンでコンボリューションをとったものである。これは疑似的なＫ-コロナのスペクトルだと思ってよい。個々の線スペクトルは完全に馴らされてしまっているが、所々に僅かなへこみが残っている。これは強い吸収線がたくさん集まっているところであり、特に波長3900Ａと4300Ａ辺りにみられる小さなへこみは、それぞれ CaIIH,K と CN 分子の吸収線群によるものである。波長3500Ａから4500Ａにおける元の太陽スペクトルとの対応を図２に示した。又、波長7500Ａ、9300Ａ、11000Ａに見られる比較的大きなへこみは、地球大気の吸収線によるもので、実際にはシャープな吸収線群として観測されるはずのものである。

図１の下は、このスペクトルが約１００ｋｍ／ｓに相当する赤方偏移を受けたとき、各波長でどれだけ強度が変化するかを、もとのスペクトルに対する相対値で示したものである。全体として右上がりなのは、プランクの山が少し赤い方へずれたためだが、この太陽風によるコロナの色温度の変化は、強度にして0.1%程度である。又、3500Ａ－4500Ａ辺りには、前述の吸収構造による0.4%程度の変化がみられる。

以上の計算から、太陽風によるコロナの運動を有意に検出し、場所による速度差（～１００ｋｍ／ｓ）を知るには、0.1%（少なくとも0.4%）程度の精度でスペクトルを観測しなければならない。具体的な方法としては、①プリズムを使ってスリットスペクトルを撮り、光球のスペクトルと比較する、②3750Ａと4000Ａ辺りを通す色フィルターを用いてコロナをできるだけ精度よく測光する、等が考えられよう。更に輝線のドップラー偏移を用いて、視線方向の速度を同時に測れば、コロナの運動を三次元的なベクトルとして知ることが出来るだろう。日食の限られた時間で以上の精度が達成できるかどうか、又、F-コロナやコロナ輝線がデータの解釈にどの様な影響を与えるか、更に検討する必要がある。

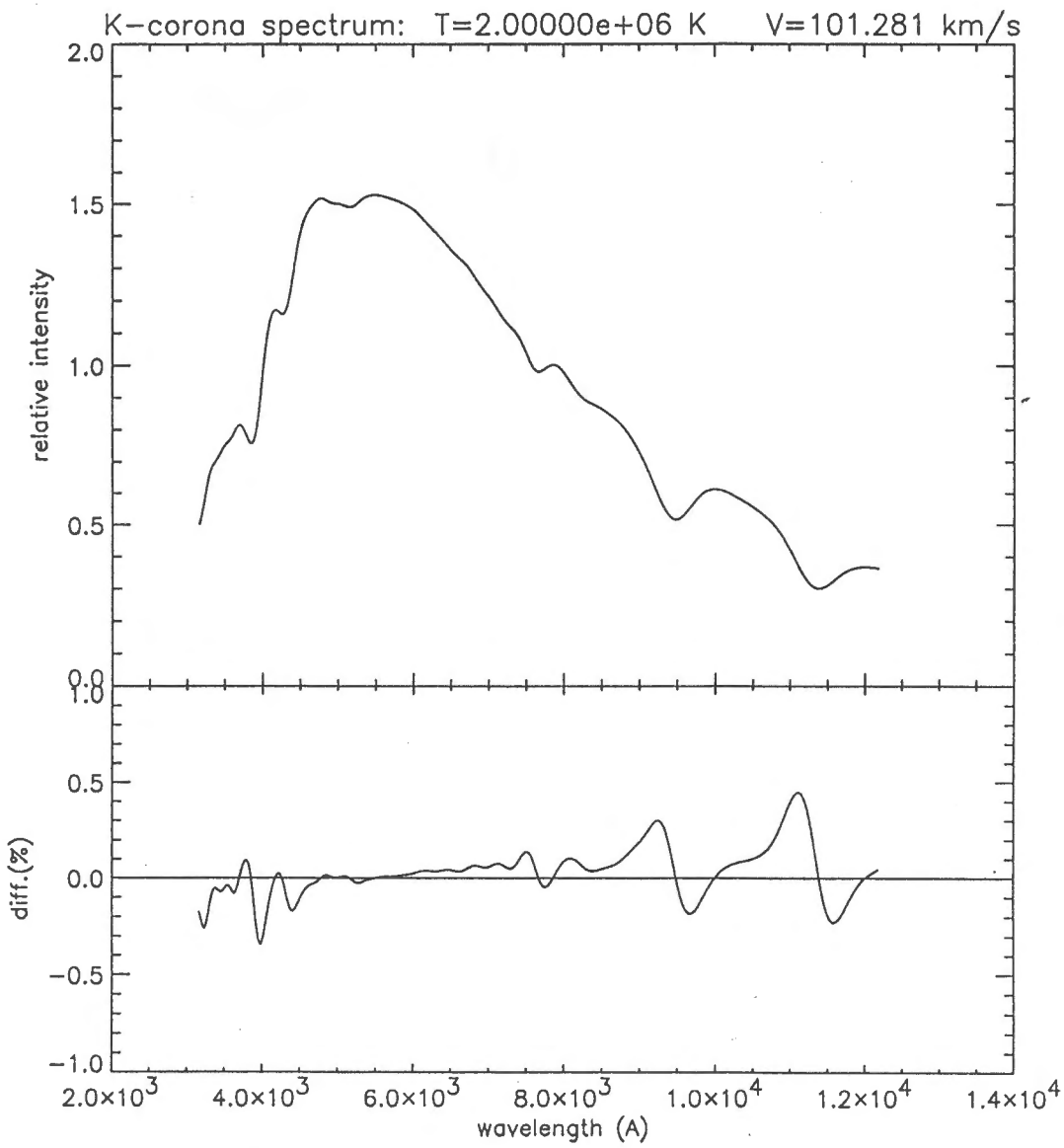

図１．プランク関数とスペクトルアトラスから計算したＫ-コロナのスペクトル（上）と、それが１００ｋｍ／ｓに相当する赤方偏移を受けた場合の相対的な強度変化（下）。

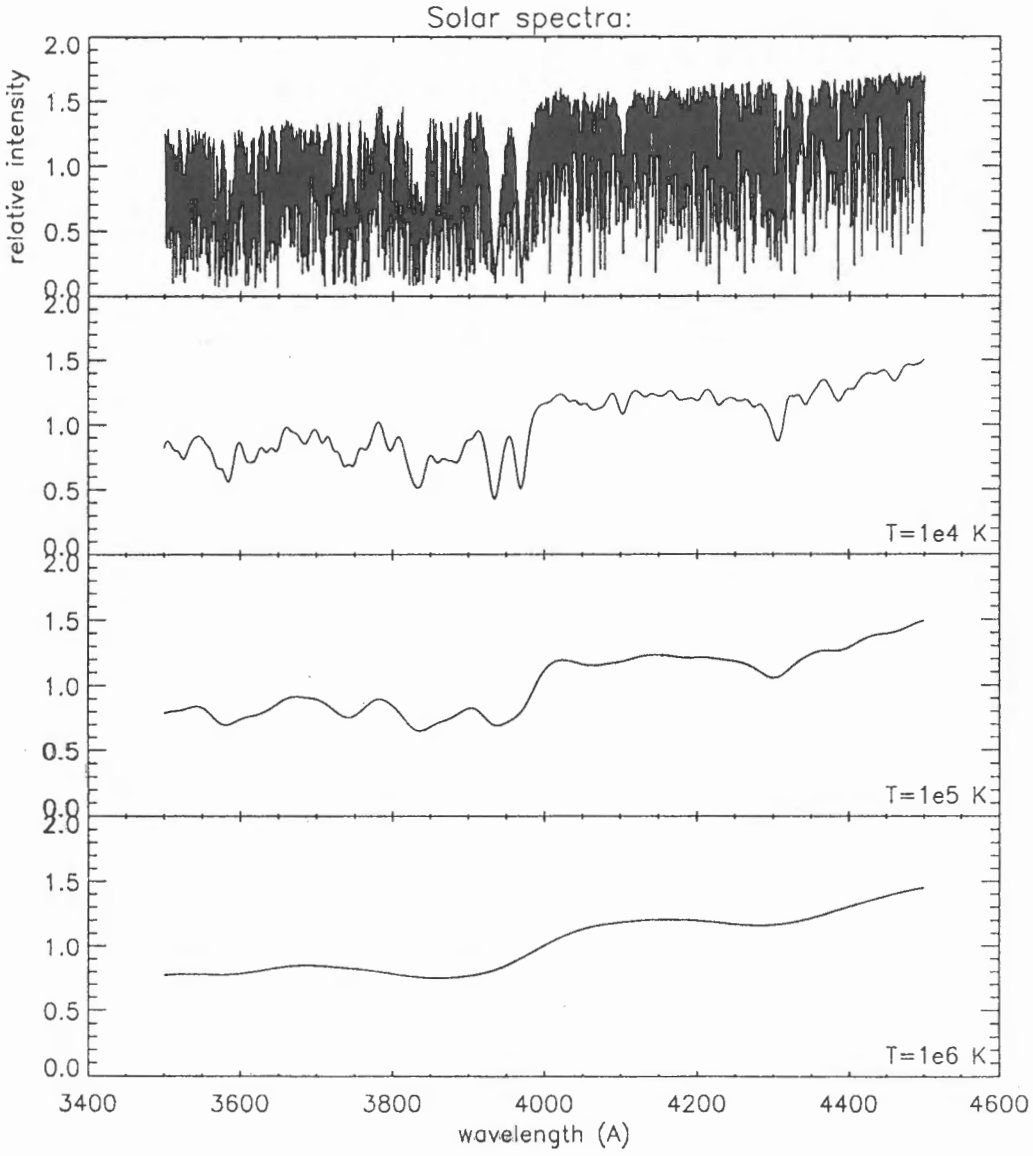

図２．（上から）3500Ａ－4500Ａの光球スペクトルと、それを１万度、１０万度、１００万度の電子で馴らしたもの。

A CCD Camera Specified for Solar Observations

Yoichiro Hanaoka

Nobeyama Radio Observatory, National Astronomical Observatory

CCD cameras are now the most popular detector in optical astronomical observations; in solar observations it is also true. However, commercial CCD cameras for the astronomical use are designed for night-time observations, and they do not have sufficient time resolutions required for solar observations. Therefore TV cameras are used as high speed CCD cameras in some solar observatories. However TV cameras are not proper for precise photometry; a high speed CCD camera tuned for solar observations are required.

There are some reasons why usual TV cameras are not proper for photometric use. The amplifier of a TV camera which convert the raw CCD signal to the TV signal is not linear one. The signal from a TV camera is distorted on the way to the digitizing device due to the long cabling. The TV signal is transformed in AC, which is not proper to measure the DC output from a CCD. Furthermore, a usual degitizing device, or a frame memory, has a 8-bit A/D convertor, which is not sufficient to measure the CCD output in the full precision (it is reasonable for the signal of a TV camera due to the low precision of the TV signal). The converting rate of the A/D convertor of the usual digutizing device is about 10Msps (or, the data rate is 10MBsec^{-1}), but the data recording rate of the usual magnetic device is much lower than 10MBsec^{-1}, then only a small part of the whole data is saved. In the conventional usage of the CCD TV camera, the high precision of the CCD's is not utilized and much data are not used.

Since a CCD camera designed for solar observations are not obtaioned commercialy, it is necessary to make a special CCD camera or a digital solar CCD camera by hand to perform high precision solar observations. My suggestion for the characteristics of the camera are shown as follows. The camera head is based on a TV camera, but the CCD chip must be cooled (the Peltier cooling is sufficient). Of course, exposures are controlled by a computer. The A/D convertor must be put as near as the CCD chip to minimize the distortion of the CCD signal. A 12-bit/10Msps A/D convertor, of which the price is 100-200 thousand yen, is necessary for high speed and high precision imaging. Such a special camera may be expensive if we develop only one camera, but now many TV cameras are used for solar observations in Japan; several cameras in Norikura, also several cameras in Mitaka, and in Hiraiso, and so on. These TV cameras can be substituted with the digital solar CCD camera. Therefore many digital solar CCD cameras can be made, then the price of each camera is not so expensive.

The data rate of such a digital camera is about 120Mbit sec^{-1}. For eclipse observations or flare observations, a high time resolution is required, therefore all the data from the camera during an eclipse or a flare must be recorded. We use very high speed data recorders, of which the recording rate is up to 256Mbit sec^{-1}, for VLBI observations and the Radio Heliograph at Nobeyama. The amount of the data recorded in a tape is 770Gbit. Such a data recorder can be used for the digital solar camera.